MOLECULAR MECHANISMS UNDERLYING INNATE IMMUNE KINASE TBK1-DRIVEN ONCOGENIC TRANSFORMATION

APPROVED BY SUPERVISORY COMMITTEE

Michael A White, Ph.D.

Melanie H. Cobb, Ph.D.

Lawrence Lum, Ph.D.

John D. Minna, M.D.

DEDICATION

This work is dedicated to my mother and Arlene for their love and support.

ACKNOWLEDGEMENTS

I am very grateful to my mentor, Dr. Michael White, for his continuous support and guidance through the entire study. I really appreciate his inspiration, patience, and generosity. I would also like to thank my committee members, Dr. Cobb, Dr. Lum, and Dr. Minna, for their invaluable advice and discussion. I thank all the White lab members and my friends for their help, suggestion, and discussion. Particularly, I would like to thank Rosie, Michael, Brian, Tzuling, and Malia for their long-term support and collaboration. I would also like to thank my friends, Veleka, Pei-Ling, Jen-Chieh, Shu-Yi, Chih-Chiang, Jen-Shuan, Yi-Chun, and Yu-San for their friendship. I am grateful to Drs. Rolf Brekken, Zhijian James Chen, Xuetao Cao, Philip Tsichlis, Charles Yeaman, William Hahn, Keqiang Ye, and Shu-Chan Hsu, Bing Su, Dos Sarbassov, Mark Magnuson, David Sabatini, Thomas Tan, and Bert Vogelstein for many of the reagents used in these studies. Finally, and most importantly, I would like to thank my mother and Arlene for their unending support and encouragement.

MOLECULAR MECHANISMS UNDERLYING INNATE IMMUNE KINASE TBK1-DRIVEN ONCOGENIC TRANSFORMATION

by

YI-HUNG OU

DISSERTATION

Presented to the Faculty of the Graduate School of Biomedical Sciences

The University of Texas Southwestern Medical Center at Dallas

In Partial Fulfillment of the Requirements

For the Degree of

DOCTOR OF PHILOSOPHY

The University of Texas Southwestern Medical Center at Dallas

Dallas, Texas

April, 2013

MOLECULAR MECHANISMS UNDERLYING INNATE IMMUNE KINASE TBK1-DRIVEN ONCOGENIC TRANSFORMATION

Publication No. _____

Yi-Hung Ou, Ph.D.

The University of Texas Southwestern Medical Center at Dallas, 2013

Michael A. White, Ph.D.

An essential kinase in innate immune signaling, TBK1 couples pathogen surveillance to induction of host defense mechanisms. The pathological activation of TBK1 in cancer can overcome programmed cell death cues, enabling cells to survive oncogenic stress. The mechanistic basis of TBK1 prosurvival signaling, however, has been enigmatic. Here we show that TBK1 directly activates AKT by phosphorylation of the canonical activation loop and hydrophobic motif sites independently of PDK1 and mTORC2. A population of AKT is bound to components of the exocyst complex. Upon mitogen stimulation, triggering of the innate immune response, re-exposure to glucose, or oncogene activation, TBK1 is recruited

to the exocyst, where it activates AKT. In cells lacking TBK1, insulin activates AKT normally, but AKT activation by these exocyst-dependent mechanisms is impaired. Discovery and characterization of a 6-aminopyrazolopyrimidine derivative, as a selective low nanomolar TBK1 inhibitor, indicates this regulatory arm can be pharmacologically perturbed independently of canonical PI3K/PDK1 signaling. Thus, AKT is a direct TBK1 substrate that connects TBK1 to prosurvival signaling. Additionally, biochemical and cell biological evidence indicates critical roles of TBK1 and its analog IKKε in the amino acid-dependent activation of mTORC1. TBK1 and IKKε are activated by amino acids and both proteins interact with mTORC1. In TBK1 and/or IKKε-deficient cells, mTORC1 activation by amino acids is impaired. Of note, we also discovered a set of TBK1 substrates and interacting proteins participating in amino acid-dependent mTORC1 signaling. In conclusion, our results suggest that TBK1 not only supports physiological and oncogenic activation of AKT, but also plays a central role in the regulation of mTORC1 activation in response to amino acids. In addition, our studies reveal novel mTORC1 components and provide new insights into the regulation of the mTORC1 signaling network.

TABLE OF CONTENTS

PRIOR PUBLICATIONS

Chang J, Meredith DM, Mayer PR, Borromeo MD, Lai HC, **Ou YH**, Johnson JE.
Prdm13 mediates the balance of inhibitory and excitatory neurons in somatosensory circuits.
Developmental Cell. 2013 (In Press)

Herman M, Ciancanelli M*, **Ou YH***, Lorenzo L, Guo Y, Sancho-Shimizu V, Pérez de Diego R, Pauwels E, Cardon A, Plancoulaine S, Klaudel-Dreszler M, Heropolitańska-Pliszka M, Rozenberg F, Lebon P, Tardieu M, White MA, Abel L, Zhang SY, and Casanova, JL.
Dominant human TBK1 mutations impair TLR3 immunity and underlie herpes simplex encephalitis.
The Journal of Experimental Medicine. 2012, 209(9):1567-82

Ou YH, Torres M, Ram RR, Formstecher E, Roland C, Cheng TL, Brekken R, Wurz R, Tasker A, Polverino T, Tan SL, and White MA.
TBK1 directly engages Akt/PKB survival signaling to support oncogenic transformation.
Molecular Cell. 2011, 41(4): 458-470

Bodemann BO, Orvedahl A, Cheng TL, Ram RR, **Ou YH**, Formstecher E, Maiti M, Hazelett CC, Wauson EM, Balakireva M, Camonis JH, Yeaman C, Levine B, and White MA.
RalB exocyst mediate the cellular starvation response by direct activation of autophagosome assembly.
Cell. 2011, 144(2): 253-1267.

Ou YH*, Chung PH*, Hsu FF, Sun TP, Chang WY, and Shieh SY.
The candidate tumor suppressor BTG3 is a transcriptional target of p53 that inhibits E2F1.
The EMBO Journal. 2007**,** 26(17): 3968-3980.

Ou YH, Chung PH, Sun TP, and Shieh SY.
p53 C-terminal phosphorylation by CHK1 and CHK2 participates in the regulation of DNA-damage-induced C-terminal acetylation.
Molecular Biology of the Cell. 2005, 16(4): 1684-1695.

Wei JH, Chou YF, **Ou YH**, Yeh YH, Tyan SW, Sun TP, Shen CY, Shieh SY.
TTK/hMps1 Participates in the Regulation of DNA Damage Checkpoint Response by Phosphorylating CHK2 on Threonine 68.
The Journal of Biological Chemistry. 2005, 280(9): 7748-7757.

Cheng TL, **Ou YH**, and White MA.
The Ras-like G-protein exchange factor family (RalGEFs) supports cancer cell viability across diverse oncogenic backgrounds.
The Journal of Biological Chemistry. (In Revision)

Potts MB*, Kim HS*, Fisher KW*, Hu Y*, Carrasco Y, Bulut GB, **Ou YH**, Herrera-Herrera ML, Cubillos F, Saurabh M, Xiao G, Hofree M, Ideker T, Xie Y, Huang LJ, Lewis RE**, MacMillan JB**, and White MA**.

Broad-scale mode-of-action annotation of natural product perturbations by functional signature ontology (FUSION).

Science. (In Revision)

Ou YH and White MA.

Book chapter on ***"Alternative mechanisms of Akt regulation"*** to the volume, **Akt Kinases in Oncogenesis**. (In Preparation)

LIST OF FIGURES

CHAPTER ONE

CHAPTER TWO

CHAPTER THREE

LIST OF DEFINITIONS

4E-BP1	Eukaryotic initiation factor 4E-binding protein 1
A20	Tumor necrosis factor inducible protein
ACK1	Activated CDC42 kinase 1
AKT	v-akt murine thymoma viral oncogene homolog
AMP	Adenosine 5′-monophosphate
AMPK	AMP-activated protein kinase
API-2	Akt/protein kinase B signaling inhibitor-2
AS160	AKT substrate 160KD (TBC1D4)
ATG13	Autophagy related 13
ATG7	Autophagy related 7
ATG9	Autophagy related 9
ATM	Ataxia telangiectasia mutated
ATP	Adenosine 5′-triphosphate
BAD	BCL2-associated agonist of cell death
BIX02189	MAP2K5 inhibitor
BrdU	5-bromo-2'-deoxyuridine
BSA	Bovine serum albumin
C7orf59	Late endosomal/lysosomal adaptor and MAPK and MTOR activator 4 (LAMTOR4)
CAD	carbamoyl-phosphate synthetase 2, aspartate transcarbamoylase, dihydroorotase
caspase	apoptosis-related cysteine peptidase
CYLD	cylindromatosis
DAPI	4',6-diamidino-2-phenylindole
DDX3	DEAD-box helicase 3
DEPTOR	DEP domain-containing mTOR-interacting protein
DNA-PK	DNA-dependent serine/threonine protein kinase
dsRNA	double-stranded RNA
EGF	Epidermal growth factor
EGFR	Epidermal growth factor receptor
eIF2K	elongation factor 2 kinase
eIF4A	The eukaryotic initiation factor-4A
eIF4B	eIF4A-binding protein
eIF4E	The eukaryotic initiation factor-4E
eNOS	endothelial NOS
ERK	Extracellular Regulated Kinase
ERK5	Mitogen-activated protein kinase 7; MAP kinase 7
FBS	Fetal bovine serum
FGF	Fibroblast growth factor
FIP200	200 kDa FAK family kinase-interacting protein (RB1CC1)

FITC	Fluorescein isothiocyanate
fMLP	N-Formylmethionyl-leucyl-phenylalanine (formylated tripeptide)
FOXO	Forkhead box transcription factors
GAP	GTPase-activating protein
GDP	Guanosine 5'-diphosphate
GEF	Guanine nucleotide exchange factor
GLUT1	Glucose transporter type 1
GLUT4	Glucose transporter type 4
Grb10	Growth factor receptor-bound protein 10
GSK3β	Glycogen synthase kinase 3 beta
GTP	Guanosine 5'-triphosphate
GβL	G protein beta subunit-like (mLST8)
HBXIP	Hepatitis B virus X-interacting protein; LAMTOR5
HEK293	Human embryonic kidney cell line
HER2	Human Epidermal Growth Factor Receptor 2
HIF1	Hypoxia-inducible factor 1
HK2	Hexokinase 2
HM	Hydrophobic motif
HRG	Heregulin
HSE	Herpes simplex virus-1 (HSV-1) encephalitis
IFNβ	Interferon beta
IGF-1	Insulin-like growth factor 1
IKKα	Inhibitor of kappaB kinase alpha
IKKβ	Inhibitor of kappaB kinase beta
IKKε	Inhibitor of kappa light polypeptide gene enhancer in B-cells, kinase epsilon
IL1b	Interleukin 1, beta
ILK1	Integrin-linked kinase
IP10	10 kDa interferon gamma-induced protein; chemokine (C-X-C motif) ligand 10
IR	Ionizing radiation
IRF3/7	Interferon regulatory factor 3/7
IRS1	Insulin receptor substrate 1
IκB	IkappaB protein
KD	Kinase domain
LC3	Microtubule-associated protein 1A/1B-light chain 3
lipin1	phosphatidate phosphatase LPIN1
LKB1	Liver kinase B1 (STK11)
LONRF1	LON peptidase N-terminal domain and ring finger 1
LPS	Lipopolysaccharide
LRS	Leucyl-tRNA synthetase
LY2940002	PI3K inhibitor

MAP2K5	Mitogen-activated protein kinase kinase 5
MAP3K3	Mitogen-activated protein kinase kinase kinase 3
MAPK	Mitogen-activated protein kinase
MAPKAPK-2	Mitogen-activated protein kinase-activated protein kinase 2
MDA-5	Melanoma Differentiation-Associated protein 5
Mdm2	p53 E3 ubiquitin protein ligase homolog
MEK	Mitogen-activated protein kinase kinase
MMTV	Mouse mammary tumor virus
MP1	MEK partner 1; LAMTOR); MAPKSP1
mTOR	mechanistic/mammalian target of rapamycin
mTORC1	mechanistic/mammalian target of rapamycin complex 1
mTORC2	mechanistic/mammalian target of rapamycin complex 2
Mx1	myxovirus (influenza virus) resistance 1
myc	v-myc myelocytomatosis viral oncogene homolog
NAK	NF-kappa-B-activating kinase
NAP1	NAK-associated protein 1 (AZI2)
NDP52	Nuclear dot protein 52
NEMO	Inhibitor of kappa light polypeptide gene enhancer in B-cells, kinase gamma
NF-κB	Nuclear factor kappa-light-chain-enhancer of activated B cells
NF1/2	neurofibromin 1/2
NSCLC	Non-small cell lung cancer
optineurin	Optic neuropathy-inducing protein (OPTN)
p14	Late endosomal/lysosomal adaptor and MAPK and MTOR activator 2 (LAMTOR2); ROBLD3
p18	Late endosomal/lysosomal adaptor and MAPK and MTOR activator 1 (LAMTOR1); c11orf59)
p21CIP1	cyclin-dependent kinase inhibitor 1A
p27KIP1	cyclin-dependent kinase inhibitor 1B
p53	Tumor protein p53
p62	SQSTM1 sequestosome 1
PAK	p21 protein (Cdc42/Rac)-activated kinase
PB1	Phox and Bem1p domain
PDCD4	Programmed cell death protein 4
PDGF	Platelet-derived growth factor
PDK1	3-phosphoinositide-dependent protein kinase-1
PFK2	Phosphofructokinase 2
PH	Pleckstrin homology
PHLPP	PH domain and leucine rich repeat protein phosphatase
PI3K	Phosphoinositide-3-kinase
PIKfyve	FYVE finger-containing phosphoinositide kinase
PIKK	Phosphatidylinositol 3-kinase-related kinase

PIP	Phosphatidylinositol 4-phosphate or Phosphatidylinositol 4-phosphate
PIP2	Phosphatidylinositol 4,5-bisphosphate,
PIP3	Phosphatidylinositol 3,4,5-trisphosphate,
PKC	Integrin-linked kinase
PMA	Phorbol-12-myristate-13-acetate
PML	promyelocytic leukemia
PP2A	Protein phosphatase 2, regulatory subunit A
PRAS40	Proline-rich Akt/PKB substrate 40 kDa
Protor1	Protein observed with Rictor-1
PTEN	Phosphatase and tensin homolog
PTK6	Tyrosine-protein kinase 6
Rab10	Ras-related protein 10
Raf	v-raf-1 murine leukemia viral oncogene homolog 1
Rag	Ras-related GTP-binding protein
Ral	Ras-like guanyl nucleotide-binding protein
RANKL	Receptor activator of nuclear factor kappa-B ligand
Raptor	Regulatory associated protein of MTOR, complex 1
Ras	Rat sarcoma
REDD1	Development and DNA Damage Responses -1
Rheb	Ras homolog enriched in brain
Rictor	RPTOR independent companion of MTOR, complex 2
RIG-1	Retinoic acid-inducible gene 1
RSK	ribosomal protein S6 kinase, 90kDa
S6	40S ribosomal protein S6
S6K	ribosomal protein S6 kinase, 70kDa,
SCF	skp, Cullin, F-box containing complex
Sec5	exocyst complex component 2 (EXOC2)
Ser	Serine
SHIP1	SH2 domain containing inositol-5-phosphatase 1
SHIP2	SH2 domain containing inositol-5-phosphatase 2
shRNA	small hairpin RNA or short hairpin RNA
SIKE	Suppressor of IKK-epsilon
Sin1	Stress-activated map kinase-interacting protein 1
SINTBAD	Similar to NAP1 TBK1 adaptor
SKP2	S-phase Kinase-associated Protein-2
SLC1A5	Solute carrier family 1 (neutral amino acid transporter), member 5
SLC7A5	Solute carrier family 7 (cationic amino acid transporter, y+ system), member 5
src	v-src sarcoma viral oncogene homolog
STING	Stimulator of interferon genes
TANK	TRAF family member-associated NF-kappa-B activator

TAS1R1	Taste receptor, type 1, member 1
TAS1R3	Taste receptor, type 1, member 3
TAX1BP1	Tax1 (human T-cell leukemia virus type I) binding protein 1
TBC1D1	TBC1 domain family, member 1
TBC1D4	TBC1 domain family, member 4
TBC1D7	TBC1 domain family, member 7
TBK1	TANK-Binding Kinase-1
TFEB	Transcription Factor EB
Thr	Threonine
TLR3	Toll-like receptor 3
TLR4	Toll-like receptor 4
Torin 1	TOR inhibitor 1
TRADD	Tumor necrosis factor (TNF)-receptor 1-associated death domain protein
TRAF3	TNF receptor-associated factor 3
TRAF6	TNF receptor-associated factor 6, E3 ubiquitin protein ligase
TRAIL	TNF-related apoptosis-inducing ligand
TRIF	TIR domain containing adaptor inducing interferon-beta
TSC1	Tuberous sclerosis 1
TSC2	Tuberous sclerosis 2
TTT-RUVBL1/2	Tel2-Tti1-Tti2 (TTT)-RUVBL1/2 complex
ULK1	unc-51-like kinase 1 (ATG1)
VEGF	Vascular endothelial growth factor
Wortmannin	PI3K inhibitor

CHAPTER ONE

INTRODUCTION

HUMAN CANCER

Maintenance of cell and tissue homeostasis in multi-cellular organisms is sophisticatedly and tightly regulated by signal transduction networks. Failure to control the dynamic balance of proliferation and cell death results in severe human diseases, such as cancer and neurodegenerative disorders. During the evolution of cancer, aberrant signaling pathways contribute to several key biological processes by which cancer cells acquire the capacity of uncontrolled proliferation and malignancy to escape from tumor suppressor-mediated surveillance network, increase cell mass to sustain rapid proliferation, induce angiogenesis for supply nutrients and oxygen to the tumor, inhibit cell death, acquire cellular immortality, and invade/metastasize to proximal or distal tissues (Hanahan and Weinberg 2011).

In the cancer arena, two broad sets of genes, tumor suppressor genes (e.g. p53 and PTEN) and oncogenes (e.g. Ras and myc), play a fundamental role in tumorigenesis. Inactivation of tumor suppressor genes caused by genomic instability, epigenetic modification, and post-translational modification results in gene silencing, loss-of-function mutation, and inactivation, which prevents tumor suppressor-mediated cell cycle arrest and apoptosis and therefore leads to aberrant cell growth and proliferation. Activation of oncogenes generally occurs through several distinct mechanisms, such as gene amplification, over-expression, fusion, and gain-of-function mutation, which sustains proliferative signals and induces cellular transformation (Pelengaris, Khan et al. 2002, Shaw and Cantley 2006, Salmena, Carracedo et al. 2008, Vousden and Prives 2009).

In addition to previously mentioned oncogenes, the small GTPase Ras is the first oncogene independently identified by several laboratories in 1982 (Der, Krontiris et al. 1982, Goldfarb, Shimizu et al. 1982, Parada, Tabin et al. 1982, Pulciani, Santos et al. 1982, Shih and Weinberg 1982). Activity of Ras and other small GTPases, such as Ral and Rheb, are controlled by guanine nucleotide exchange factors (GEF) and GTPase-activating proteins (GAP). GDP-bound Ras is activated by GEFs which facilitate the substitution of GTP for GDP, and then active GTP-bound Ras promotes cell proliferation, survival, and differentiation by stimulating three major downstream effector pathways, including RalGEF/Ral, PI3K/AKT and Raf/MEK/ERK kinase cascade (Karnoub and Weinberg 2008). Ral, Ras-like guanyl nucleotide-binding proteins, has two family members, RalA and RalB, which are constitutively activated in most cancer cells. RalA has been shown to participate in anchorage-independent cancer cell growth. Although RalA and RalB are more than 90% identical in amino acid level, the function of RalB, in contrast to RalA, is required for cancer cell survival but is not essential for the proliferation of non-tumorigenic epithelial cells (Chien and White 2003, Bodemann and White 2008). Recent findings indicate that the RalB/Sec5 effector complex directly recruits and activates TBK1 in the innate immune response, whereas cancer cells hijack this RalB/Sec5/TBK1 pathway to deflect apoptosis (Chien, Kim et al. 2006). However, the role of TBK1-mediated cancer cell survival and proliferation remains ill-understood.

AKT SIGNALING PATHWAY

The PI3K-AKT axis is one of the most recognized signaling pathways, which participates in a range of physiological processes and disease settings, including cell growth, proliferation, survival, angiogenesis and metabolism. Active PI3K converts PIP2 to PIP3, which functions as signaling intermediates to regulate several important biological processes, including membrane trafficking, signal transduction, cell movement, cell growth, proliferation, and complex metabolic processes. After PIP3 docks at the plasma membrane, it recruits AKT to the plasma membrane, where AKT is subsequently phosphorylated by PDK1 at Thr308 residue and by either mTORC2 or other hydrophobic motif kinases at Ser473 residue. Cumulative evidence suggest that phosphorylation of AKT at Thr308 and Ser473 is critical for full activation of the AKT kinase in response to upstream signaling (Manning and Cantley 2007, DeBerardinis, Lum et al. 2008, Chalhoub and Baker 2009, Engelman 2009).

In humans, there are three AKT genes, AKT1, AKT2 and AKT3, which play a non-redundant role in numerous cellular and organismal processes, such as animal size and metabolism. From a peptide structure aspect, the three AKT isoforms share very similar domain structures that are composed of an N-terminal pleckstrin homology (PH) domain, a kinase domain (KD), and a C-terminal regulatory domain known as hydrophobic motif (HM) (Figure 1.1). AKT1 is expressed quite ubiquitously in almost all tissues, whereas AKT2 is preferentially expressed in insulin-responsive tissues and lymphocytes. Expression of AKT3 is confined in the brain region. Genetic mouse models further confirm that spatial expression of AKT in those tissues is critical for the development and physiology of those tissues. Membrane targeting of AKT relies on the PH domain that binds to PIP3 concentrated at the plasma membrane. Since

PIP3 is required for AKT membrane localization, PIP3 phosphatases, PTEN, SHIP1 and SHIP2, negatively regulate AKT signaling (Matheny and Adamo 2009, Song, Salmena et al. 2012).

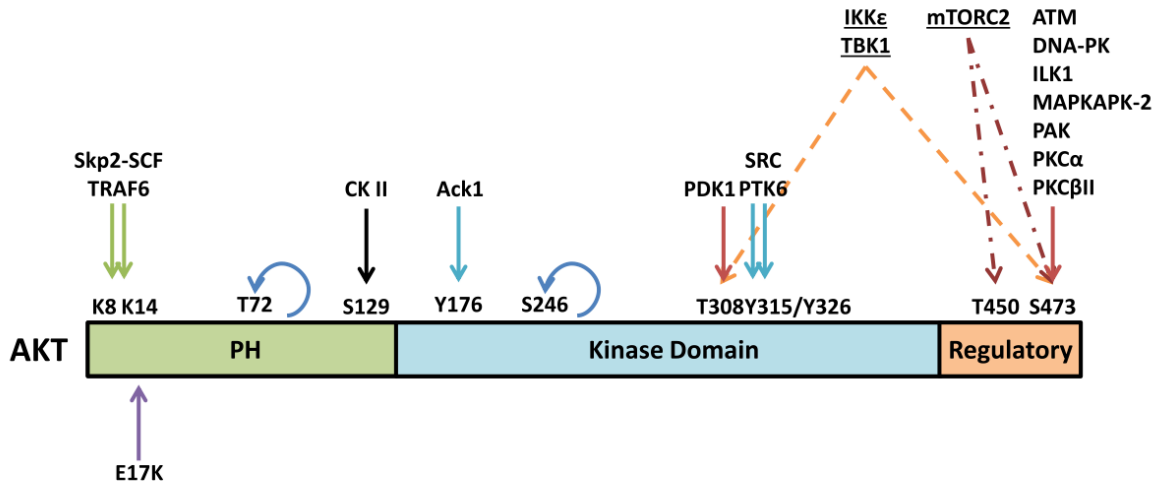

Figure 1.1 AKT domain structure and its regulatory network.

Activation of AKT

It's been well documented that Ras and receptor tyrosine kinases activate PI3K-AKT pathway in both physiological and pathological conditions. It's been proposed that phosphorylation of AKT at both Ser473 and Thr308 and AKT membrane localization are required for full activation of AKT (Manning and Cantley 2007). More than 15 years ago, several groups reported that PDK1 directly phosphorylates AKT at Thr308. Nevertheless, identification of kinases targeting AKT-HM took several years. Mounting evidence suggests that multiple kinases are involved in phosphorylation of AKT at Ser473 in a stimuli-dependent and cell type-specific manner (Figure 1.1 and 1.2). Among those AKT-HM kinases, mTORC2 composed of mTOR, Rictor, Sin1, GβL, and Protor1, is the most fully characterized AKT-HM

kinase and activates AKT by directly phosphorylating AKT at Ser473 when cells are exposed to insulin and other growth factors (Liao and Hung 2010, Vasudevan and Garraway 2010, Zoncu, Efeyan et al. 2011).

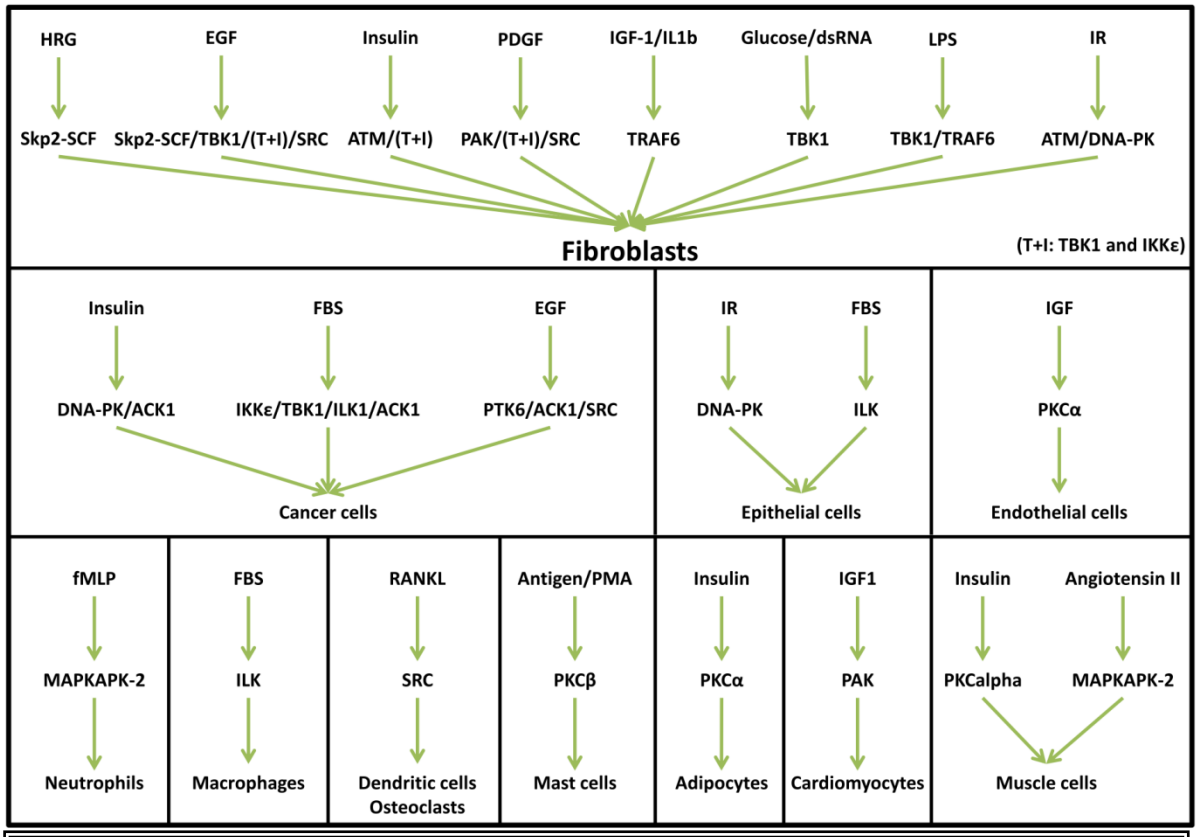

Figure 1.2 Cell-type and stimuli-specific regulation of AKT.

Regulation of AKT by E3 Ubiquitin Ligases

Yang and co-workers found that TRAF6 directly mediates AKT ubiquitination and is indispensible for AKT membrane targeting and activation after IGF-1 stimulation (Yang, Wang et al. 2009). Overexpression of TRAF6 enhances K63-linked ubiquitination of AKT in HEK293T cells, and also specifically drives phosphorylation of AKT at Thr308 that leads to the activation of AKT as indicated by GSK3β phosphorylation. *In vitro* ubiquitination experiments

also reveal that TRAF6 is a direct E3 ligase for AKT. Moreover, IGF1-induced AKT ubiquitination and phosphorylation is largely impaired in TRAF6 knockdown and knockout cells. Importantly, suppression of TRAF6 expression by shRNAs reduces tumorigenicity in a xenograft model that uses human PC-3 prostate tumor cells. Substitution of glutamate to lysine on AKT enhances ubiquitination of AKT at the PH domain and inhibits AKT phosphorylation and kinase activity, which is primarily due to promote AKT membrane targeting. Taken together, these findings suggest that TRAF6 is a potential drug target candidate for hyperactivation of AKT signaling.

In addition to TRAF6, Skp2-SCF complex is another E3 ligase directly controlling AKT ubiquitination, membrane localization, and activation (Chan, Li et al. 2012). Interestingly, the Skp2-SCF complex, but not TRAF6, is required for EGF-mediated AKT phosphorylation and activation, suggesting that different growth factor receptors may engage distinct E3 ligases to activate AKT signaling. Similar to TRAF6 deficient cells, AKT ubiquitination and membrane targeting is disrupted in Skp2 knockdown cells, emphasizing that K63-linked ubiquitination is a crucial step for AKT activation. Downregulation of Skp2 by shRNAs results in reduction of glucose uptake and glycolysis *in vitro* and *in vivo*, which has been associated with AKT activity. Loss of Skp2 in the MMTV- HER2 breast mouse model reduces activation of AKT signaling and malignancy. Moreover, higher expression levels of Skp2 are associated with higher AKT phosphorylation and poor prognosis in HER2 positive tumors. Importantly, silencing of Skp2 renders HER2 overexpression cells and tumors sensitive to Herceptin treatment. Taken together, these findings suggest that Skp2 is not only pivotal for the ErbB-mediated AKT activation and oncogenic transformation, but also an emerging diagnostic marker and drug target for HER2-positive breast tumors.

Suppression of AKT

In addition to PIP3 phosphatases, protein phosphatases, PP2A and PHLPP1/PHLPP2, also inhibit AKT activity via direct dephosphorylation. PP2A-mediated dephosphorylation of AKT at Thr308 reduces AKT activity (Sato, Fujita et al. 2000, Ugi, Imamura et al. 2004, Kuo, Huang et al. 2008). However, PHLPP1 and PHLPP2 selectively target AKT isoforms. For example, PHLPP1 preferentially dephosphorylates AKT2 and AKT3, whereas PHLPP2 specifically dephosphorylates AKT1 and AKT3 (O'Neill, Niederst et al. 2013). Nevertheless, how these protein phosphatases are controlled remains not fully understood. AKT activity is also controlled by several negative feedback regulation loops. AKT-mediated mTORC1 activation results in S6K-dependent phosphorylation and degradation of IRS1 protein, which abrogates insulin/IGF1 signaling and thus reduces mTORC2-dependent AKT-Ser473 phosphorylation and AKT activity (Harrington, Findlay et al. 2004, Shah, Wang et al. 2004). Moreover, it's been proposed that S6K also phosphorylates Rictor at Thr1135 to negatively regulate the capability of mTORC2 to phosphorylate AKT at Ser473 (Boulbes, Chen et al. 2010, Julien, Carriere et al. 2010, Treins, Warne et al. 2010). Nevertheless, the physiological significance of the phosphorylation of Rictor-Thr1135 remains largely unknown. Another AKT substrate FOXO1 also participates in the negative feedback loop by controlling the expression of Rictor. Activation of AKT inhibits FOXO1 transcription activity, which suppresses FOXO1-mediated expression of Rictor and thus reduces mTORC2-AKT signaling (Chen, Jeon et al. 2010).

DOWNSTREAM ACTIONS OF AKT

Cell survival and cell cycle

AKT regulates many different cell biological processes by directly targeting more than dozens of downstream substrates. One of the key roles of AKT is the regulation of cell survival by suppressing proapoptotic proteins, such as BAD and pro-caspase-9 (Blume-Jensen, Janknecht et al. 1998, Cardone, Roy et al. 1998). AKT also promotes the cytoplasmic retention of FOXO proteins, which prevents FOXO protein-induced expression of proapoptotic genes, such as TRAIL and TRADD (Zhang, Tang et al. 2011). Furthermore, AKT promotes the progression of cell cycle and cell proliferation by inhibiting p21CIP1, p27KIP1 and GSK3β. Phosphorylation of E3 ligase MDM2 by AKT promotes its nuclear translocation where it mediates ubiquitination and degradation of p53 via a proteasome-dependent mechanism (Liao and Hung 2010, Vasudevan and Garraway 2010). (Figure 1.3)

AKT and mTORC1 signaling

Besides inducing gene transcription, AKT supports protein translation and cell growth mainly through the downstream effector mTORC1. TSC2 and PRAS40 and DEPTOR are known negative regulators of mTORC1, whereas only TSC2 and PRAS40 are AKT immediate substrates (Dan, Sun et al. 2002, Inoki, Li et al. 2002, Potter, Pedraza et al. 2002, Sancak, Thoreen et al. 2007, Thedieck, Polak et al. 2007, Wang, Harris et al. 2007, Peterson, Laplante et al. 2009). Phosphorylation of TSC2 by AKT suppresses its GAP activity toward Rheb, a key component of mTORC1, which leads to accumulation of active GTP-bound Rheb that binds to mTORC1 complex and activates the mTORC1 pathway (Zoncu, Efeyan et al. 2011). PRAS40 was first identified as an AKT substrate, whereas studies later demonstrated that PRAS40 not only inhibits mTORC1 through direct binding, but also acts as mTORC1 substrates (Wang,

Harris et al. 2008). Phosphorylation of PRAS40 by AKT and mTORC1 induces its dissociation from mTORC1 complex, which relieves its inhibitory effect on mTORC1 activity.

AKT and angiogenesis

Phosphorylation of eNOS by AKT promotes nitric oxide secretion and angiogenesis. AKT is not only an important signaling protein downstream of VEGF, but also significantly contributes to expression of VEGF through an mTORC1-HIF1 axis. Therefore, AKT functions as a central hub promoting angiogenesis through feed-forward amplification loops (Vasudevan and Garraway 2010).

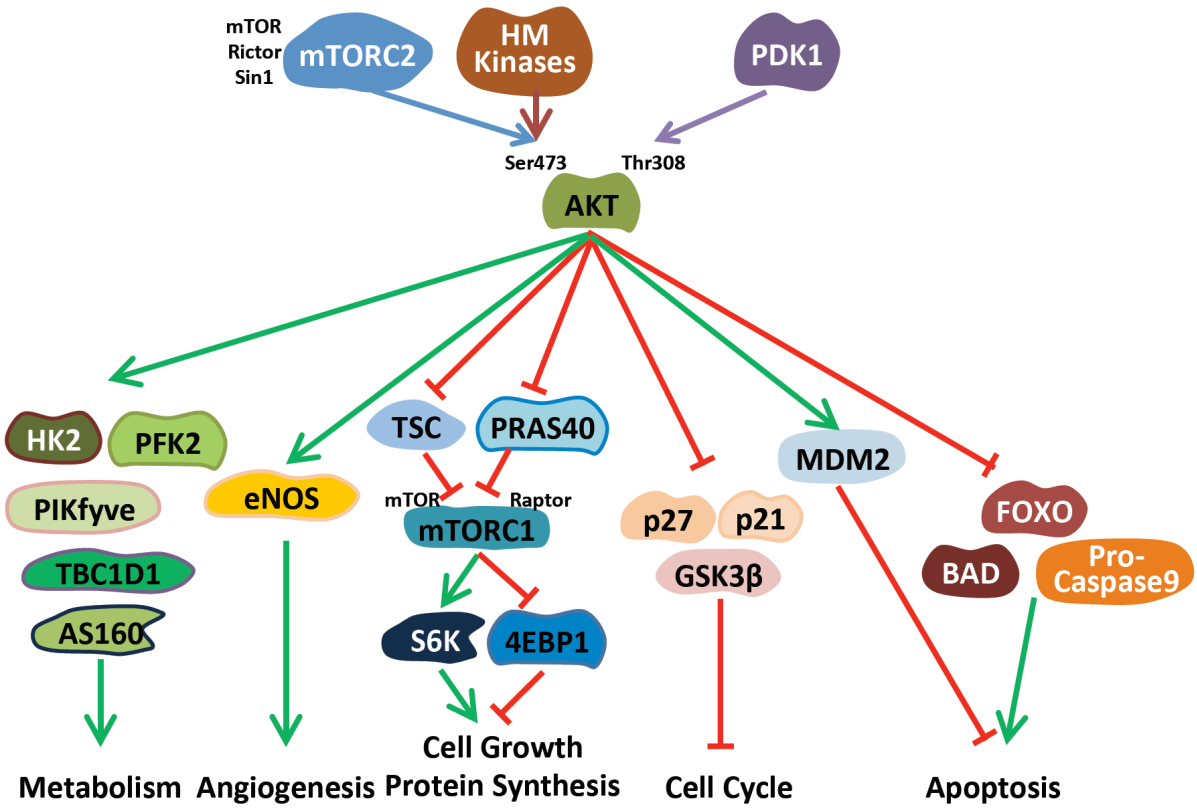

Figure 1.3 AKT signaling networks.

AKT and metabolism

AKT regulates glucose homeostasis by a variety of mechanisms. AKT directly phosphorylates phosphofructokinase 2 (PFK2) to enhance glycolysis (Deprez, Vertommen et al. 1997). AKT also promotes the translocation of glycolytic enzyme hexokinase 2 (HK2) to the outer mitochondrial membrane, which is critical for HK2-dependent glucose phosphorylation and proliferative effects (Wolf, Agnihotri et al. 2011). When adipose tissue and skeletal muscle cells are exposed to insulin, AKT phosphorylates Rab-GTPase-activating protein AS160 (AKT substrate 160KD, also known as TBC1D4) and TBC1D1 to promote glucose uptake by enhancing trafficking of intracellular glucose transporter GLUT4 storage vesicles to the cell surface. Inhibitory AKT phosphorylation on AS160 and TBC1D1 at several sites induces 14-3-3 binding to AS160 and TBC1D1, which suppresses their GAP activities. This leads to the accumulation of GTP-bound Rab, which promotes the trafficking and tethering of GLUT4 storage vesicles to the plasma membrane. Consequently, this robust process increases the level of GLUT4 at the cell surface to import glucose in response to acute insulin exposure (Sano, Roach et al. 2008, Stockli, Fazakerley et al. 2011). Studies from Sano and colleagues reveal that Rab10 is the target of the AS160 and is essential for insulin-induced translocation of GLUT4 to the plasma membrane in adipocytes (Sano, Eguez et al. 2007, Sano, Roach et al. 2008). Besides AS160, the phosphoinositide 3P-5-kinase PIKfyve is also an AKT substrate that has been linked to GLUT4 translocation and glucose uptake. Phosphorylation of PIKfyve by AKT may facilitate the sorting of GLUT4 from internalized endosomes into GLUT4 storage vesicles (Berwick, Dell et al. 2004, Welsh, Hers et al. 2005).

In addition to GLUT4, another widely distributed glucose transporter GLUT1 is also regulated by AKT signaling at the transcription level. Zhou and colleagues suggest that TBC1D1

may contribute to the expression of GLUT1 gene through the AKT downstream effector mTORC1 (Zhou, Jiang et al. 2008). In TSC2 mutant cells, hyperactive mTORC1 up-regulates the expression of GLUT1 gene and glucose uptake. Interestingly, expression of GLUT1 also elevates mTORC1 activity by a TSC2 and AMPK-independent mechanism, suggesting that there is a novel feed-forward amplification loop between mTORC1 and GLUT1 (Buller, Loberg et al. 2008, Buller, Heilig et al. 2011). Furthermore, mTORC1-mediated up-regulation of HIF1 also contributes to GLUT1 expression in Peutz-Jeghers syndrome patients and LKB1-deficient mice (Shackelford, Vasquez et al. 2009).

As mentioned previously, AKT2 is preferentially expressed in insulin responsive tissues such as liver, kidney, heart and skeletal muscle, which indicates that AKT2 may play an important role in insulin signaling. AKT2 deficient mice show significant diabetic phenotype, including insulin resistance, glucose intolerance, and reduced level of circulating leptin (Cho, Mu et al. 2001, Garofalo, Orena et al. 2003). It's been reported that mutation of AKT2 contributes to severe insulin resistance and diabetes in humans (George, Rochford et al. 2004). However, AKT1 or AKT3 knockout mice do not display any significant diabetic phenotype. Instead, AKT1 deficient mice show growth retardation, which phenocopies the mice growing in an mTORC1 suppressive background. Brains of AKT3 knockout mice are smaller compared to the wild-type mice (Hay 2011).

AKT pathway in cancer

Frequent activation of AKT signaling has been found in more than 50% of human cancer (Altomare and Testa 2005). Among all three AKT isoforms, AKT2 is the only one frequently amplified or overexpressed in human tumors (Stephens, Tarpey et al. 2012). However, activating mutation of RTK (e.g EGFR and HER2), Ras and PI3K, and inactivation of tumor suppressor (e.g. PTEN and NF1/2) in human cancer all leads to the activation of AKT. Although it's quite uncommon that mutation of AKT results in cancer, several studies identified somatic mutation on the AKT PH domain, indicating that the AKT (E17K) mutation found in human cancers promotes anchorage-independent growth and cellular transformation. This oncogenic AKT (E17K) mutant is constitutively activated and localized to the plasma membrane. Of note, membrane recruitment of this mutant is resistant to the inhibition of PI3K by LY2940002 (Carpten, Faber et al. 2007, Sasaki, Okuda et al. 2008, Boormans, Korsten et al. 2010, Do, Salemi et al. 2010, Poduri, Evrony et al. 2012, Salhia, Van Cott et al. 2012).

TBK1/ IKKε SIGNALING NETWORK

The atypical IκB kinase family members TANK-Binding Kinase 1 (TBK1 as known as NAK and T2K) and its analog IκB kinase ε (IKKε as known as IKKi), share 61% sequence identity at the amino acid level, and have been defined as a central hub in cell regulatory networks responsive to inflammatory cytokines and pathogen surveillance receptors. The role of TBK1 and IKKε in innate immune response is originally reported as central modulators regulating the transcriptional activity of interferon regulatory factor 3/7 (IRF3/7) host defense gene expressions. TBK1 is constitutively expressed in normal cells and highly up-regulated in a panel of human tumor samples and cancer cell lines, whereas IKKε expresses is an immediate

early gene product in response to LPS, viruses, and cytokines. After viral or bacterial infection, TBK1 and IKKε phosphorylate several residues at the c-terminal regions of IRF3, and then activated and dimerized IRF3 translocates into the nucleus to induce the transcription of interferon and interferon-stimulated genes to mediate innate immune and antiviral responses to defend a host (Fitzgerald, McWhirter et al. 2003, Hacker and Karin 2006, Hiscott 2007, Kawai and Akira 2007, Chau, Gioia et al. 2008).

Roles of TBK1 and IKKε in innate immune response

TBK1 are IKKε were initially identified as upstream kinases regulating NF-κB activity via genetic and biochemical experiments. At developmental stage E14.5, TBK1 knockout mice show severe liver degeneration, which photocopys p63, IKKβ and NEMO knockout mice (Beg, Sha et al. 1995, Li, Van Antwerp et al. 1999, Pomerantz and Baltimore 1999, Bonnard, Mirtsos et al. 2000, Rudolph, Yeh et al. 2000, Tojima, Fujimoto et al. 2000). Overexpression of TBK1 and IKKε also induce NF-κB activity and phosphorylation of p65 at Ser536 (Buss, Dorrie et al. 2004). However, in TBK1 and IKKε (but not IKKα and IKKβ) single knockout MEFs, classical NF-κB response remains intact with respect to degradation of IκB and DNA binding activity of NF-κB. Of note, a small group of NF-κB target genes is still affected in TBK1 or IKKε knockout MEFs (Bonnard, Mirtsos et al. 2000). In stimulated T cells, IKKε phosphorylates p65 at Ser468 and leads to activation of NF-κB signal (Mattioli, Geng et al. 2006). These data suggests that TBK1 and IKKε may partially contribute to NF-κB by regulating transcription of a specific set of NF-κB downstream genes in some type of cells or tissues. However, there is no doubt that TBK1 and IKKε mainly contribute to the innate immunity by regulating transcription factors IRF3 and IRF7.

Pathogen surveillance sensors and adaptors are required for proper innate immune responses and also participate in the regulation of TBK1 and IKKε activity. For example RIG-1 and MDA-5 are well-known cytosolic RNA sensors that activate TBK1 and IKKε through mitochondrial adaptor MAVS-TRAF3 or MAVS-STING pathways. Upon association with MAVS, STING, a mitochondria and ER protein, may function as a scaffold protein to recruit TBK1 and IRF3(Arnoult, Soares et al. 2011). TLR3 is localized at the endosomes and senses dsRNA, whereas TLR4 is a plasma membrane protein responding to bacterial LPS. Both ligand-bound TLRs recruit TRIF-TRAF3 to activate TBK1 and IKKε (O'Neill 2008). Cytosolic DNA sensors, DAI and RNA polymerase III activate TBK1 in a STING-dependent manner (Takaoka, Wang et al. 2007, Ablasser, Bauernfeind et al. 2009, Chiu, Macmillan et al. 2009, Ishikawa, Ma et al. 2009). Clearly, scaffolding proteins, such as TRAF3, STING, TANK, NAP1, and SINTBAD, play an important role in promoting TBK1 and IKKε activity in response to pathogens (Chau, Gioia et al. 2008, Bowie 2012). The DEAD-box helicase 3 (DDX3) inhibited by some viruses is also critical for TBK1 and IKKε-mediated innate immunity (Schroder, Baran et al. 2008, Soulat, Burckstummer et al. 2008). Moreover, association of TBK1 with autophagy adaptors, including p62, NDP52, and optineurin, contributes to the autophagic clearance of bacteria (Weidberg and Elazar 2011). There are several negative regulators involved in TBK1-IRF3 axis, including SHIP2, SIKE, CYLD, and A20 (Zhao 2013). However, TBK1-mediated signal transduction in both physiological and pathological settings remains largely unknown.

TBK1 in cancer

TBK1 is highly expressed in sarcoma, lung, breast, ovarian tumors, and mutation of TBK1 has been reported in a wide range of human malignancies, including glioblastoma, breast,

colon, uterine, and lung cancer (Cerami, Gao et al. 2012) (Figure 1.4). Nonetheless, it remain unclear what is the impact of those mutations on the function of TBK1 in tumorigenesis, although it has been reported that heterozygous TBK1 mutations diminish TLR3 immunity and cause herpes simplex encephalitis in childhood (Herman, Ciancanelli et al. 2012). TBK1 has been reported to support angiogenesis and malignant transformation (Korherr, Gille et al. 2006, Clement, Meloche et al. 2008, Shen and Hahn 2011). Our laboratory has reported that the RalB/Sec5 effector complex directly recruits and activates TBK1 in TLR-mediated innate immune responses. Moreover, cancer cells hijack this RalB/Sec5/TBK1 pathway to deflect apoptosis. In this disease setting, depletion of TBK1 or Sec5 is selectively toxic. RalB activation promotes TBK1/Sec5 assembly and phosphorylation of Sec5 by TBK1. Furthermore, studies using TBK1 knockout MEFs shows that TBK1 is required for fibroblasts to tolerate acute oncogenic stress caused by overexpression of K-Ras (Chien, Kim et al. 2006). Functional genomics approach also identified the dependency of TBK1 on K-Ras-driven cancer, indicating that a group of K-Ras-expressed lung cancer cell lines are highly addicted to a TBK1-mediated survival pathway and that TBK1-driven NF-κB activation is required for the survival of this group of tumors (Barbie, Tamayo et al. 2009). TBK1 also contributes to anti-apoptotic signaling by mediating NF-κB-dependent expression of PAI-2 and transglutaminase 2, which suppresses the conversion of pro-caspase 3 to caspase 3 (Delhase, Kim et al. 2012). Recent findings also indicate that TBK1 signals to a noncanonical NF-κB pathway through TAX1BP1/NDP52-modulated autophagy, which promotes cell survival and proliferation (Newman, Scholefield et al. 2012). (Figure 1.5)

Cancer	TBK1 Mutations									
Brain	V39L	G99R	L281I	A535T	K691N					
Breast	D13E	R72S	D296H							
Colon	W9*	F56C	S206I	M263V	S347Y	R357*	T389I	D407Y	G410R	S632L
Head and Neck	Q660H									
Lung	V58M	L59F	S151F	K323N	S510I	Q553E	K691N			
Ovarian	R525S									
Skin	R25C	P90S	P182L	S398F	G420A	E653Q				
Thyroid	A22P									
Endometrium	R25C	K65E	(F112L, L281I)	R143C	F158C	K461N	L704F			
Haematopoietic and Lymphoid tissues	R117*	Y185C	I334L	E643(IF-D)	N652(IF-D)					
Pancreas	V458A	F663L								
Kidney	G106V									
Urinary Tract	E561K									
Stomach	R357*					(*: nonsense mutation)				

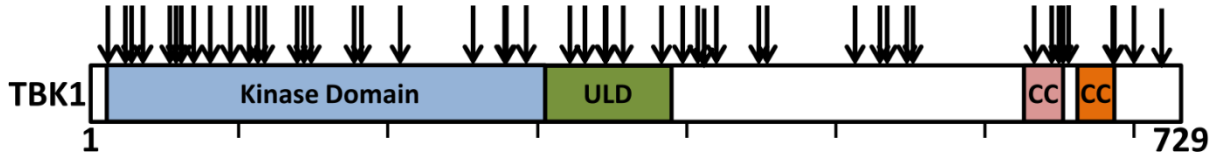

Figure 1.4 TBK1 domain structure and mutations of TBK1 found in human cancers. Arrows indicate individual mutations. (IF-D: in-frame deletion)

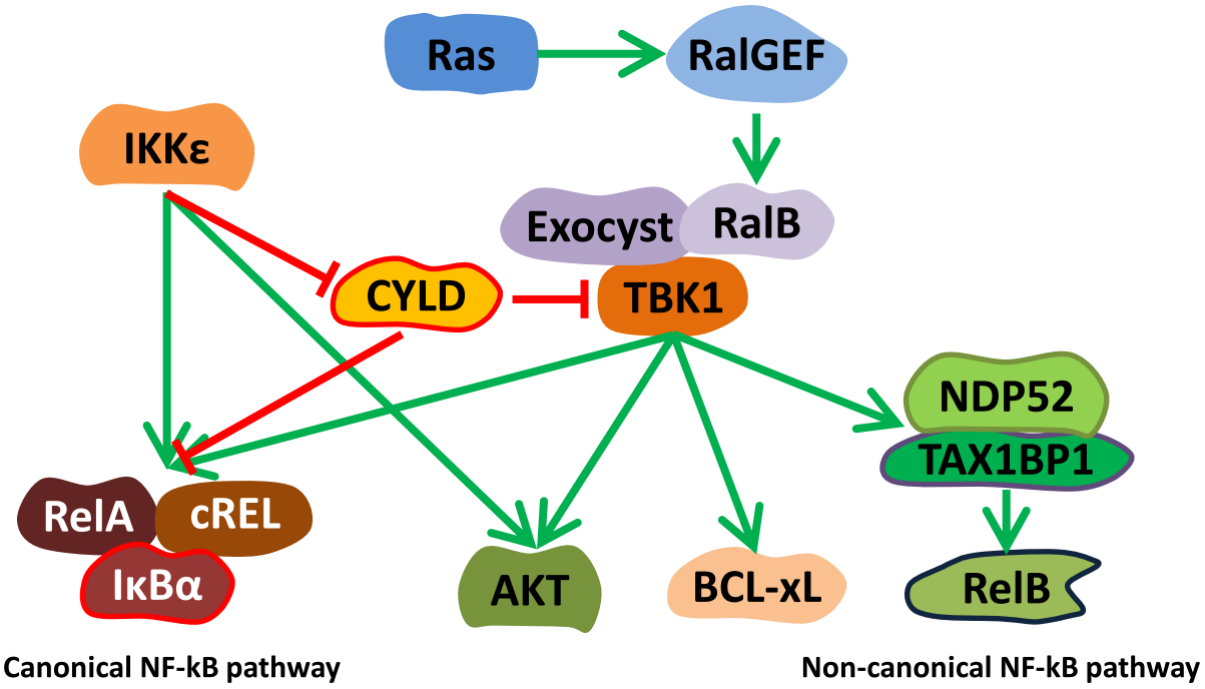

Figure 1.5 TBK1 signaling networks.

CHAPTER TWO

TBK1 DIRECTLY ENGAGES AKT/PKB SURVIVAL SIGNALING TO SUPPORT ONCOGENIC TRANSFORMATION

INTRODUCTION

The atypical IκB kinase family member TBK1 (TANK-binding kinase 1) has been defined as a principle hub in cell regulatory networks responsive to inflammatory cytokines and pathogen surveillance receptors (Fitzgerald, McWhirter et al. 2003, Hacker and Karin 2006, Kawai and Akira 2007). Together with its homologue IKKε, TBK1 marshals the IRF3 and IRF7 transcription factors to induce type I interferon expression and activation of other components of the immediate early host defense response. As such, TBK1 and IKKε are required elements of innate immune signaling in most epithelia and stromal cell types (Hacker and Karin 2006, Hiscott 2007, Kawai and Akira 2007, Chau, Gioia et al. 2008).

In cancer cells, pathological TBK1 activation supports oncogenic transformation by suppressing a programmed cell death response to oncogene activation (Bodemann and White 2008). TBK1 kinase activity is engaged by Ras through the RalGEF-RalB-Sec5 effector pathway, is elevated in transformed cells, and is required for their survival in culture (Chien, Kim et al. 2006, Korherr, Gille et al. 2006). Systematic RNAi screens of diverse tumor-derived cell lines confirmed that a codependent relationship between oncogenic Ras and the RalB/Sec5/TBK1 pathway is conserved in a variety of disease settings (Barbie, Tamayo et al. 2009).

While IRF3 is a direct TBK1 substrate that clearly accounts for much of the role of TBK1 in support of innate immune signaling (Fitzgerald, McWhirter et al. 2003, Sharma, tenOever et al. 2003), TBK1 substrates that mediate cancer cell survival are ill defined. Studies employing IRF3$^{-/-}$ MEFs or RNAi-mediated IRF3 depletion from cancer cell lines indicated this canonical TBK1 substrate is not an obligate component of TBK1-driven cell survival signaling (Chien, Kim et al. 2006, Barbie, Tamayo et al. 2009), but may be important for pro-angiogenic signaling (Korherr, Gille et al. 2006). Using TBK1$^{-/-}$ cells to parse TBK1-dependent Ras-induced regulatory events, we found TBK1 is required for oncogenic Ras activation of AKT and concomitant mTOR activation and GSK3β suppression. Insulin-induced AKT activation is intact in TBK1$^{-/-}$ MEFs, however TLR4, TLR3, EGFR and glucose-induced AKT activation is impaired. In human epithelial cells, these TBK1-dependent signals recruit endogenous TBK1 to the exocyst where it activates AKT. Furthermore, TBK1 depletion impairs both mitogen and oncogene activation of AKT in human cells. We find that TBK1 directly interacts with AKT and is sufficient to drive both activation loop, T308, and hydrophobic motif, S473, phosphorylation in cells and within an *in vitro* biochemical reconstitution system. Consistent with these observations, TBK1 activation of AKT in cells can occur in the absence of the canonical AKT-T308 and AKT-S473 kinases, PDK1 and mTORC2. Loss of TBK1 is toxic to most, but not all oncogenic Ras expressing tumor lines *in vitro* and *in vivo*, and this toxicity can be rescued by expression of mutationally activated AKT. A novel chemical inhibitor of TBK1 kinase activity, with potency in the nanomolar range, was isolated from a 250,000 compound screen. This 6-aminopyrazolopyrimidine derivative is selectively toxic to TBK1-dependent cancer cell lines.

Furthermore, the compound can inhibit AKT activation in these cells without affecting the canonical AKT activators PDK1 or mTOR. Thus AKT likely represents a bona fide TBK1 substrate protein that mediates TBK1-dependent signaling in normal and tumorigenic contexts. The phenotypic concordance of TBK1 homozygous deletion, RNAi-mediated TBK1 depletion and pharmacological inhibition of TBK1 kinase activity reveals TBK1 as a targetable link supporting context-selective mobilization of the AKT regulatory network.

RESULTS

Previous observations that TBK1$^{-/-}$ MEFs fail to support oncogenic Ras-induced transformation, at least in part due to survival defects (Chien, Kim et al. 2006), prompted us to examine survival pathway activation in this setting. As expected, lentiviral-mediated transient expression of K-RasG12V in wild-type mouse embryo fibroblasts resulted in excess AKT activation as indicated by accumulation of activation site phosphorylation (Downward 2003, Mitin, Rossman et al. 2005, Manning and Cantley 2007). In contrast, despite equivalent K-RasG12V expression, TBK1$^{-/-}$ MEFs did not support AKT activation by oncogenic Ras (Figure 2.1A). Selection of stable populations of wild-type and TBK1$^{-/-}$ MEFs, with similar amounts of K-RasG12V expression, showed marked differences in the formation of growth transformed foci, accumulation of active AKT, and concomitant engagement of the mTOR pathway (Figure 2.1B). Transient siRNA-mediated TBK1 depletion in human osteosarcoma cells and telomerase-immortalized airway epithelial cells with multiple independent siRNAs resulted in reduced accumulation of active AKT as

compared to controls (Figure 2.1C). Collectively, these observations suggest TBK1 supports AKT pathway activation in multiple regulatory contexts.

We have previously defined the heterooctameric Sec6/8 a.k.a. exocyst complex as a hub for Ras activation of TBK1 via the RalB effector pathway (Moskalenko, Henry et al. 2002, Chien and White 2003, Chien, Kim et al. 2006). A protein/protein interaction map, generated by saturating genome-wide yeast two-hybrid screens of each human exocyst subunit against a human placenta library, identified AKT1 and AKT2 interactions with two distinct exocyst subunits- Exo70 and Sec3 (Figure 2.1D). The association of AKT with the exocyst was validated by expression co-IP (Figure 2.1E) as well as recovery of native exocyst components from endogenous AKT immunoprecipitates (see Figure 3D). The functional relevance of this association is suggested by impaired accumulation of active AKT upon Sec3 depletion from U2OS cells (Figure 2.1C). Immunoprecipitates of native exocyst complexes from multiple cell types selectively coprecipitated endogenous TBK1 versus the closely related family member, IKKε, further implicating TBK1 and the exocyst in AKT activation (Figure 2.1F).

Figure 2.1

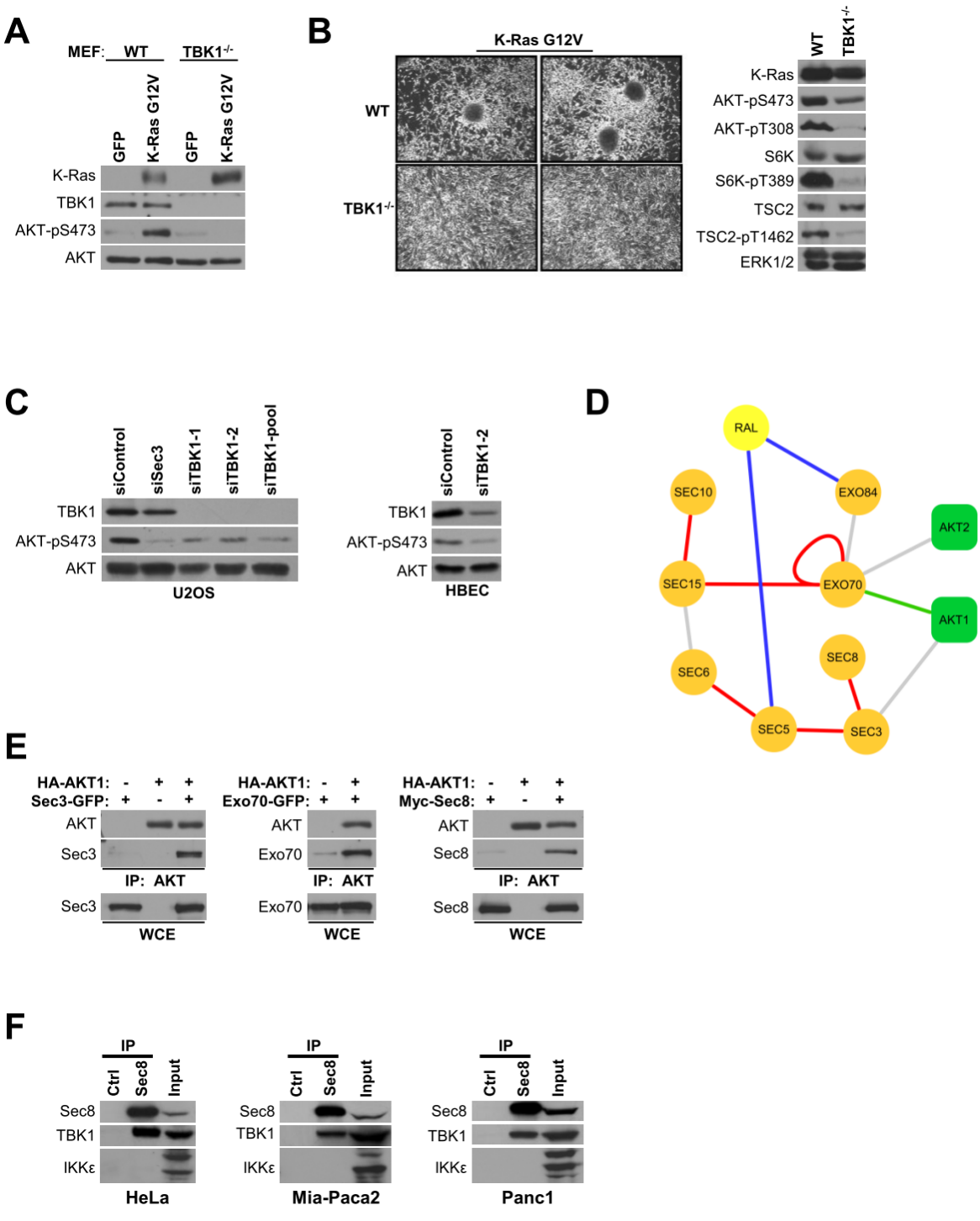
A
MEF: WT TBK1-/-
GFP
K-Ras G12V
GFP
K-Ras G12V
K-Ras
TBK1
AKT-pS473
AKT
B
K-Ras G12V
WT
TBK1-/-
WT
TBK1-/-
K-Ras
AKT-pS473
AKT-pT308
S6K
S6K-pT389
TSC2
TSC2-pT1462
ERK1/2
C
siControl
siSec3
siTBK1-1
siTBK1-2
siTBK1-pool
TBK1
AKT-pS473
AKT
U2OS
siControl
siTBK1-2
TBK1
AKT-pS473
AKT
HBEC
D
RAL
SEC10
EXO84
AKT2
SEC15
EXO70
AKT1
SEC6
SEC8
SEC5
SEC3
E
HA-AKT1: - + +
Sec3-GFP: + - +
AKT
Sec3
IP: AKT
Sec3
WCE
HA-AKT1: - +
Exo70-GFP: + +
AKT
Exo70
IP: AKT
Exo70
WCE
HA-AKT1: - + +
Myc-Sec8: + - +
AKT
Sec8
IP: AKT
Sec8
WCE
F
IP
Ctrl
Sec8
Input
Sec8
TBK1
IKKε
HeLa
IP
Ctrl
Sec8
Input
Sec8
TBK1
IKKε
Mia-Paca2
IP
Ctrl
Sec8
Input
Sec8
TBK1
IKKε
Panc1

Figure 2.1. TBK1 and the exocyst support AKT activation.

(A) Wild-type (WT) and TBK1 homozygous null ($TBK1^{-/-}$) mouse embryonic fibroblasts (MEF) were infected with lentivirus encoding GFP or K-RasG12V (Chien, Kim et al. 2006). Five days post-infection, whole cell lysates were prepared and relative accumulation of AKT-pS473, total K-Ras, TBK1, and AKT was assessed by immunoblot. (Approximate detected molecular size: K-Ras, 21KDa; TBK1, 84KDa; AKT, 60KDa; AKT-pS473, 60KDa; AKT-pT308, 60KDa)

(B) WT and $TBK1^{-/-}$ MEFs with equivalent stable expression of K-Ras G12V were seeded at low density and grown to confluence under standard culture conditions. Representative bright field images of monolayer cultures are shown (left panels). Whole cell lysates were probed by immunoblot for the indicated proteins and selectively phosphorylated proteins (right panels). In addition to evaluation of AKT phosphorylation, the AKT substrate site on TSC2 (T1462) and the mTor-responsive site on p70S6K (T389) were evaluated as shown. ERK1/2 is shown as a loading control. (Approximate detected molecular size: AKT-pT308, 60KDa; S6K, 70KDa; S6K-pT389; TSC2, 200KDa; TSC2-pT1462, 200KDa; ERK1/2, 42/44KDa; others as described above)

(C) U2OS and HBEC cells were transfected with the indicated siRNAs. Seventy-two hours post transfection, whole cell lysates were assessed for TBK1 expression and accumulation of phosphorylated AKT as indicated. (Detected molecular sizes were as described above).

(D) The exocyst/Ral/AKT protein-protein interaction network as derived from whole-genome yeast two-hybrid screens. Edges are colored according to the confidence score attributed to each interaction in the screens (confidence score is detailed in (Formstecher, Aresta et al. 2005)): red = A, blue = B, green = C, grey =D scores.

(E) HEK293T cells were transfected with the indicated constructs. 48 hours post transfection, AKT was immunoprecipitated using anti-HA beads and coprecipitating proteins were detected as indicated. Mammalian expression constructs encoding Sec3-GFP, Exo70-GFP, Myc-Sec8 and HA-AKT were transfected into HEK293T cells as indicated. IP indicates immunoprecipitation. WCE indicates whole cell extract. (Molecular size: Sec3, 102KDa; Exo70, 78KDa; Sec8, 110KDa; others as described above)

(F) Endogenous Sec8 was immunoprecipitated from the indicated cell lines using anti-Sec8 monoclonal antibodies. Immunoprecipitates were probed for endogenous TBK1 or IKKε as indicated. Anti-Myc monoclonal antibodies were used as a specificity control (Ctrl). (Molecular size: IKKε, a triplet centered on 80KDa; others as described above)

To assess the context-selective contribution of TBK1 to AKT activation, we evaluated the responsiveness of TBK1$^{-/-}$ cells to a variety of germane AKT pathway agonists (Figure 2.2). We found that AKT was equivalently responsive to insulin in both wild-type and TBK1$^{-/-}$ MEFs, indicating that insulin-induced AKT activation is TBK1-independent (Figure 2.2A). In contrast, AKT-responsiveness to EGF or glucose was impaired in the absence of TBK1 (Figure 2.2B,D). In addition, AKT-responsiveness to innate immune pathway activation by either Sendai virus infection or LPS exposure was severely blunted in the absence of TBK1 as compared to wild-type MEFs (Figure 2.2F). Complementation of TBK1$^{-/-}$ MEFs using human wild-type TBK1 rescued AKT activation by EGF and glucose (Figure 2.2C,E). We did not observe activation of IFNβ expression, a canonical TBK1 effector pathway, in response to EGF or glucose reexposure in these cells (Figure 2.2G). However, TBK1$^{-/-}$ MEFs were refractory to EGF-induced proliferation (Figure 2.2H) and sensitized to apoptosis upon serum or glucose withdrawal (Figure 2.2I). Together, these observations reveal a stimulus-selective contribution of TBK1 to AKT pathway activation.

Figure 2.2

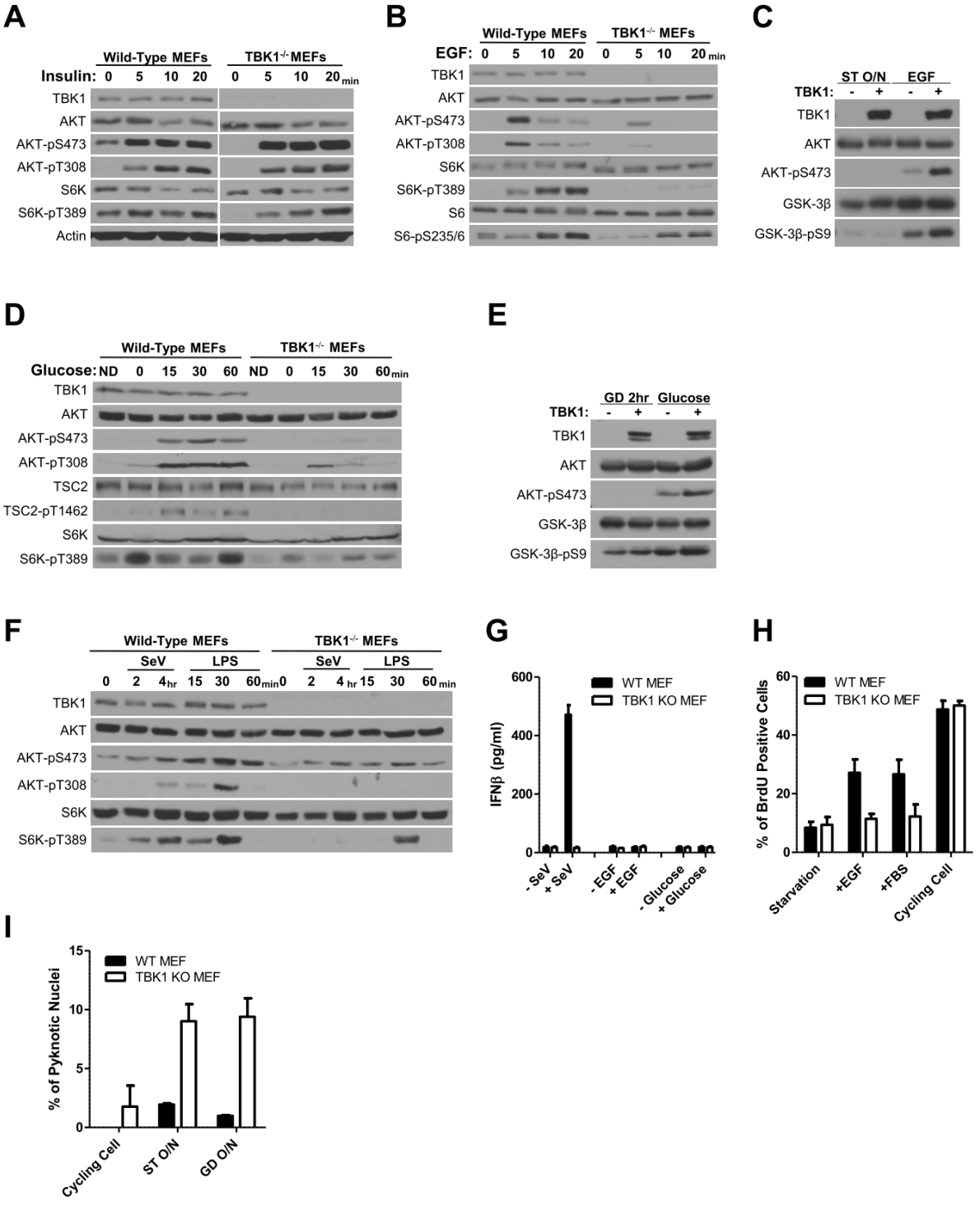
A
Wild-Type MEFs
TBK1-/- MEFs
Insulin: 0 5 10 20 0 5 10 20 min
TBK1
AKT
AKT-pS473
AKT-pT308
S6K
S6K-pT389
Actin
B
Wild-Type MEFs
TBK1-/- MEFs
EGF: 0 5 10 20 0 5 10 20 min
TBK1
AKT
AKT-pS473
AKT-pT308
S6K
S6K-pT389
S6
S6-pS235/6
C
ST O/N
EGF
TBK1: - + - +
TBK1
AKT
AKT-pS473
GSK-3β
GSK-3β-pS9
D
Wild-Type MEFs
TBK1-/- MEFs
Glucose: ND 0 15 30 60 ND 0 15 30 60 min
TBK1
AKT
AKT-pS473
AKT-pT308
TSC2
TSC2-pT1462
S6K
S6K-pT389
E
GD 2hr
Glucose
TBK1: - + - +
TBK1
AKT
AKT-pS473
GSK-3β
GSK-3β-pS9
F
Wild-Type MEFs
TBK1-/- MEFs
SeV
LPS
SeV
LPS
0 2 4hr 15 30 60min 0 2 4 hr 15 30 60 min
TBK1
AKT
AKT-pS473
AKT-pT308
S6K
S6K-pT389
G
WT MEF
TBK1 KO MEF
IFNβ (pg/ml)
600
400
200
0
- SeV
+ SeV
- EGF
+ EGF
- Glucose
+ Glucose
H
WT MEF
TBK1 KO MEF
% of BrdU Positive Cells
60
40
20
0
Starvation
+EGF
+FBS
Cycling Cell
I
WT MEF
TBK1 KO MEF
% of Pyknotic Nuclei
15
10
5
0
Cycling Cell
ST O/N
GD O/N

Figure 2.2. Selective contribution of TBK1 to stimulus-dependent AKT activation.

(A) Wild-type and TBK1$^{-/-}$ MEFs were incubated overnight in the absence of serum and then treated with insulin (1 μg/ml) as indicated. Whole cell extracts were probed for the indicated proteins and selectively phosphorylated proteins. Actin is shown as a loading control. (Molecular size: Actin, 45KDa; others as described)

(B) Wild-type and TBK1$^{-/-}$ MEFs were incubated overnight in the absence of serum and then treated with EGF (100 ng/ml) as indicated. Whole cell extracts were probed as in (A). (Molecular size: S6, 32KDa; S6-pS235/6, 32KDa; others as described)

(C) TBK1$^{-/-}$ MEFs were infected with lentivirus encoding GFP or TBK1. Cell were starved without serum overnight (ST O/N) and then treated with EGF (100 ng/ml) as indicated. Whole cell extracts were probed as in (A). The AKT substrate site on GSK3β (S9) was evaluated as an indication of AKT pathway activation. (Molecular size: GSK-3β, 46KDa; GSK-3β-pS9, 46KDa; others as described)

(D) Wild-type and TBK1$^{-/-}$ MEFs were incubated cells in DMEM with 10% serum but without glucose for 2 hours followed by addition of 25 mM glucose as indicated. Whole cell extracts were probed as in (A). ND indicates the normal DMEM control. (Molecular size: as described)

(E) TBK1$^{-/-}$ MEFs were infected with lentivirus encoding GFP or TBK1. Cells were incubated in DMEM with 10% serum but without glucose for 2 hours (GD 2hr) followed by addition of 25mM glucose as indicated. Whole cell extracts were probed as in (A). (Molecular size: as described)

(F) Wild-type and TBK1$^{-/-}$ MEFs were either exposed to Sendai virus (SeV, 100 HA/ml) or treated with LPS (1 μg/ml) as indicated. Whole cell extracts were probed as in (A). (Molecular size: as described)

(G) WT and TBK1$^{-/-}$ MEFs were either maintained in the presence of serum, serum starved, or glucose deprived overnight, and then treated with Sendai virus (SeV, 100 HA/ml), EGF (100 ng/ml), or glucose (25 mM) as indicated. After 19 hours, media was collected for measuring interferonβ accumulation.

(H) WT and TBK1$^{-/-}$ MEFs were either maintained in the presence of serum (cycling cells) or serum starved 44 hr, and then treated with either EGF (100ng/ml) or FBS (10%) as indicated in the presence of BrdU (10 μM). BrdU incorporation is shown as a percentage of total nuclei.

(I) WT and TBK1$^{-/-}$ MEFs were either maintained in the presence of serum (cycling cells), serum starved, or glucose deprived. After 24hr cells were fixed and stained with DAPI. Pyknotic nuclei are shown as a percentage of total nuclei.

To examine the TBK1-AKT relationship in cellular level, we perform immunofluorescence staining. My data suggests that expression of wild-type TBK1 protein in Mia-Paca2 and HCC44 is sufficient to induce the phosphorylation of AKT on Serine 473. However, expression of TBK1 kinase-dead protein slightly reduced phosphorylation of AKT (Figure 2.3).

Figure 2.3

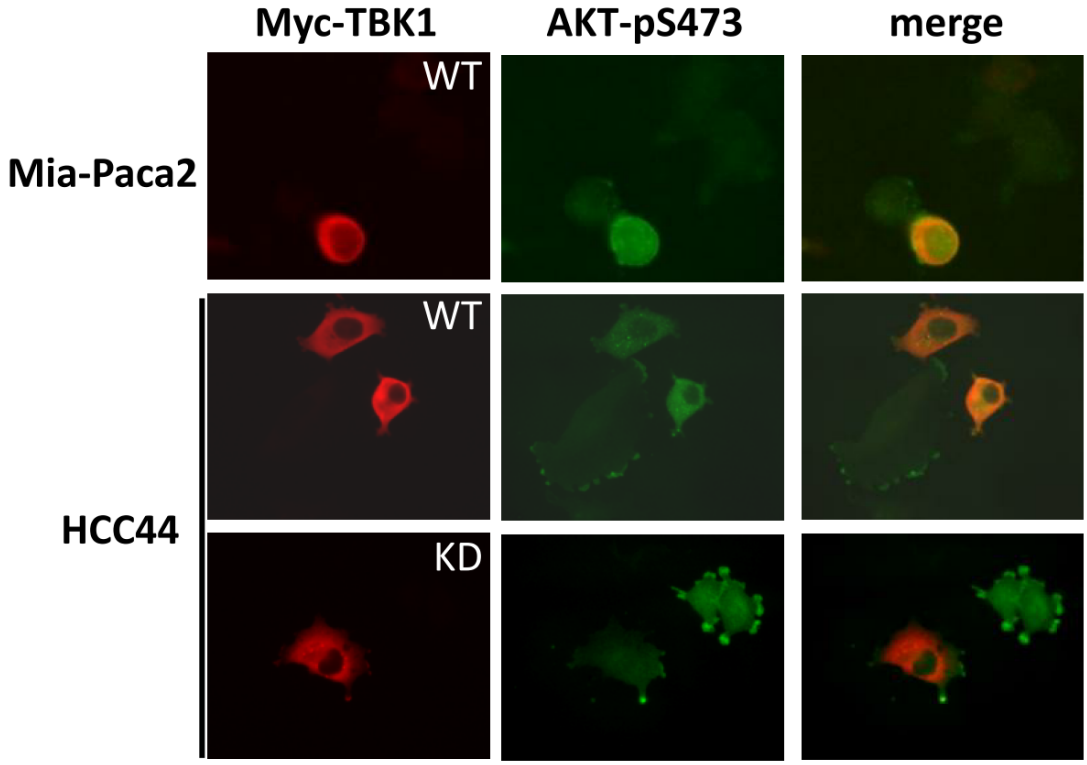

Figure 2.3 TBK1 regulates phosphorylation of AKT at Ser473. Mia-Paca2 and HCC44 cells were transfected with either a wildtype or a kinase-dead mammalian Myc-TBK1 expression vector as indicated. After 24 hours, cells were fixed and stained with anti-Myc (9E10, Santa Crzu) mouse monoclonal antibody and Anti-AKT-pS473 (D9E, Cell Signaling) to view Myc-TBK1 and AKT-pS473.

Examination of full-length and truncated proteins indicated that TBK1 and AKT can be reciprocally isolated in either TBK1 or AKT immunoprecipitates (Figure 2.4A) and that the association in cells is likely mediated through their respective kinase domains (Figure 2.4B,C). To examine native TBK1/AKT complex assembly, we tested the capacity of endogenous AKT to coimmunoprecipitate endogenous TBK1 in response to glucose exposure or innate immune pathway activation- two settings requiring TBK1 for AKT activation as indicated by observations in TBK1$^{-/-}$ MEFs (Figure 2.2). In glucose starved cells, the exocyst but not TBK1 coimmunoprecipitated with AKT. However, glucose stimulation recruited TBK1 to AKT complexes in all 4 human cell lines tested (Figure 2.4D). Sorbitol exposure was used as an osmolarity control (Figure 2.4D, middle top panel). These observations indicate that a population of AKT is constitutively associated with the exocyst, while TBK1 is recruited into the complex in a stimulus-dependent manner. Similarly, Sendai virus infection or LPS exposure drove assembly of native TBK1/AKT complexes (Figure 2.4E).

Figure 2.4

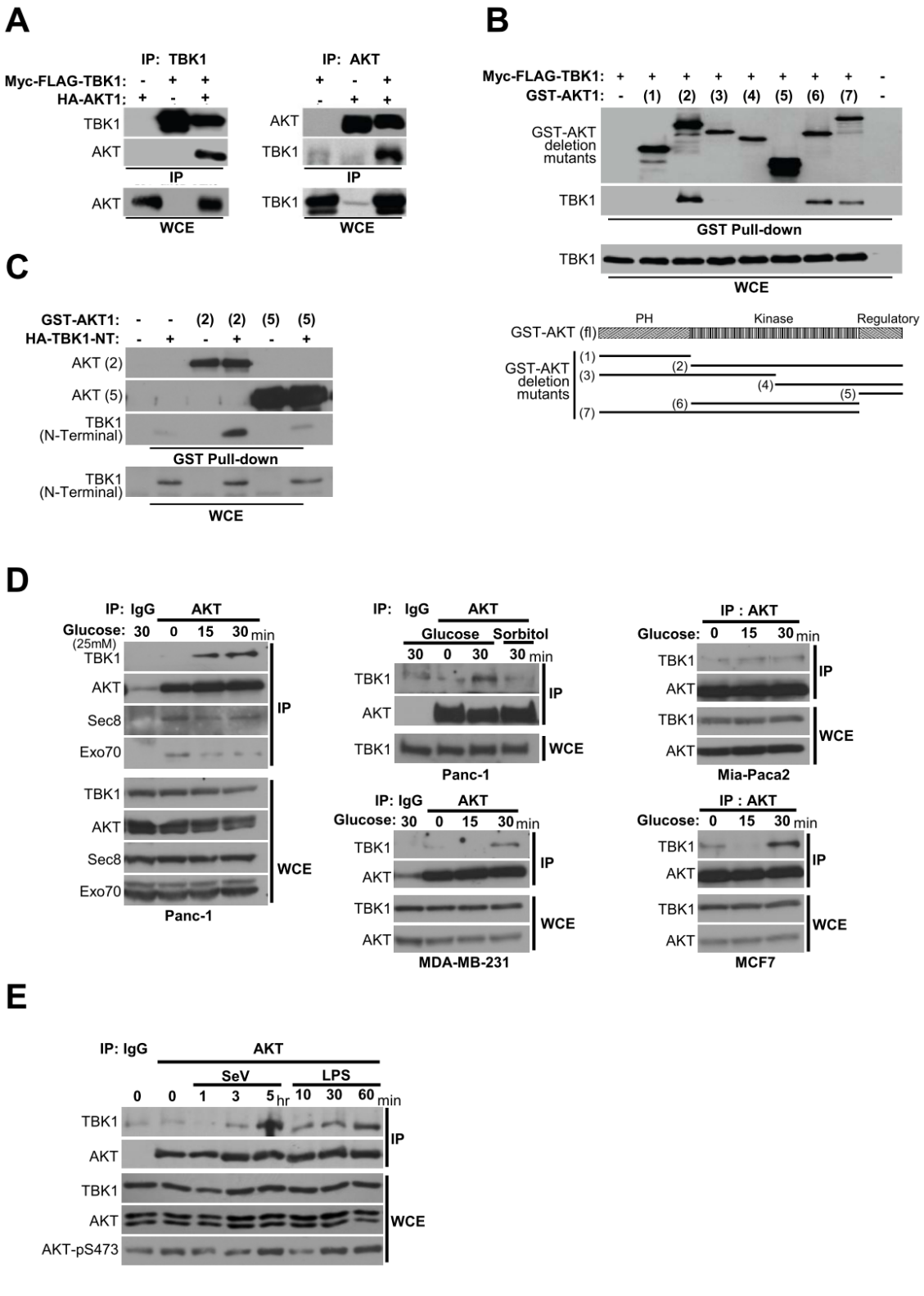
A
IP: TBK1
IP: AKT
Myc-FLAG-TBK1:
HA-AKT1:
TBK1
AKT
IP
WCE
B
Myc-FLAG-TBK1:
GST-AKT1:
GST-AKT deletion mutants
GST Pull-down
WCE
PH
Kinase
Regulatory
GST-AKT (fl)
C
GST-AKT1:
HA-TBK1-NT:
AKT (2)
AKT (5)
TBK1 (N-Terminal)
GST Pull-down
WCE
D
IP: IgG
AKT
Glucose:
(25mM)
Sec8
Exo70
Panc-1
Sorbitol
MDA-MB-231
IP : AKT
Mia-Paca2
MCF7
E
SeV
LPS
AKT-pS473

Figure 2.4. TBK1/AKT complex formation is stimulus-specific.

(A) HEK293T cells were transfected as indicated. Reciprocal co-expression/co-immunoprecipitations are shown. (Molecular size: as previously described)

(B) GST-AKT expression constructs encoding a panel of truncation variants were coexpressed with Myc-FLAG-TBK1 in HEK293T cells. Glutathione-mediated affinity isolation of the AKT variants (GST Pull-down) was used to define a minimally sufficient TBK1 interaction domain as indicated. Whole cell extracts (WCE) are shown as controls for TBK1 expression.

(C) HA-tagged TBK1 amino-terminal fragment (1-242) that encompasses the catalytic domain [TBK1 (N-terminal)] was coexpressed with either GST-AKT expression constructs [AKT(2)] or [AKT(5)]. Affinity isolation of AKT was probed for co-isolation of N-terminal TBK1as in (B).

(D) Panc-1, MDA-MB-231, Mia-Paca2, and MCF7 cells were deprived of glucose for 2 hr followed by incubation with 25 mM glucose or sorbitol as indicated. Endogenous AKT was immunoprecipitated from extracts taken at the indicated time points. Immunoprecipitates were assayed for coprecipitation of the indicated proteins. Normal mouse IgG was used as a control for specificity (IgG lanes). (Molecular size: as described)

(E) H1993 cells were either exposed to Sendai virus (SeV, 100 HA/ml) or treated with LPS (1 μg/ml), and harvested at the indicated time intervals. Co-immunoprecipitation and immunoblot were performed as in (D). Normal mouse IgG was used as a control for specificity (IgG lane). (Molecular size: as described)

Both wild-type and kinase-dead TBK1 associated with AKT, however, only wild-type TBK1 immunoprecipitates contained active AKT, as indicated by serine 473 phosphorylation and *in vitro* kinase activity using a GSK3α/β fusion peptide as substrate (Figure 2.5A). Remarkably, TBK1 expression was sufficient to drive AKT activation in the face of pharmacological inactivation of the PI3K family (Figure 2.5B). Moreover, TBK1 induced AKT activation loop (T308) and hydrophobic motif (S473) phosphorylation in cells in the absence of PDK1 (Figure 2.5C,D) or the mTORC2 subunits Sin1 (Figure 2.5E) or Rictor

(Figure 2.5F). These observations indicate that TBK1 is sufficient to induce AKT activation independently of the canonical PDK1/mTORC2 collaboration (Alessi, James et al. 1997, Sarbassov, Guertin et al. 2005, Guertin, Stevens et al. 2006, Jacinto, Facchinetti et al. 2006, Shiota, Woo et al. 2006, Manning and Cantley 2007, Engelman 2009).

In the presence of ATP and Mg^{++}, purified recombinant TBK1 was sufficient to drive phosphorylation of both T308 and S473 on otherwise inactive recombinant AKT1 *in vitro* (Figure 2.5G). Moreover, this correlated with a 100-fold increase in AKT1 specific activity as detected using a GSK3α/β–derived peptide substrate (Figure 2.5G), and with significant accumulation of phosphorylation of AKT autosubstrate sites (Figure 2.5H) (Li, Lu et al. 2006). Endogenous TBK1 immunoprecipitated from MEFs also directly phosphorylated recombinant AKT (Figure 2.5I). Consistent with a role for TBK1 in EGF-induced AKT activation in MEFs (Figure 2.2B) TBK1 kinase activity was enhanced by EGF stimulation (Figure 2.5I). Similar observations using kinase-dead and wild-type proteins immunopurified from HEK293T cells indicated that TBK1-induced phosphorylation of AKT-T308 and AKT-S473 was dependent upon an intact TBK1 kinase domain, and independent of AKT kinase activity (Figure 2.5J). As expected, TBK1 induction of AKT autosubstrate site phosphorylation only occurred with catalytically intact AKT (Figure 2.5J). Thus, to our knowledge, TBK1 is the first kinase identified as sufficient to directly activate AKT. The disease significance of this non-canonical regulatory arm is suggested by the observation that, in the absence of PDK1, oncogenic Ras signaling to AKT is only partially blunted and the responsiveness of AKT effectors is unaffected (Figure 2.5K).

Figure 2.5

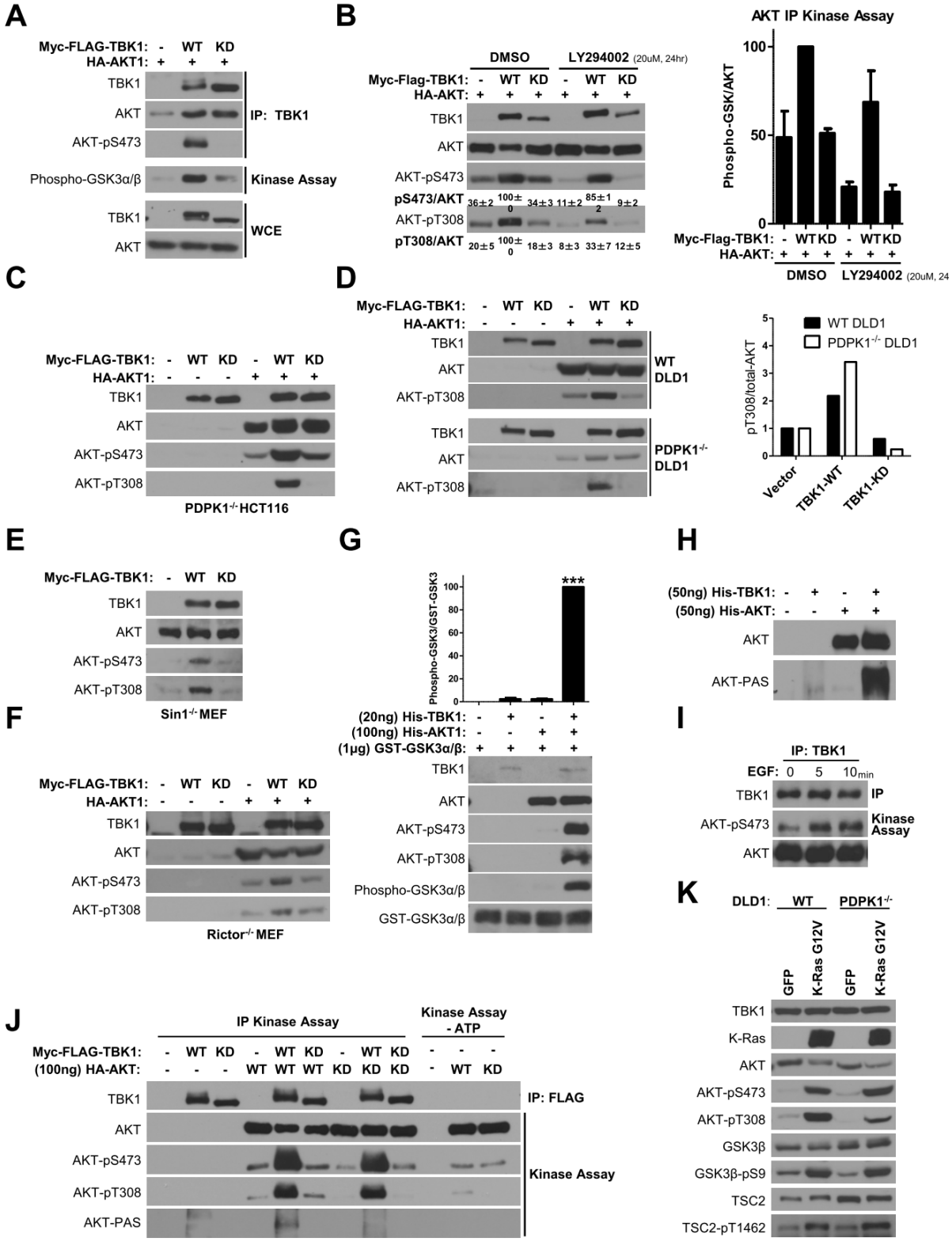
A
Myc-FLAG-TBK1: - WT KD
HA-AKT1: + + +
TBK1
AKT
AKT-pS473
IP: TBK1
Phospho-GSK3α/β
Kinase Assay
TBK1
AKT
WCE
B
DMSO
LY294002 (20uM, 24hr)
Myc-Flag-TBK1: - WT KD - WT KD
HA-AKT: + + + + + +
TBK1
AKT
AKT-pS473
pS473/AKT 36±2 100±0 34±3 11±2 85±12 9±2
AKT-pT308
pT308/AKT 20±5 100±0 18±3 8±3 33±7 12±5
AKT IP Kinase Assay
Phospho-GSK/AKT
100
50
0
Myc-Flag-TBK1: - WT KD - WT KD
HA-AKT: + + + + + +
DMSO
LY294002 (20uM, 24
C
Myc-FLAG-TBK1: - WT KD - WT KD
HA-AKT1: - - - + + +
TBK1
AKT
AKT-pS473
AKT-pT308
PDPK1-/- HCT116
D
Myc-FLAG-TBK1: - WT KD - WT KD
HA-AKT1: - - - + + +
TBK1
AKT
AKT-pT308
WT DLD1
PDPK1-/- DLD1
pT308/total-AKT
WT DLD1
PDPK1-/- DLD1
Vector
TBK1-WT
TBK1-KD
E
Myc-FLAG-TBK1: - WT KD
TBK1
AKT
AKT-pS473
AKT-pT308
Sin1-/- MEF
F
Myc-FLAG-TBK1: - WT KD - WT KD
HA-AKT1: - - - + + +
TBK1
AKT
AKT-pS473
AKT-pT308
Rictor-/- MEF
G
Phospho-GSK3/GST-GSK3
***
(20ng) His-TBK1: - + - +
(100ng) His-AKT1: - - + +
(1μg) GST-GSK3α/β: + + + +
TBK1
AKT
AKT-pS473
AKT-pT308
Phospho-GSK3α/β
GST-GSK3α/β
H
(50ng) His-TBK1: - + - +
(50ng) His-AKT: - - + +
AKT
AKT-PAS
I
IP: TBK1
EGF: 0 5 10min
TBK1
IP
AKT-pS473
Kinase Assay
AKT
J
IP Kinase Assay
Kinase Assay - ATP
Myc-FLAG-TBK1: - WT KD - WT KD - WT KD - - -
(100ng) HA-AKT: - - - WT WT WT KD KD KD - WT KD
TBK1
IP: FLAG
AKT
AKT-pS473
AKT-pT308
Kinase Assay
AKT-PAS
K
DLD1: WT PDPK1-/-
GFP
K-Ras G12V
GFP
K-Ras G12V
TBK1
K-Ras
AKT
AKT-pS473
AKT-pT308
GSK3β
GSK3β-pS9
TSC2
TSC2-pT1462

Figure 2.5. TBK1 directly activates AKT.

(A) Myc-FLAG-tagged TBK1 was immunoprecipitated from HEK293T cells coexpressing HA-tagged AKT. Immunoprecipitates were probed for the presence of AKT and AKT-pS473 (IP). In addition, immunoprecipitates were assayed for AKT kinase activity, *in vitro*, using recombinant GST-GSK3α/β fusion peptides as substrate, and the phospho-GSK-3α/β (Ser21/9) antibody to detect substrate phosphorylation (Kinase Assay). Whole cell extracts (WCE) are shown as expression controls. (Molecular size: phospho-GST-GSK3α/β, 27KDa; others as described)

(B) HEK293T cells transfected as indicated were treated with DMSO or 20 μM LY294002 (PI3K inhibitor) for 24 hr prior to collection of protein extracts. Left panel: Whole cell extracts probed with the indicated proteins are shown. AKT-pS473 and AKT-pT308 signal intensity was quantitated as a percent of total AKT. Values shown are the mean and standard errors from three experiments. Right panel: HA-tagged AKT was immunoprecipitated and AKT kinase activity in the immunoprecipitates was assayed as in (A).Error bars represent standard error from the mean (Right panel). (Molecular size: as described)

(C) PDPK1$^{-/-}$ HCT116 cells were transfected with plasmids encoding HA-AKT1, wild-type (WT) or kinase-dead (KD) TBK1 as indicated. Two days post-transfection, whole cell lysates were assessed for TBK1 and AKT expression, and accumulation of phosphorylated AKT as indicated. (Molecular size: as described)

(D) WT and PDPK1$^{-/-}$ DLD1 cells were transfected and treated as indicated in (C) (Left panel). Accumulation of AKT-pT308 signal intensity was normalized to total AKT signal intensity. Values are presented normalized to vector control (Right Panel). (Molecular size: as described)

(E) Sin1$^{-/-}$ MEFs were transfected with plasmids encoding wild-type (WT) or kinase-dead (KD) TBK1. Two day post-transfection, whole cell lysates were assessed for TBK1 expression and accumulation of phosphorylated AKT as indicated. (Molecular size: as described)

(F) Rictor$^{-/-}$ MEFs were transfected and treated as indicated in (C). (Molecular size: as described)

(Continued)

Figure 2.5. TBK1 directly activates AKT. (Continued)

(G) Recombinant AKT and TBK1 proteins were incubated in kinase buffer with ATP at 30°C as indicated. After 30min incubation, GSK3α/β fusion peptides and additional ATP were added into each reaction at 30°C for an additional 30min. Reactions were separated by SDS-PAGE and immunoblotted to detect the indicated proteins and phosphorylation events. The products of kinase reactions were quantitated from multiple independent experiments. Error bars represent standard error mean. Significance was evaluated by One-way ANOVA, Bonferroni's Multiple Comparison Test. ***, indicates $p<0.0001$.

(H) The indicated purified recombinant proteins were incubated in kinase buffer with ATP at 30°C for 30min. Reactivity of recombinant AKT (top panel) with anti-phospho-AKT substrate site (R-X-R-X-X-pS/pT) antibodies (PAS) is shown (bottom panel).

(I) WT MEFs were serum starved overnight and then treated with EGF (100 ng/ml) as indicated. Endogenous TBK1 was immunoprecipitated and assayed for TBK1 kinase activity, *in vitro*, using recombinant His-AKT protein as substrate, and the anti-pS473-AKT antibody to detect substrate phosphorylation (Kinase Assay).

(J) Immunopurified Myc-FLAG-tagged TBK1 wild-type (WT) or kinase-dead (KD) was incubated with purified inactive HA-tagged AKT wild-type (WT) or kinase-dead (KD) as indicated. Kinase reactions were separated by SDS-PAGE and immunoblotted to detect the indicated proteins and phosphorylation events. (Molecular size: AKT-PAS: 70KDa; others as described)

(K) WT and PDPK1$^{-/-}$ DLD1 were infected with lentivirus encoding GFP or K-RasG12V. Three days post-infection, whole cell lysates were prepared and probed by immunoblot for the indicated proteins and selectively phosphorylated proteins. (Molecular size: as described)

The observation that these kinases associate through their respective catalytic domains (Figure 2.4B,C), prompted us to examine the consequence of AKT on TBK1 activation. We found that expression of AKT markedly enhanced TBK1 activation as monitored by accumulation of phosphorylation of the autoactivating TBK1 substrate site S172 (Figure 2.6A) (Kishore, Huynh et al. 2002, Clark, Plater et al. 2009). Tandem mass spectrometry analysis of TBK1 peptides revealed two novel candidate phosphorylation sites on S510 and S716 (Figure 2.6B). The flanking residues for both sites indicated conservation with known AKT substrate sites (ScanSite) (Obenauer, Cantley et al. 2003). Consistent with this, TBK1 immunoisolated from cell culture reacts with the AKT substrate-site selective anti-phosphopeptide antibody (Zhang, Zha et al. 2002), while mutation of either S510 or S716 alone reduces reactivity, and mutation of both S510 and S716 sites together eliminates this reactivity (Figure 2.6C). Importantly, mutation of the candidate AKT substrate sites also markedly impairs accumulation of active TBK1 in cells as indicated by loss of S172 autoactivation site phosphorylation (Figure 2.6C bottom panels). Finally, we found that incubation with purified recombinant AKT1 in vitro was sufficient to enhance activation of recombinant TBK1 as indicated by accumulation of S172 phosphorylation (Figure 2.6D). This was observed using either enzymatically active AKT or AKT initially lacking activation site phosphorylation. The later displayed reduced mobility upon incubation with TBK1 as would be expected from the capacity of TBK1 to induce AKT activation site phosphorylation. Thus there is likely a direct and reciprocal activation loop between AKT and TBK1.

Figure 2.6

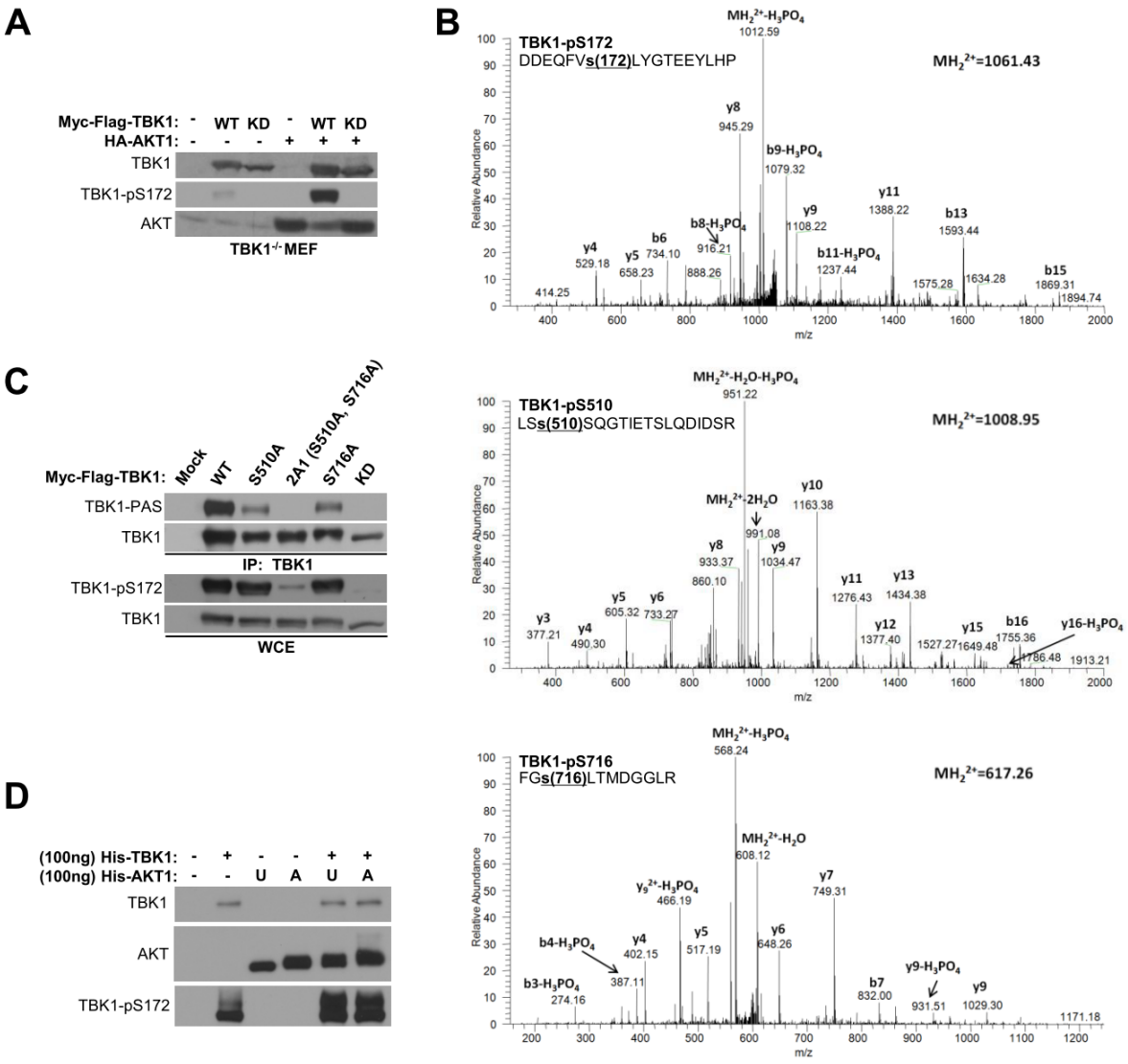
A
Myc-Flag-TBK1: - WT KD - WT KD
HA-AKT1: - - - + + +
TBK1
TBK1-pS172
AKT
TBK1-/- MEF
B
TBK1-pS172
DDEQFVs(172)LYGTEEYLHP
MH2 2+=1061.43
TBK1-pS510
LSs(510)SQGTIETSLQDIDSR
MH2 2+=1008.95
TBK1-pS716
FGs(716)LTMDGGLR
MH2 2+=617.26
Relative Abundance
m/z
C
Myc-Flag-TBK1: Mock WT S510A 2A1 (S510A, S716A) S716A KD
TBK1-PAS
TBK1
IP: TBK1
TBK1-pS172
TBK1
WCE
D
(100ng) His-TBK1: - + - - + +
(100ng) His-AKT1: - - U A U A
TBK1
AKT
TBK1-pS172

Figure 2.6. AKT activates TBK1.

(A) Whole cell extracts from TBK1$^{-/-}$ MEFs expressing TBK1 and/or AKT as indicated were probed for accumulation of phosphorylation of the autoactivating TBK1 substrate site S172.

(B) CID MS/MS spectra from TBK1 peptides purified from cell lysates. Top panel: CID MS/MS spectum of **DDEQFVs(172)LYGTEEYLHP** with a precursor ion of 1061.43(2+). Sufficient b and y ions were detected to identify Ser172 as the phosphorylated site. Middle panel: CID MS/MS spectrum of **LSs(510)SQGTIETSLQDIDSR** with a precursor ion of 1008.95(2+) . Sufficient fragment ions (especially the y15 and y16-H_3PO_4) were detected to identify Ser510 as the phosphorylated site. Bottom panel: CID MS/MS spectrum of **FGs(716)LTMDGGLR** with a precursor ion of 617.26(2+). Sufficient b and y ions (especially the b3-H_3PO_4) were detected to identify Ser716 as the phosphorylated site. "y" designates ions that contain the C-terminal region of the peptide generated from amide bond cleavage by CID. "b" designates ions that contain the N-terminal region of the peptide generated from amide bond cleavage by CID.

(C) The indicated TBK1 variants were expressed in HEK293T cells followed by immunoprecipitation to detect reactivity with the phosphorylated AKT substrate site-specific antibody. This antibody selectively reacts with phosphorylated AKT consensus substrate sites (labeled as TBK1-PAS). Whole cell extracts were probed for accumulation of autophosphorylated TBK1.

(D) Recombinant His_6-TBK1 (100ng) was incubated with either unactivated (U) or activated (A) His_6-AKT (100ng) in kinase reaction buffer for 30min at 30°C. The products were assayed for accumulation of the TBK1 autophosphorylation site (S172) using phospho-specific antibodies.

To examine the consequence of TBK1 on tumorigenicity, we first depleted TBK1 using lentiviral transduction of shRNAs in Mia-Paca2 cells, a pancreas cancer cell line with the K-RasG12C mutation (Forbes, Tang et al. 2009). Two of three hairpins resulted in detectable TBK1 depletion by 2 days post transduction with concomitant reduction in AKT activation (Figure 2.7A). By 6 days post transduction, the viability of TBK1 depleted cells was severely compromised (Figure 2.7B), but could be rescued by expression of an artificially activated myristoylated AKT fusion protein (Figure 2.7C). To examine if the cell death observed in cultured cells was recapitulated in an orthotopic setting, Mia-Paca-2 cells were surgically implanted beneath the capsule of the tail of the pancreas of immune-compromised mice two days post transduction with shRNA expressing lentiviral constructs. Two independent TBK1 shRNAs impaired primary tumor initiation (Figure 2.7D) and progression (Figure 2.7E) as compared to controls. Equivalent experiments were also performed in MDA-MB-231 cells, a triple negative breast cancer derived cell line with activating mutations in both K-Ras and B-Raf (Forbes, Tang et al. 2009). MDA-MB-231 cells, transduced with shRNA-expressing lentivirus, were implanted into the mammary fat pad of immune compromised mice and tumor growth was followed (Figure 2.7F). By 45 days post-implantation, control samples had progressed substantially (Figure 2.7G) and metastasized to other organs (Figure 2.7H). In contrast, TBK1-depleted samples progressed very poorly and failed to metastasize (Figure 2.7F,G,H). These observations indicate that TBK1 is required to support AKT activation in cancer cells, and is required for primary tumor initiation and progression, at least in the context of two different orthotopic xenograft models.

Figure 2.7

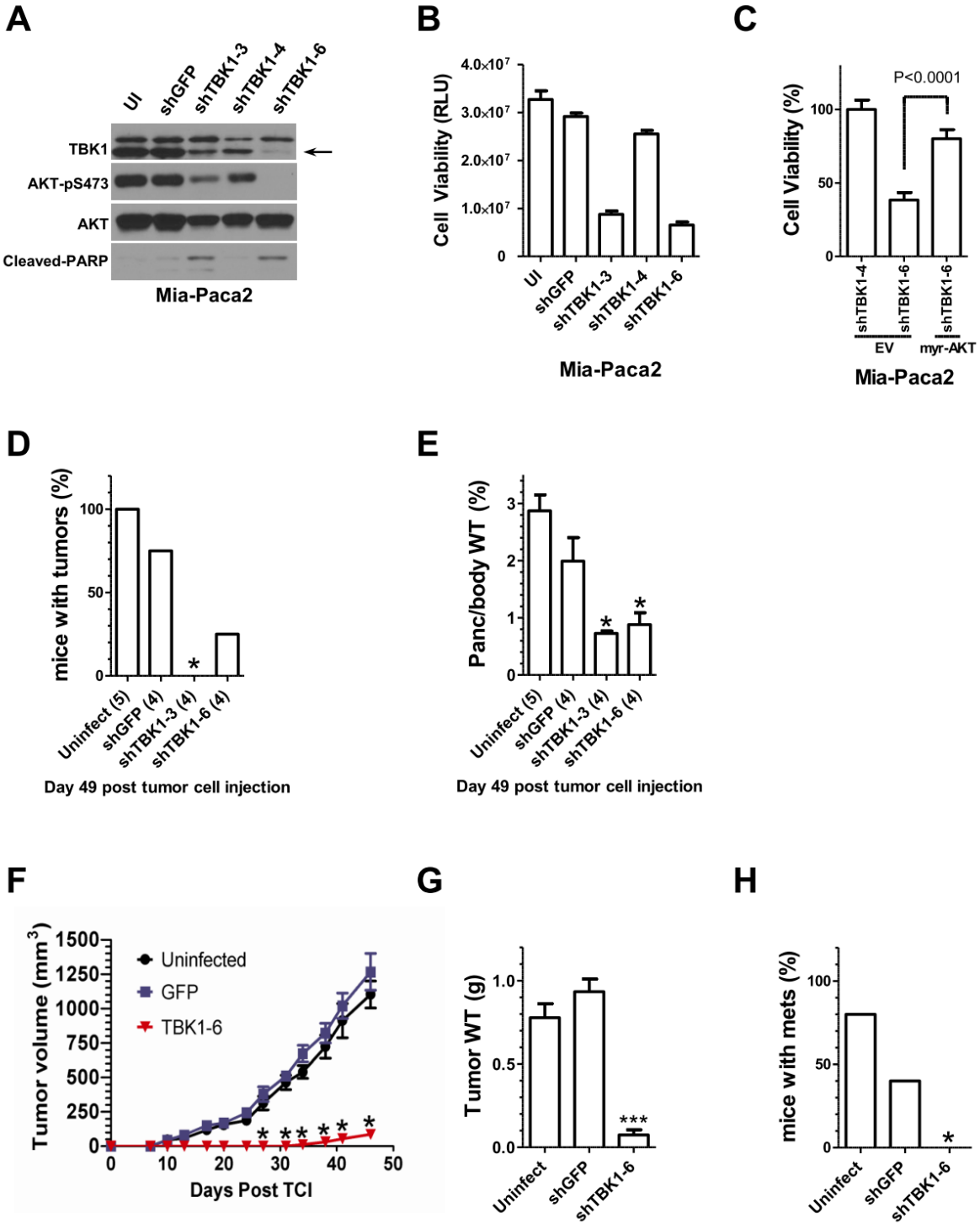
A
UI
shGFP
shTBK1-3
shTBK1-4
shTBK1-6
TBK1
AKT-pS473
AKT
Cleaved-PARP
Mia-Paca2
B
Cell Viability (RLU)
4.0x10^7
3.0x10^7
2.0x10^7
1.0x10^7
0
UI
shGFP
shTBK1-3
shTBK1-4
shTBK1-6
Mia-Paca2
C
Cell Viability (%)
P<0.0001
100
50
0
shTBK1-4
shTBK1-6
shTBK1-6
EV
myr-AKT
Mia-Paca2
D
mice with tumors (%)
100
50
0
*
Uninfect (5)
shGFP (4)
shTBK1-3 (4)
shTBK1-6 (4)
Day 49 post tumor cell injection
E
Panc/body WT (%)
3
2
1
0
*
*
Uninfect (5)
shGFP (4)
shTBK1-3 (4)
shTBK1-6 (4)
Day 49 post tumor cell injection
F
Tumor volume (mm3)
1500
1250
1000
750
500
250
0
Uninfected
GFP
TBK1-6
*
**
*
*
*
0
10
20
30
40
50
Days Post TCI
G
Tumor WT (g)
1.0
0.5
0.0
***
Uninfect
shGFP
shTBK1-6
H
mice with mets (%)
100
50
0
*
Uninfect
shGFP
shTBK1-6

Figure 2.7. TBK1 is required to support cancer cell tumorigenicity *in vivo*.

(A) Mia-Paca2 cells were infected with lentivirus encoding shRNAs targeting GFP (shGFP) or TBK1 (shTBK1-3, shTBK1-4 and shTBK1-6). UI indicates uninfected control. Three days post-infection, whole cell extracts were assayed for the indicated proteins. (Molecular size: as previously described)

(B) Mia-Paca2 cells were treated as in (A), and assayed for relative viability 6 days post-infection using an ATP-coupled luminescence assay (CellTiter-Glo, Promega). Bars indicated standard deviation from the mean of three independent experiments.

(C) Mia-Paca2 cells were transfected with plasmids encoding a constitutively active variant of AKT (myr-AKT) or empty vector (EV) as a control (Bellacosa, Chan et al. 1998). One-day post-transfection, cells were infected as indicated in (A) with lentivirus encoding shTBK1-4 and shTBK1-6. Five-day post-infection, cell viability was assayed as in (B). Significance was evaluated using the student's two-tailed T-test.

(D) $1x10^6$ Mia-Paca2 cells uninfected (n=5) or stably expressing GFP (n=4) or shRNA constructs targeting TBK1 (TBK1-3, n=4; TBK1-6; n=4) were injected into the pancreas of SCID mice. All cells were collected two days post lentiviral infection and viability was confirmed by trypan blue exclusion. At this time-point, TBK1 depletion has not proceeded to the point that begins to engage cell death. Animal health and tumor growth was monitored and a cohort of animals sacrificed on Day 49 post tumor cell injection. Total tumor incidence is shown.

(E) Pancreas weight (tumor burden) was normalized to total body weight at the end of the study and is displayed as % of body weight.

(F) MDA-MB-231 cells uninfected or stably expressing GFP or shRNA targeting TBK1 (TBK1-6) (n=5/group) were injected into the mammary fat pad of female SCID mice. Again, all cells were collected two days post lentiviral infection and viability was confirmed by trypan blue exclusion. Animal health and tumor volume were followed throughout the duration of the experiment.

(G) Tumor burden at the time of sacrifice is displayed as final tumor weight.

(H) Metastatic incidence.

(D-H) *, indicates $p<0.05$; and ***, indicates $p<0.005$ vs. uninfected control by ANOVA with a Bonferroni correction for multiple comparison testing.

To discriminate the consequence of TBK1 depletion from inhibition of TBK1 kinase activity, we wished to employ small molecule TBK1 inhibitors for pharmacological interrogation of the TBK1/AKT regulatory relationship in normal and cancer cells. The currently available compound, BX795 (Bamborough, Christopher et al. 2006, Clark, Plater et al. 2009), has significant activity against both TBK1 and PDK1, which limits its application to these studies (Bain, Plater et al. 2007). Therefore, we isolated additional chemical TBK1 inhibitors from a biochemical screen of ~250,000 small molecules. A 6-aminopyrazolopyrimidine derivative (Compound II, Figure 2.8A) was identified as a lead compound with an IC_{50} of 13 nM against TBK1 and 59 nM against the TBK1 homolog IKKε, but with 100- to 1000-fold less activity against other tested protein kinases including PDK1, PI3K family members and mTOR (Figure 2.8B). Consistent with inhibition of TBK1-dependent signaling, compound II inhibited LPS-induced expression of IFNβ (IC_{50} =62nM), and the IFNβ target genes IP10 (IC_{50} =78nM) and Mx1 (IC_{50} =20nM) (Figure 2.8C). Consistent with selective activity on canonical TBK1 pathway activation (Sato, Sugiyama et al. 2003, Yamamoto, Sato et al. 2003), Compound II effectively blocked TLR3-dependent IRF3 nuclear translocation in cells with an IC_{50} under 100 nM, but did not impair TNFR1-dependent p65 NFκB nuclear translocation with doses as high as 20 μM (Figure 2.8D). This later response has been defined as TBK1-independent (Sato, Sugiyama et al. 2003, Perry, Chow et al. 2004, Chien, Kim et al. 2006). Concordant with our observations in $TBK1^{-/-}$ MEFs, a 30-minute pretreatment of wild-type MEFs with Compound II impaired AKT activation by glucose (Figure 2.8E). Similarly, a 30-minute incubation of the TBK1-sensitive cell line HCC44 with doses of Compound II as low as 500 nM was sufficient to

blunt baseline AKT activity (Figure 2.8F). Notably, Compound II had no activity against the canonical AKT kinases PDK1 and mTOR *in vitro* (Figure 2.8B), indicating the defective AKT response is likely a consequence of impaired TBK1 activity. Concordant with mTORC2-independent activation of AKT by TBK1, the AKT response to host defense signaling in $Sin1^{-/-}$ and $Rictor^{-/-}$ cells was blocked by Compound II (Figure 2.8G). Concordant with the consequence of siRNA and shRNA-mediated TBK1 depletion, a 24-hour exposure to Compound II inhibited AKT pathway activation and survival in multiple cancer cell lines at doses close to those affecting IRF-3 nuclear localization (Figure 2.8H). Importantly, the extent of AKT inhibition was equivalent or better than that observed with 40 μM of the PI3K inhibitor LY294002 (Figure 2.8H).

Figure 2.8

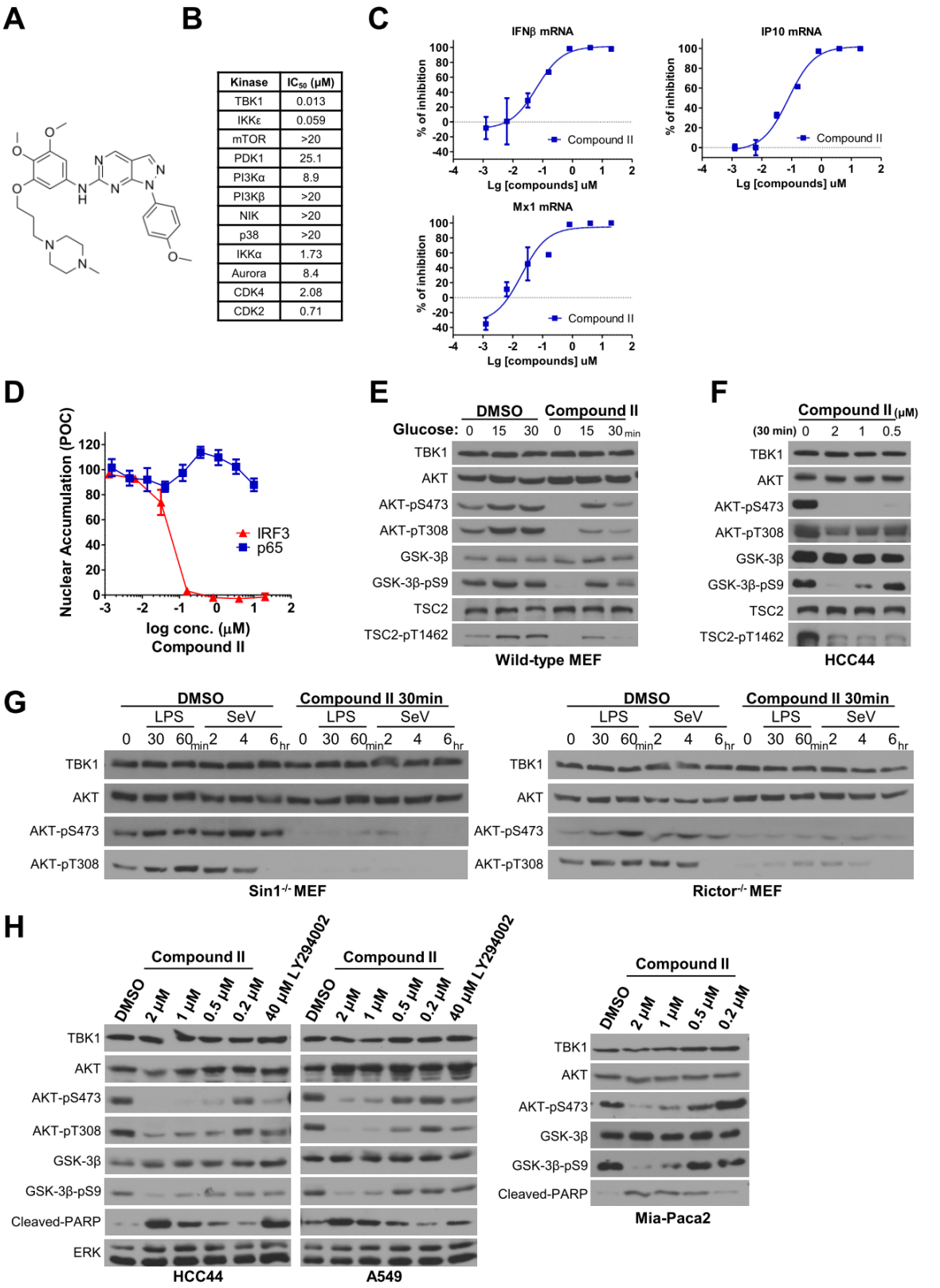
A
B
C
D
E
F
G
H
Kinase | IC50 (μM)
TBK1 0.013
IKKε 0.059
mTOR >20
PDK1 25.1
PI3Kα 8.9
PI3Kβ >20
NIK >20
p38 >20
IKKα 1.73
Aurora 8.4
CDK4 2.08
CDK2 0.71
IFNβ mRNA
IP10 mRNA
Mx1 mRNA
% of inhibition
Lg [compounds] uM
Compound II
Nuclear Accumulation (POC)
log conc. (μM) Compound II
IRF3
p65
DMSO
Compound II
Glucose:
TBK1
AKT
AKT-pS473
AKT-pT308
GSK-3β
GSK-3β-pS9
TSC2
TSC2-pT1462
Wild-type MEF
Compound II (μM)
(30 min)
HCC44
LPS
SeV
Compound II 30min
Sin1-/- MEF
Rictor-/- MEF
Cleaved-PARP
ERK
HCC44
A549
Mia-Paca2
40 μM LY294002

Figure 2.8. Pharmacological inhibition of TBK1 impairs AKT signaling.

(A) Structure of Compound II.

(B) IC_{50} values for *in vitro* inhibition of the indicated purified recombinant kinases by Compound II.

(C) Primary macrophages from mouse bone marrow were treated with LPS and increasing concentrations concentration of Compound II. LPS induced accumulation of interferonβ (IFNβ) and interferonβ target gene (IP10 and Mx1) mRNAs were measured by quantitative PCR and shown as percent of inhibition. Error bars represent S.D.M. from triplicate experiments.

(D) HeLa cells incubated in the indicated concentrations of Compound II were stimulated with 10 ng/ml TNFα for 10 minutes (p65 assays), or transfected with poly I:C for 2 hours (IRF3 assays), followed by immunofluorescence-based detection of IRF3 and p65 nuclear accumulation. Nuclear accumulation is plotted as percent of control (POC). Error bars represent S.D.M. from triplicate analysis.

(E) Wild-type MEFs were incubated cells in DMEM with 10% serum but without glucose for 2 hours. Cells were then pretreated with 2 μM Compound II for 30 minutes as indicated followed by addition of 25 mM glucose as indicated. Whole cell extracts were prepared post glucose stimulation and immunoblotted as shown. (Molecular size: as described)

(F) Asynchronous proliferating cultures of HCC44 cells were exposed to the indicated concentrations of Compound II for 30 minutes. Whole cell extracts were immunoblotted for detection of the indicated proteins and phospho-proteins. (Molecular size: as described)

(G) $Sin1^{-/-}$ and $Rictor^{-/-}$ MEFs were pretreated with DMSO or Compound II for 30 minutes as indicated, followed by exposure to LPS (1 μg/ml) or Sendai virus (SeV, 100 HA/ml). Whole cell extracts prepared at the indicated time-points were immunoblotted for detection of AKT activation. (Molecular size: as described)

(H) Whole cell extracts from HCC44, A549 and Mia-Paca2 cells exposed to the indicated concentrations of Compound II or LY294002 for 24 hours were immunoblotted to detect consequences on AKT pathway activation. (Molecular size: cleaved-PARP: 89KDa; others as described)

We next examined if cancer cell lines selectively sensitive to shRNA-mediated TBK1 depletion were also selectively sensitive to Compound II. First, to assess the incidence of TBK1-sensitivity across diverse oncogenotypes within a discrete disease setting, we employed a panel non-small cell lung cancer (NSCLC) derived cells lines for which the oncogenic Ras status had been defined. We collected 15 lines, 10 of which express oncogenic K-Ras, and examined the consequence of TBK1 depletion on cell viability using two independent TBK1 shRNAs. We found that TBK1 depletion was toxic to approximately 50% of this cohort (Figure 2.9A). Of note, H1993 (TBK1-sensitive) and H2073 (TBK1-resistant) are derived from a lymph node metastasis and the primary tumor, respectively, from the same patient. Although many lines with oncogenic Ras mutations were in the TBK1-dependent class (6 of 10), the presence of this oncogene is not solely sufficient to specify TBK1-sensitivity. A recent study examining the relative addiction of NSCLC cell lines to oncogenic Ras expression indicated that lines with epithelial characteristics, including elevated E-cadherin expression, were selectively dependent on the continued expression of oncogenic Ras (Singh, Greninger et al. 2009). However, this relationship also failed to specify TBK1-sensitivity (Figure 2.9A, lower panels), suggesting additional key biological determinants driving TBK1 addiction remain to be discovered. A549 (TBK1-dependent) and H441 (TBK1-independent) were exposed to Compound II for 96 hours across a nanomolar to micromolar dose range, with cell viability as the endpoint assay. Importantly A549 cells (IC_{50} ~ 0.4 micromolar) were acutely responsive to compound II concentrations at least 10 fold lower than those required for significant toxicity in H441 cells (IC_{50} ~ 4.2 micromolar) (Figure 2.9B). In addition, TBK1-dependent lines were selectively sensitive to

induction of apoptosis upon a 24-hour exposure to 2 micromolar Compound II as compared to TBK1-independent lines (Figure 2.9C). Compound II exposure strongly suppressed accumulation of active AKT in all TBK1-sensitive NSCLC lines tested (H358, H1993, and HCC44). In contrast the TBK1-independent cell lines H2073 and H441 maintained chronic AKT activation in the presence of Compound II (Figure 2.9D). Calu1, which displays intermediate sensitivity to TBK1 depletion (Figure 2.9A), also displayed intermediate sensitivity to Compound II-dependent inhibition of AKT activation (Figure 2.9D). These concordant observations between RNAi-mediated TBK1 depletion and small molecule mediated inhibition of TBK1 activity indicate that TBK1 represents an important direct regulatory input to AKT survival signaling (Figure 2.10).

Figure 2.9

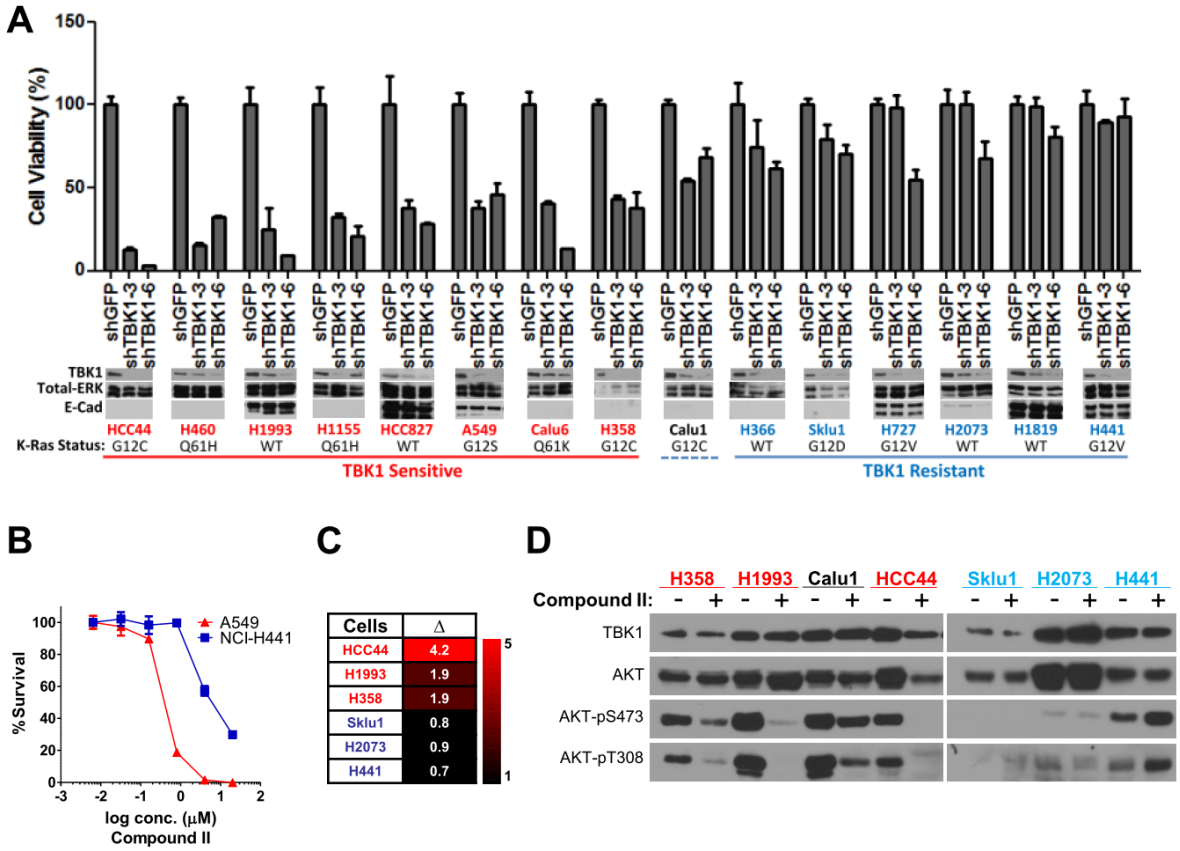

Figure 2.9. TBK1 sensitivity in non small cell lung cancer.

(A) The indicated cell lines were infected with lentivirus encoding shRNAs targeting GFP or two independent shRNAs targeting TBK1 as indicated. Relative cell viability was assayed 6 days post infection as in Figure 5. Whole cell extracts from parallel infections were collected and probed for the indicated proteins.

(B) Following a 96-hour exposure to the indicated concentrations of Compound II, A549 and H441 cell viability was measured as indicated. Bars represent standard error from the mean of three independent experiments.

(C) The indicated cell lines were exposed to DMSO or 2 μM Compound II for 24 hours. Cells were then labeled with FITC-conjugated Annexin V, and scored by FACS. Values shown in the heat-map represent fold-induction of Annexin V positive cells over the DMSO controls (Δ).

(D) Whole cell extracts from cells treated for 24 hours as in (C) were immunoblotted as indicated. Lysates were loaded based on equivalent cell numbers for each sample.

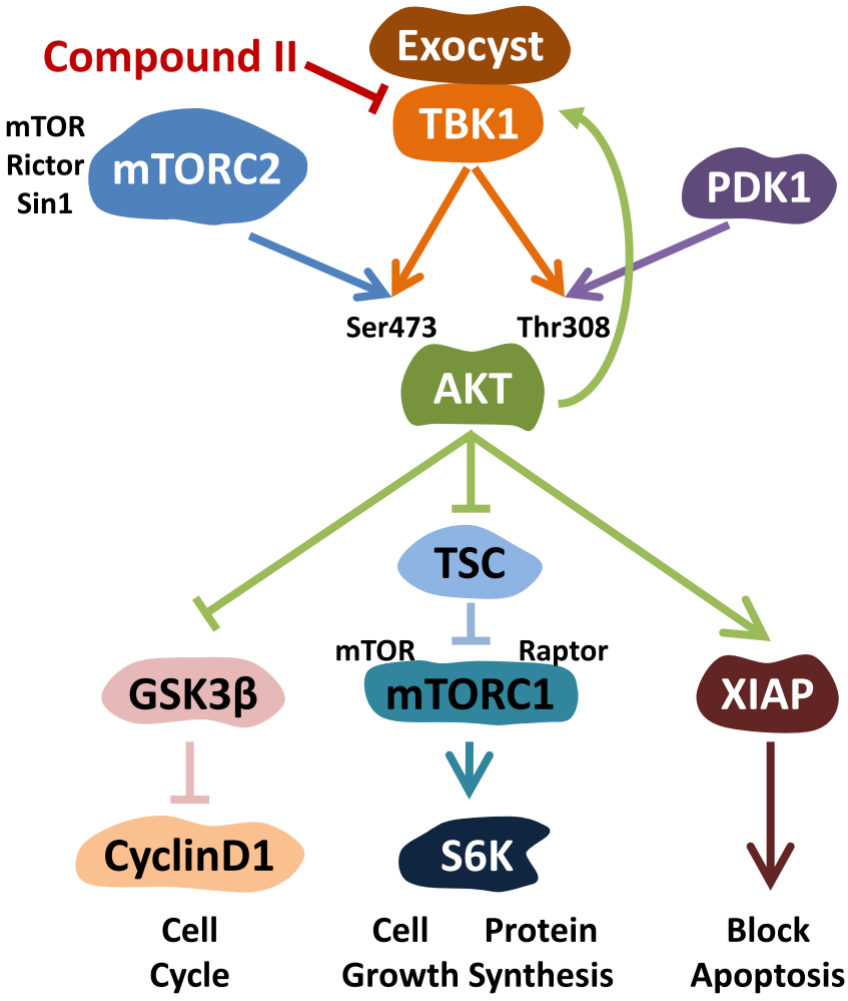

Figure 2.10 TBK1-AKT signaling networks.

DISCUSSION

Beyond its canonical occupation as a core component of innate immune and inflammatory cytokine signaling, TBK1 has attracted attention as a potential therapeutic target in cancer given its selective support of cancer cell viability (Chien, Kim et al. 2006, Barbie, Tamayo et al. 2009). Here, we have identified the survival signaling kinase AKT/PKB as a direct TBK1 effector. Upon genetic ablation, RNAi-mediated depletion, or pharmacological inactivation of TBK1, AKT activity is diminished and cancer cell viability is impaired. The mechanistic basis of TBK1 support of AKT activation is direct stimulation of AKT catalytic activity as a consequence of TBK1-induced phosphorylation of both the T308 activation loop residue and the S473 hydrophobic domain residue. TBK1 expression is required to support pathological oncogene-dependent AKT signaling, and is required to fully engage AKT in response to EGF, glucose, and host defense signaling. Insulin responsiveness, on the other hand, is TBK1-independent.

The PDK1 kinase and mTORC2 complex have been defined as key proximal determinants of AKT activation. mTORC2 directly phosphorylates AKT-S473, which in turn promotes direct phosphorylation of T308 by PDK1 in the presence of appropriate collateral accumulation of the PI3K product phosphatidylinositol-3,4,5-trisphosphate (PIP_3) (Alessi, James et al. 1997, Sarbassov, Guertin et al. 2005, Manning and Cantley 2007, Engelman 2009). This collaborative action is required for AKT activation by insulin (Hresko and Mueckler 2005), though the mechanism of mTORC2 activation in this context is currently unknown (Manning and Cantley 2007). Our observations suggest that the contribution of TBK1 to AKT activation is non-redundant to the PDK1/mTORC2 pathway.

For example, the PDK1/mTORC2 pathway is apparently intact in TBK1$^{-/-}$ MEFs given the wild-type responsiveness of AKT to insulin in these cells. However, the defective AKT responsiveness to EGF, glucose, or innate immune signaling indicates that PDK1/mTORC2 are not sufficient to engage AKT downstream of all germane regulatory inputs. Most importantly, TBK1 retains the capacity to activate AKT in cells where PDK1 or the mTORC2 subunits Sin1 or Rictor have been homozygously deleted.

We find that a subpopulation of AKT in cells is associated with the Sec6/8 a.k.a. exocyst complex. This heterooctameric protein complex was originally identified through its role in the regulated targeting and tethering of selected secretory vesicles to specialized dynamic plasma membrane domains (Grindstaff, Yeaman et al. 1998, Guo, Sacher et al. 2000). Subsequently, it was discovered that the exocyst plays a direct role in host defense signaling by marshaling TBK1 and STING (stimulator of interferon genes) in response to cellular detection of viral replication intermediates (Chien, Kim et al. 2006, Bodemann and White 2008, Ishikawa and Barber 2008, Ishikawa, Ma et al. 2009). The recruitment of TBK1 to the exocyst in response to AKT pathway agonists that are TBK1 dependent, together with the observation that exocyst integrity supports AKT activation, suggests that this protein complex may represent an architecturally discrete signaling platform. Distinct regulatory inputs to AKT, which can be separately or simultaneously operative, could support compartmentalization of AKT activity within a cell, perhaps as a mechanism to specify the cadre of client substrates engaged by AKT in response to diverse agonists (Jacinto, Facchinetti et al. 2006, Bozulic and Hemmings 2009).

Chemical inhibitors of TBK1 will be valuable in further clarifying the role of TBK1 in AKT survival signaling, and defining the therapeutic value of this kinase target. As a tool compound, Compound II was found to be effective in the low nanomolar range in vitro, cell permeable, and a potent and selective TBK1 inhibitor in cells. Importantly, Compound II exposure impaired accumulation of active AKT, and displayed selective toxicity in TBK1-dependent cancer cell lines. The concordant observations with Compound II exposure and TBK1 depletion strongly suggest that the phenotypes reported here is most likely a consequence of TBK1 catalytic activity as opposed to activity-independent consequences of TBK1 depletion. This indicates that TBK1 support of pathological AKT activation can likely be pharmacologically targeted in disease. In conclusion, our observations define AKT as a direct TBK1 effector and reveal a non-canonical context-selective regulatory mechanism for mobilization of AKT signaling.

In addition to somatic mutations found in human cancers, heterozygous TBK1 mutations have been reported in patients suffered from childhood herpes simplex virus-1 (HSV-1) encephalitis (HSE). Both TBK1 mutations (D50A and G159A) result in lost-of-function mutants through different mechanisms. TBK1-D50A mutation reduces TBK1 protein stability, which leads to haploinsufficiency. However, TBK1-G159A mutation impairs TBK1 kinase activity and mutant proteins behave in a dominant-negative fashion. Importantly, these observations suggest that pharmacological inhibition of TBK1 for therapeutic intervention in human cancers may not have substantial side effects since both patients carrying TBK1 lost-of-function mutations are healthy before suffered from HSE (Herman, Ciancanelli et al. 2012) (Figure 2.11).

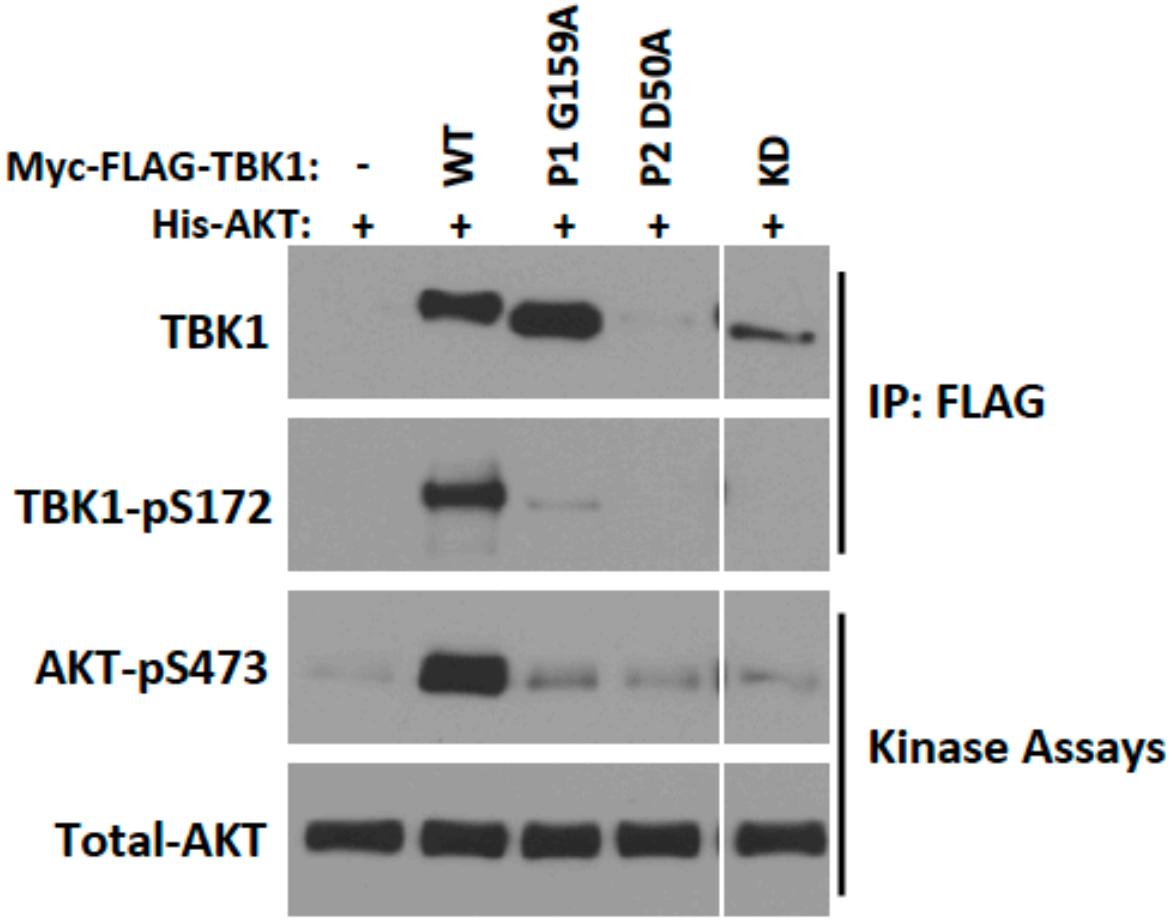

Figure 2.11. Both mutant TBK1 alleles are loss-of-function but through different mechanisms. HEK293T cells were transfected with control vector or either WT or mutant TBK1 expression constructs. Myc-FLAG-tagged TBK1 was immunoprecipitated from HEK293T cells. Immunoprecipitates were assayed for TBK1 kinase activity, *in vitro*, using recombinant AKT as substrate, and the phospho-AKT-Ser473 antibody to detect substrate phosphorylation (Kinase Assays).

MATERIAL AND METHODS

Cell culture and transfection. TBK1$^{+/+}$ and TBK1$^{-/-}$ MEFs, Mia-Paca2, U2OS, Panc-1, HEK293T, HBEC, HeLa and MCF7 cells were cultured as previously described (Chien, Kim et al. 2006), and Sin$^{-/-}$ MEFs, kindly provided by Dr. Bing Su (Yale University), Rictor$^{-/-}$ MEFs, kindly provided by Drs. Mark Magnuson (Vanderbilt University School of Medicine), Dos Sarbassov (The University of Texas MD Anderson Cancer Center) and David Sabatini (Massachusetts Institute of Technology), and MDA-MB-231 cells were cultured in DMEM supplemented with 10% fetal bovine serum (Atlanta Biologicals), 100 U/mL penicillin and 100 μg/mL streptomycin (Invitrogen). Wild-type and PDPK1$^{-/-}$ HCT116 and DLD1 cells were kindly provided by Dr. Bert Vogelstein (Johns Hopkins University) and cultured as described (Ericson, Gan et al. 2010). Lung cancer cell lines A549, Calu1, Calu6, H1155, H1819, H1993, H2073, HCC366, H358, H441, H460, H727, HCC827, HCC44 and Sklu1 cells were cultured in RPMI supplemented with 5% fetal bovine serum (Atlanta Biologicals), 100 U/mL penicillin and 100 μg/mL streptomycin (Invitrogen). For siRNA transfection, U2OS and HBEC cells were transfected with siRNA using DharmaFECT 1 (Dharmacon) as described (Whitehurst, Bodemann et al. 2007). Sin$^{-/-}$ MEFs, Rictor$^{-/-}$ MEFs, PDK1$^{-/-}$ HCT116 and DLD1 cells were transfected with ExGen 500 (Fermentas) according to manufacturer's instructions. HeLa cells were transfected with LF2000 (Invitrogen).

Plasmids, reagents and antibodies. The mammalian expression plasmids pCDNA-FLAG-TBK1 (WT) and (K38M) were generously provided by Dr. James Chen (UT Southwestern Medical Center), and are as described (Seth, Sun et al. 2005). To construct the pRK5-Myc-FLAG-TBK1 (WT) and (K38M) mammalian expression plasmids, TBK1 coding sequences were excised from pCDNA-FLAG-TBK1 (WT) and (K38M) and subcloned into the *BamHI* and *XbaI* sites of pRK5-Myc. HA-TBK1 (WT) and HA-TBK1 (NT) expression vectors were generously provided by Dr. Xuetao Cao (Second Military Medical University, Shanghai, China) (An, Zhao et al. 2006). Wild-type and kinase-dead HA-AKT1, and myristoylated-HA-AKT1 were generously provided by Dr. Philip N. Tsichlis (Tufts Medical Center) (Bellacosa, Chan et al. 1998). GST-AKT1 full-length and truncation mutants were generously provided by Dr. Keqiang Ye (Emory University School of Medicine) (Ahn, Rong et al. 2004, Tang, Jang et al. 2007). Lenti-virus shRNA expression constructs were generously provided by Dr. William Hahn (Harvard Medical School). Myc-Sec8, Sec3-GFP, and Exo70-GFP expression constructs were generously provided by Dr. Charles Yeaman (University of Iowa) (Matern, Yeaman et al. 2001). Recombinant His-TBK1 (no. 14-628), and His-AKT1 (inactive, no. 14-279) were purchased from Upstate/Millipore Corp. AKT Kinase Assay kits (no. 9840) were purchased from Cell Signaling Technology. Glutathione (GSH)-Sepharose 4B (no. 17-0756-01) was purchased from GE Healthcare Amersham. Protein A/G (sc-2003) and anti-HA antibody conjugated beads (sc-7392ac) were purchased from Santa Cruz. Anti-FLAG antibody conjugated beads (A2220), 3xFLAG peptide (F4799) and LY294002 (L9908) were purchased from Sigma. HA peptide (RP11735) was purchased from GenScript. Anti-Sec8 mouse monoclonal antibodies were

kindly provided by Dr. Charles Yeaman (University of Iowa) (Matern, Yeaman et al. 2001) and anti-Exo70 mouse monoclonal antibodies were generously provided from Dr. Shu-Chan Hsu (Rutgers University) (Vega and Hsu 2001). Additional antibodies were purchased from Sigma (anti-Actin, A1978), BioChain (anti-IKKε, Z5020108), Santa Cruz Technology (anti-K-Ras, sc-30; anti-ERK1/2, sc-93; anti-Myc, sc-40; anti-HA, sc-805; anti-IRF3, sc-9082), Cell Signaling Technology (anti-AKT1, 2967; anti-AKT-pS473, 4060; anti-AKT-pT308, 2965; anti-phospho-(Ser/Thr) AKT substrate, 9611; S6K, 9202; S6K-pT389, 9234 and 9206; S6, 2217; S6-pS235/236, 4858; TBK1, 3504; TSC2, 3635; TSC2-pT1462, 3611; Cleaved-PARP, 9541;), Upstate/Millipore Corp. (anti-TBK1, 04-856; anti-AKT1, 05-796) and Imgenex Corp. (anti-TBK1, IMG-139A).

Lentiviral transduction. Lentiviral-based expression constructs were packaged by cotransfection of HEK293FT cells with VSV-G and Δ-8.9 plasmids. Growth media was replaced with Opti-MEM 24 hours post transfection, and incubated a further 24 hours prior to viral particle collection. $TBK1^{+/+}$ and $TBK1^{-/-}$ MEFs were plated at a density of $4x10^4$ cells/well into 6-well plates. Twenty-four hours later, cells were infected with lentiviral particles and polybrene (10 μg/ml). $PDPK1^{+/+}$ and $PDPK1^{-/-}$ DLD1 cells were plated at a density of $1.25x10^5$ cells/well into 6-well plates. Twenty-four hours later, cells were infected with lentiviral particles and polybrene (10 μg/ml). Mia-Paca2 and MDA-MB-231 cells were seeded at $1x10^5$ cells/well in 6-well plates. Twenty-four hours later, cells were infected with 1ml of lenti-viral particles containing indicated shRNAs for 2 hours, and then virus-containing medium (Opti-MEM) was replaced with 2 ml of normal medium. All

NSCLC cell lines were seeded at $5x10^3$ cells/well into 96-well microtiter plates in triplicate and incubated overnight. Twenty-four hours later cells were infected with 90 µl of lenti-viral particles in Opti-MEM and polybrene (10 µg/ml) for 2 hours followed by a medium exchange with RPMI containing 5% FBS. On day 3 post-infection, cells were given fresh medium. On day 6, cells were equilibrated at r.t. for 30 min and then CellTiter-Glo reagent (15µl) was added to each well. Following 10 min incubation, samples were analyzed using an Envision plate reader.

Immunoprecipitation and affinity purification. Whole cell extracts were prepared in non-denaturing IP buffer (20 mM Tris HCl [pH 7.5], 10 mM $MgCl_2$, 2 mM EGTA, 10% Glycerol, 137 mM NaCl, 1% Triton X-100 (vol/vol), 0.5% Na Deoxycholate, 1 mM DTT, phosphatase and protease inhibitors [Roche]) were incubated with anti-AKT1 mouse monoclonal antibody (Cell Signaling) and 30 µl Protein A/G beads (Santa Cruz) overnight at 4^oC. Immunoprecipitates were washed three times in (20 mM Tris HCl [pH 7.5], 10 mM $MgCl_2$, 2 mM EGTA, 10% Glycerol, 137 mM NaCl, 1% Triton X-100 (vol/vol), 0.5% Na Deoxycholate, 1 mM DTT, and 1 mM PMSF) then boiled in standard SDS sample buffer. Samples were separated by SDS-PAGE followed by immunoblot analysis. Co-immunoprecipitation of overexpressed proteins from HEK293T cell lysates was performed with 30 µl of anti-HA agarose beads (25% slurry) or anti-FLAG M2 beads (50% slurry). For mapping TBK1-interacting domain on AKT, a variety of GST-tagged AKT deletion mutants and Myc-FLAG-tagged TBK1 were expressed in HEK293T cells. Two-day post-transfection, cells were lysed in IP buffer, and then cell lysates were incubated with 30 µl

GSH-Sepharose beads for 3 hours. After three washes with wash buffer, beads were boiled for 5 min in SDS sample buffer, and subjected to SDS-PAGE and immunobloting analysis. For mapping TBK1/AKT interaction domains, GST-tagged AKT kinase-domain and either HA-tagged full-length or N-terminal TBK1 were expressed in HEK293T cells. Two-day post-transfection, cells were lysed in IP buffer, and then cell lysates were incubated with 30 μl GSH-Sepharose beads for 3 hours. After three washes with wash buffer, beads were boiled for 5 min in SDS sample buffer, and subjected to SDS-PAGE and immunoblot analysis.

Immunofluorescence. For quantitative detection of endogenous IRF3 nuclear localization in response to Poly I:C, 15,000 HeLa cells/well were seeded in 96-well plates in medium containing 10% FBS. Compound (10 doses, starting from 20 μM, then 1:5 serially diluted) and 5 μg/ml of poly I:C (Sigma, P-9582) mixed with 3 μl/ml of LF 2000 were added and cells were incubated for 2 hrs. Cells were then fixed with 3.7% formaldehyde for 15 min., permeabilized with 0.5% Triton-X for 15 min., then stained with anti-IRF3 antibody for an hour followed by Alexa488 secondary antibody and Hoechst nuclear staining for another hour. Intensity of IRF3 in nucleus vs. IRF3 in cytoplasm was measured using Cellomics ArrayScan and analyzed using vHCS View and GraphPad Prism. For quantitative detection of endogenous p65 nuclear translocation in response to TNF, HeLa cells were handled as described above except that cells were pretreated with serially diluted compound for 10 minutes prior to exposure to 10 ng/ml TNFα for 10 minutes. p65 was detected with a rabbit polyclonal anti-p65 and the Alexa488 secondary antibody and nuclear accumulation was

quantitated as above. For Annexin V labeling, cells were harvested with trypsin, washed two times in PBS, resuspended in 100 µl Annexin V binding buffer (10 mM HEPES pH 7.4, 140 mM NaCl, 2.5 mM $CaCl_2$) and incubated with 5 µl FITC Annexin V (BD Pharmingen, 51-65874X) at r.t. for 15 min. Samples were then subjected to FACS Calibur (BD Biosciences) and analyzed using CellQuest software (BD Biosciences). For BrdU incorporation assays, WT and $TBK1^{-/-}$ MEFs were seeded onto cover slips overnight and then either maintained in the presence or absence of serum for 44 hr. Cells were treated with BrdU (10 µM; Sigma, B9285) together with either carrier, EGF (100ng/ml) or FBS (10%) simultaneously. After 4 hours, cells were washed with PBS, fixed by 3.7% Formaldehyde for overnight at 4 ^{0}C, and then permeabilized with cold acetone for 5 min. Following PBS washes, cells were treated with 2N HCl for 10min at R.T. then washed again. Cover slips were blocked with PBTA (PBS, 1% Tween 20, and 1% BSA) for 30 min at R.T., and then incubated with anti-BrdU antibody (1:20; Invitrogen, A21303) for 1 hr. Following extensive washing, cells were stained with DAPI and mounted. BrdU positive cells were counted as percentage relative to total nuclei (DAPI stain). For measuring cell death, WT and $TBK1^{-/-}$ MEFs were seeded onto cover slips overnight. Cells were either maintained in the presence of serum, serum starved, or glucose deprived. After 24hr cells were fixed and stained with DAPI. Pyknotic cells were counted as percentage relative to total nuclei (DAPI stain).

AKT affinity purification. HA-AKT wild-type or kinase-dead was expressed in HEK293T cells. Two days post-transfection, cells were incubated overnight in DMEM without serum, and then lysed in IP buffer. HA-AKT proteins were purified with anti-HA beads, and

washed extensively (20 mM Tris-HCl, and 1 M NaCl; pH 7.5). HA-AKT proteins were then released with elution buffer (1 mg/ml HA peptide, 20 mM Tris-HCl, 0.1 M NaCl, and 0.1 mM EDTA; pH 7.5). The concentrations and purity of HA-AKT wild-type and kinase-dead proteins were determined by Coomassie blue staining.

In Vitro protein kinase activity assays. For *in vitro* kinase assays with purified recombinant proteins, 20 ng of His-tagged TBK1 and 100 ng of His-tagged AKT were mixed as indicated in kinase buffer (25 mM Tris HCl [pH 7.5], 10 mM $MgCl_2$, 5 mM β-Glycerophosphate, 2 mM DTT, and 0.1 mM Na_3VO_4) containing 200 μM ATP at 30^{o}C. After 30 min. incubation, 1 μg of GST-GSK3α/β AKT substrate peptides (CGPKGPGRRRTSSFAEG) and 200 μM ATP were added and kinase reactions were performed for additional 30 min at 30^{o}C. Phosphorylation of the AKT substrate sites on the GSK3α/β peptide was detected using the phospho-GSK-3α/β (Ser21/9) antibody (Cell Signaling). For IP kinase assays, HA-AKT and Myc-FLAG-TBK1 were expressed in HEK293T cells. Cells were lysed in IP buffer and immunoprecipitation was performed with anti-HA beads or anti-FLAG M2 beads, respectively. Following extensive washing with IP buffer containing 0.1% SDS, beads were suspended in kinase buffer (25 mM Tris HCl [pH 7.5], 10 mM $MgCl_2$, 5 mM β-Glycerophosphate, 2 mM DTT, and 0.1 mM Na_3VO_4), and reactions were performed at 30^{o}C in 50 μl kinase buffer containing 100 μg/ml 3xFLAG peptides, 200 μM ATP, and either purified HA-AKT wild-type or kinase-dead as indicated. After 30 minutes, reaction mixtures were boiled for 5 min in SDS sample buffer, and subjected to SDS-PAGE and immunoblot analysis. For measuring native TBK1 kinase activity, WT MEFs were starved overnight and

treated as indicated. IP kinase assays were then performed by using anti-TBK1 antibody (Cell Signaling) and His-tagged AKT as substrate following above-mentioned procedure.

Chemical compound screen. A library of 256,953 kinase inhibitor-biased compounds were screened against full-length TBK1 (Invitrogen) using an HTRF assay from the CisBio KinEase system. Compounds were screened at single dose of 25 μM in the presence of 6 nM TBK1, 1 μM STK3, and 10 μM ATP (2xKm) using the HTRF KinEASE S3 kit. 917 compounds which inhibited >40% of TBK1 activity were selected for single-point reconfirmation. Dose-response studies were performed on 818 confirmed hits, and compounds with IC_{50} < 1 μM were selected for follow-up studies. Compound II was found to be a potent inhibitor of TBK1 and IKKε in both biochemical and cell-based assays. In-house kinase cross-screening revealed a reasonable selectivity profile in that Compound II does not inhibit IKK α/β kinases and known kinase mediators of the PI3K-AKT-mTOR pathway.

Yeast two-hybrid screens. The coding sequences for amino acids 1-222 of human AKT1 (GenBank gi:6224101) and amino acids 111 – 222 of human AKT2 (GenBank gi: 6715585) were cloned into pB6 as a C-terminal fusion to Gal4 DNA Binding Domain. The constructs were used as baits to screen at saturation a highly complex, random-primed human placenta cDNA library constructed in pP6. pB6 and pP6 derive from the original pAS2ΔΔ (Fromont-Racine, Rain et al. 1997) and pGADGH (Bartel, Chien et al. 1993) plasmids, respectively. 60 million clones (6-fold the complexity of the library) were screened with each bait using a

mating approach with Y187 (matα) and CG1945 (mata) yeast strains as previously described (Fromont-Racine, Rain et al. 1997). Positive colonies were selected on a medium lacking tryptophan, leucine and histidine. The prey fragments of the positive clones were amplified by PCR and sequenced at their 5' and 3' junctions. The resulting sequences were used to identify the corresponding interacting proteins in the GenBank database (NCBI) using a fully automated procedure. A confidence score (PBS, for Predicted Biological Score) was attributed to each interaction as previously described (Formstecher, Aresta et al. 2005). The PBS relies on two different levels of analysis. First, a local score takes into account the redundancy and independency of prey fragments, as well as the distribution of reading frames and stop codons in overlapping fragments. Second, a global score takes into account the interactions found in all the screens performed at Hybrigenics using the same library. This global score represents the probability of an interaction being nonspecific. For practical use, the scores were divided into four categories, from A (highest confidence) to D (lowest confidence). A fifth category (E) specifically flags interactions involving highly connected prey domains previously found several times in screens performed on libraries derived from the same organism. Finally, several of these highly connected domains have been confirmed as false-positives of the technique and are now tagged as F. The PBS scores have been shown to positively correlate with the biological significance of interactions (Rain, Selig et al. 2001, Wojcik, Boneca et al. 2002).

Orthotopic xenograft tumor models. 6-8 week old female NOD/SCID mice were purchased from an on-campus supplier. Animals were housed in a pathogen free facility and all animal

studies were performed on a protocol approved by the IACUC at the University of Texas Southwestern Medical Center. For the orthotopic breast cancer model, SCID mice were anesthetized using inhaled isoflurane and 5 x 10^6 naïve or infected MDA-MB-231 cells were injected into the mammary fat pad (MFP) using previously described techniques (Roland, Dineen et al. 2009). Briefly, a small incision was made over the right axillary fat pad and the cells were injected in a volume of 50 µl using a 30-gauge needle. The incision was closed with a simple suture. Caliper measurements were performed twice weekly and tumor volume was calculated as D x d^2 x 0.52, where D is the long diameter and d is the perpendicular short diameter. Animals were sacrificed on post-injection day 48. At necropsy, tumor weights were calculated and lung metastases were evaluated by visual inspection. For the orthotopic pancreatic cancer model, animals were anesthetized using inhaled isoflurane. The abdominal wall and peritoneum were opened and the inferior pole of the spleen and tail of the pancreas were externalized through the wound. 1 x 10^6 naïve or infected Mia-Paca-2 cells in 50 µl PBS were injected into the tail of the pancreas using a 30g needle. The skin and abdominal musculature were closed with a non-absorbable suture. Mice were monitored and weighed twice weekly. Animals were sacrificed at 7 weeks post-injection. At necropsy, liver, nodal, splenic, GI and peritoneal metastases were evaluated by visual inspection. Tumors weights were calculated in conjunction with residual pancreas (Dineen, Lynn et al. 2008).

Complementation assays. Mia-Paca2 cells were seeded at 2.5x10^3 into 96-well format in triplicate and incubated overnight. Twenty-four hours later cells were transfected with constructs encoding either empty vector (EV) or constitutively-activated myristoylated-AKT

(myr-AKT) by using ExGen 500. Forty-eight hours post-transfection, cells were infected with 90 µl of lentiviral particles containing indicated shRNAs for 2 hours, and then virus-containing medium (Opti-MEM) was replaced with 100 µl normal medium. On day 3 post-infection, cells were given fresh medium. On day 6, cells were equilibrated at r.t. for 30 min and then CellTiter-Glo reagent (15 µl) was added to each well. After 10 min incubation, samples were analyzed using an Envision plate reader.

Measurement of interferonß production. Wild WT and TBK1$^{-/-}$ MEFs were seeded at $3x10^3$ into 96-well format in triplicate and incubated overnight. Cells were either maintained in the presence of serum, serum starved, or glucose deprived overnight, and then treated with Sendai viruses, EGF, or glucose respectively for 19 hours as indicated. Expression of interferonβ was measured using the mouse interferonβ ELISA (PBL Biomedical Laboratories).

Quantitative cytokine gene expression assays. Bone marrow derived macrophages were obtained by culturing C57/BL6 mice bone marrow cells in RPMI medium containing 10% FBS and 100ng/ml CSF-1 (Amgen Inc) for 6 days. To test the effect of TBK1 inhibitors on LPS induced gene expression, bone marrow derived macrophages were stimulated with 10ng/ml LPS (Sigma Aldrich) for 3 hours. mRNA was prepared using a standard mRNA extraction kit (Qiagen Inc). Real-time PCR was performed using the ABI PRISM 7900HT sequence detection system (PerkinElmer). Primers and probes were purchased from Applied

Biosystems. Values were calculated based on standard curves generated for each gene. Expression levels of gene of interest were expressed relative to GAPDH.

Primers, siRNAs, and shRNAs. Synthetic siRNAs targeting TBK1 and Sec3 were obtained from Dharmacon. The followings are sense sequences of siRNA: Sequences of siTBK1-1 (5'-GACAGAAGUUGUGAUCACAdTdT-3') and siTBK1-2 (5'-CCUCUGAAUACCAUAGGAUdTdT-3') were previously described. siRNA pools targeting TBK1 (siGENOME) were a mixture of four independent siRNA containing the following sense sequences:

D-003788-01 (5'-GAACGUAGAUUAGCUUAU-3');

D-003788-02 (5'-UGACAGAGAUUUACUAUCA-3');

D-003788-06 (5'-UAAAGUACAUCCACGUUAU-3');

D-003788-07 (5'-GGAUAUCGACAGCAGAUUA-3').

siRNA pools targeting Sec3 (siGENOME) were a mixture of four independent siRNA containing the following sense sequences:

D-013312-01 (5'- 5'-GAAAUUAACUGGAUCUACU-3'-3');

D-013312-02 (5'- GUAAAGUCAUUAAGGAGUA-3');

D-013312-03 (5'- GAAUGUAGCUCUUCGACCA-3');

D-013312-04 (5'- GAUUAUUUAUCCCGACUAU-3').

Lentiviral shRNAs expression constructs were based on the following hairpin sequences:

pLKO.1-shTBK1-3 (Clone ID: TRCN0000003183: CCGGGTATTTGATGTGGTCGTGTA ACTCGAGTTACACGACCACATCAAATACTTTTT);

pLKO.1-shTBK1-4 (Clone ID: TRCN0000003184: CCGGCCAGGAAATATCATGCGTGT

TCTCGAGAACACGCATGATATTTCCTGGTTTTT);

pLKO.1-shTBK1-6 (Clone ID: TRCN0000003186: CCGGCGGGAACCTCTGAATACCA

TACTCGAGTATGGTATTCAGAGGTTCCCGTTTTT);

pLKO.1-shGFP: GCCCGCAAGCTGACCCTGAAGTTCATTCAAGAGATGAACTTCA

GGGTCAGCTTGCTTTTT)

CHAPTER THREE

AMINO ACID SENSING AND REGULATION OF mTORC1

INTRODUCTION

mTORC1 Signaling

Dynamic balance of cell growth and cell death is sophisticatedly and tightly regulated by various molecular mechanisms in eukaryotic cells. Among these signaling pathways, mechanistic/mammalian target of rapamycin complex 1 (mTORC1) is the master regulator of cell growth. Thus, deregulation of mTORC1 pathway is frequently observed in human cancers and metabolic disorders. During the development of human cancer, deletion or suppression of tumor suppressors, including NF1, PTEN, TSC1/2, and LKB1, as well as activating mutation or amplification of oncogenes, such as receptor tyrosine kinases, Ras and PI3K, all lead to the activation of mTORC1 pathway. Moreover, autophagy, nutrients (e.g. glucose and amino acids), stress resulted from hypoxia, energetic imbalance, inflammation and DNA damage, are known to regulate mTORC1 activity. Collectively, these findings not only show the complexity of mTORC1 signaling network, but also demonstrate the biological significance of mTORC1 pathway in molecular, cellular and organismal aspects (Shaw and Cantley 2006, Polak and Hall 2009, Howell and Manning 2011, Proud 2011, Zoncu, Efeyan et al. 2011, Inoki, Kim et al. 2012)

.

Molecular components of mTORC1

mTOR is a conserved Ser/Thr protein kinase belonging to the PIKK family and forms mTORC1 and mTORC2 by associating with adaptor proteins, Raptor and Rictor respectively, which are required for complex assembly and determination of substrate specificity. mTORC2 contains five core components (mTOR, mLST8, Rictor, mSIN1, and PROTOR) and one suppressor (DEPTOR), whereas mTORC1 is composed of three core components (mTOR, mLST8 and Raptor) as well as two negative regulators (DEPTOR and PRAS40) (Sengupta, Peterson et al. 2010, Yecies and Manning 2011, Efeyan, Zoncu et al. 2012).

mTORC1 and protein synthesis

Ribosomal S6 kinase (S6K) and eukaryotic initiation factor 4E-binding protein 1 (4E-BP1) are the most well-known mTORC1 substrates participating in mTORC1-mediated protein translation. mTORC1 activates S6K by directly phosphorylating multiple residues at the c-terminal region of S6K. Upon activation, S6K then phosphorylates 40S ribosomal protein S6, elongation factor 2 kinase (eIF2K), eIF4A-binding protein (eIF4B), and programmed cell death protein 4 (PDCD4) that binds to and inhibits eIF4A. Association of 4E-BP1with eIF4E negatively regulates eIF4E-modulated translation initiation. Phosphorylation of 4EBP1 by mTORC1 disrupts this 4EBP1-eIF4E complex, and then released eIF4E recruits translation initiation factors and ribosomal subunits to the 5'end of mRNA to activate mRNA translation. To stimulate protein synthesis, mTORC1 also enhances ribosome biogenesis and expression of 5'-terminal oligo pyrimidine (5'TOP)

mRNAs that include ribosomal proteins, translation and elongation factors. Besides 5'TOP mRNA, mTOR also stimulates a subset of mRNAs to promote cell growth and metabolism. These mRNAs contain complex secondary structure of 5'UTR and encode transcription factors (e.g. Myc and HIF1), growth factors (EGF, IGF, and FGF) and cyclin D, which are all well recognized proteins involved in both physiological settings and tumorigenesis (Wullschleger, Loewith et al. 2006, Ma and Blenis 2009, Sengupta, Peterson et al. 2010, Topisirovic and Sonenberg 2011, Yecies and Manning 2011).

mTORC1 and autophagy

Autophagy is a recycling process to maintain the homeostasis of proteins and organelles, which is mediated by an ULK1-ATG13-FIP200 protein complex and lysosome-dependent catabolic machinery (Ganley, Lam du et al. 2009, Hosokawa, Hara et al. 2009, Jung, Jun et al. 2009). Mounting evidence suggests that the Ying-Yang relationship between mTORC1 and autophagy is critical for the equilibrium of catabolic and anabolic cell growth. Upon nutrient deprivation or environmental stresses, ULK1 negatively regulates mTORC1 activity by disrupting mTORC1 complex and hindering the mTORC1 substrate accessibility by phosphorylating Raptor (Dunlop, Hunt et al. 2011, Jung, Seo et al. 2011). In the nutrient-rich environment, however, mTORC1 inhibits ULK1 kinase activity by directly phosphorylating ULK1 and ATG13 (Chan 2009, Hosokawa, Hara et al. 2009). Recent findings suggest that RalB, Sec5, and Exo84 exocyst subcomplexes play an essential role to function as a platform to mobilize mTORC1 and ULK1 in response to nutrient availability (Bodemann, Orvedahl et al. 2011). In the presence of nutrients, transcription factor EB

(TFEB), which contributes to lysosome biogenesis, is phosphorylated and inhibited by mTORC1. Nevertheless, in nutrition-deficient conditions, TFEB is released due to suppression of mTORC1. Thus TFEB shuttles into the nucleus to coordinate lysosome biogenesis by inducing lysosomal genes (Pena-Llopis, Vega-Rubin-de-Celis et al. 2011, Martina, Chen et al. 2012, Roczniak-Ferguson, Petit et al. 2012, Settembre, Zoncu et al. 2012, Martina and Puertollano 2013).

mTORC1 and metabolism

Accumulation of building blocks is a key step for cell growth and proliferation. mTORC1 pathway controls numerous metabolic pathways, including glycolysis, lipid and amino acid metabolisms as well as *de novo* pyrimidine synthesis and pentose phosphate pathway. For example, mTORC1 modulates glycolysis through regulating transcription factors Myc and HIF-1(Yecies and Manning 2011). Several reports also suggest that mTORC1 coordinates lipid metabolism by regulating SREBPs through lipin1 and S6K1 (Porstmann, Santos et al. 2009, Laplante and Sabatini 2010, Peterson, Sengupta et al. 2011, Yecies and Manning 2011, Owen, Zhang et al. 2012, Shao and Espenshade 2012). Recent findings also suggests that mTORC1-S6K axis contributes to *de novo* pryrimdine synthesis by phosphorylating S1859 on CAD (carbamoyl-phosphate synthetase 2, aspartate transcarbamoylase, dihydroorotase). Thus, activated CAD facilitates *de novo* pyrimidine synthesis by catalyzing the first three steps in this reaction (Ben-Sahra, Howell et al. 2013, Robitaille, Christen et al. 2013).

Regulation of mTORC1

Growth factors (e.g. EGF, Insulin, IGF-1) activate mTORC1 mainly by promoting the phosphorylation and inhibition of TSC2 that associates with TSC1/TBC1D7 and functions as a GAP of small GTPase Rheb (Dibble, Elis et al. 2012). AKT as well as MAPK and RSK directly phosphorylate TSC2, which disrupts the TSC complex and leads to accumulation of GTP-loaded Rheb that subsequently activates mTORC1 (Mendoza, Er et al. 2011). AMPK is responsive to reduced AMP/ATP ratio, caused by glucose deprivation and hypoxic stress. Upon stimulation, AMPK directly phosphorylates and activates TSC2 to suppress mTORC1(Inoki, Zhu et al. 2003). Phosphorylation of Raptor by AMPK also suppresses mTORC1 activity (Gwinn, Shackelford et al. 2008). REDD1, a HIF-1 target gene and stress response protein, negatively regulates mTORC1 in response to hypoxic stress, DNA damage, and energy depletion while the molecular mechanism underlying REDD1-mediated mTORC1 inhibition remains unclear (DeYoung, Horak et al. 2008, Horak, Crawford et al. 2010, Vadysirisack, Baenke et al. 2011, Wolff, Vega-Rubin-de-Celis et al. 2011, Tan and Hagen 2013). IKKβ-mediated phosphorylation and inhibition of TSC1 also induce mTORC1 activity (Lee, Kuo et al. 2007). Recent phosphoproteomic studies indicate that mTORC1 substrate Grb10 is a negative regulator of the growth factor-mediated mTORC1 signaling (Hsu, Kang et al. 2011, Yu, Yoon et al. 2011). The assembly of TTT-RUVBL1/2 complex is required for mTORC1 lysosomal localization and dimerization. Metabolic catastrophe caused by depletion of glucose and glutamine results in the disassembly of TTT-RUVBL1/2 complex, which leads to the inactivation of mTORC1 (Kim, Hoffman et al. 2013).

mTORC1 and amino acid sensing

mTORC1 integrates signaling inputs from nutrients, growth factors, stress, and environmental cues. During anabolic processes, one of the limiting steps of protein synthesis is amino acid availability. Not surprisingly, amino acids, such as leucine, glutamine, and arginine, harness mTORC1 activity to promote cell growth. Recent findings shed new light on the molecular mechanism underlying amino acid-induced mTORC1 activation. Upon exposure to amino acids, vATPase signals to lysosomal Ragulator complex (p18, p14, MP1, HBXIP and C7orf59) which controls the nucleotide exchanges of Rag heterodimeric. By Ragulator-dependent switch of GDP-RagA/B-GTP-RagC/D to GTP-RagA/B-GDP-RagC/D, Rag heterodimers recruits mTORC1 to lysosomes, where mTORC1 is activated and phosphorylates its downstream substrates (Wang and Proud 2011, Efeyan, Zoncu et al. 2012, Jewell, Russell et al. 2013). Recent studies suggest autophagic adaptor, p62, which binds to polyubiquitin chains and LC3, participates in amino acid-induced mTORC1 signaling by interacting with mTOR and Raptor to mobilize the mTORC1 complex to lysosomes and also facilitate the formation of active Rag heterodimer (Duran, Amanchy et al. 2011, Moscat and Diaz-Meco 2011). Additionally, it's been reported that SLC1A5 promotes glutamine uptake to create an intracellular glutamine pool that is required for bi-directional transporter SLC7A5, by pumping out glutamine, to facilitate leucine influx to activate mTORC1 (Nicklin, Bergman et al. 2009). Moreover, leucine and glutamine signal to Rag GTPase to activate mTORC1 via glutaminolysis and production of α-ketoglutarate (Duran, Oppliger et al. 2012). Interestingly, recent findings suggest Leucyl-tRNA synthetase (LRS) contributes to

mTORC1 signaling by functioning as an intracellular leucine sensor (Han, Jeong et al. 2012). Furthermore, G protein-coupled taste receptors TAS1R1 and TAS1R3 support mTORC1 signaling by sensing extracellular amino acids and promoting the translocation of mTORC1 to lysosomes (Han, Jeong et al. 2012, Wauson, Zaganjor et al. 2012, Wauson, Zaganjor et al. 2013).

IKKε: an innate immune response and cancer gene

IKKε, like TBK1, is a family member of the non-canonical IKK protein kinases and activates IRF3 and IRF7 to mediate the interferon response to bacterial and viral infection. Unlike TBK1, which is ubiquitously expressed in human cells, IKKε protein is inducible in lymphoid and other cell types upon exposure to pathogens. Although IKKε was initially identified as an amplified and overexpressed breast cancer oncogene that deflects apoptosis by activating the NF-κB pathway, amplification and overexpression of IKKε gene has been observed in a variety of human tumors, including pancreatic ductal adenocarcinoma, glioma, prostate, ovarian and non-small cell lung cancers (Boehm, Zhao et al. 2007, Barbie, Tamayo et al. 2009, Guo, Shu et al. 2009, Cheng, Guo et al. 2011, Guan, Zhang et al. 2011, Guo, Coppola et al. 2011, Li, Chen et al. 2012). IKKε is critical for cells to tolerate DNA-damage-induced apoptosis via the NF-κB pathway. In response to DNA damage, sumoylated IKKε translocates to the nucleus, where it colocalizes with PML nuclear bodies and phosphorylates p65 (Renner, Moreno et al. 2010). These findings implicate IKKε as a potential therapeutic target in chemoresistance. Another known IKKε substrate is tumor suppressor CYLD. IKKε directly phosphorylates CYLD at Ser418 both *in vitro* and *in vivo* to suppress CYLD

deubiquitinase activity, which is critical for IKKε -mediated cellular transformation (Hutti, Shen et al. 2009). During innate immune response, CYLD negatively regulates RIG-I-IKKε /TBK1 axis by controlling RIG-I ubiquitination. Loss of CYLD results in constitutive activation of IKKε and TBK1 as well as interferon hyper-production upon viral infection (Friedman, O'Donnell et al. 2008, Zhang, Wu et al. 2008). Nevertheless, it remains unclear if CYLD suppresses tumorigenesis by negatively regulating oncogenic IKKε and TBK1 signaling.

William Hahn and colleagues demonstrated that IKKε is essential for breast cancer cell survival and the gene encoding IKKε is frequently amplified in human breast tumors. IKKε can substitute for PI3K-AKT signaling in malignant transformation, implicating that IKKε may activate the AKT pathway or IKKε may share some downstream signaling components with the AKT pathway (Boehm, Zhao et al. 2007). Accumulating evidence indicates that IKKε directly phosphorylates AKT at both Thr308 and Ser473 in vitro and activates AKT in cells via an mTORC2-independent pathway, whereas it remains controversial if PI3K plays a critical role for IKKε -mediated AKT phosphorylation and activation (Guo, Coppola et al. 2011, Xie, Zhang et al. 2011). Of note, pharmacological inhibition of PI3K does not suppress phosphorylation of AKT in IKKε-overexpressed human lung cancer cell line H1299 and IKKε knockout cells. Moreover, IKKε -induced AKT activation is resistant to AKT inhibitor API-2, a small molecule inhibitor targeting the AKT PH domain, and IKKε -mediated AKT phosphorylation is independent of AKT PH domain and PDK1 protein. Expression of dominant negative p85a mutant only selectively inhibits insulin-induced AKT phosphorylation but has no effect towards IKKε expression-induced

AKT phosphorylation (Guo, Coppola et al. 2011). Notably, insulin-induced AKT phosphorylation in IKKε expressing HeLa cells is reduced only by PI3K inhibitors, LY294002 and Wortmannin, but not by mTOR kinase inhibitor Torin 1 (Xie, Zhang et al. 2011). However, it remains unclear whether endogenous IKKε activates AKT through a PI3K-dependent mechanism or not. Importantly, increased IKKε protein expression is associated with elevated phosphorylation of AKT in human primary breast tumors and AKT signaling is required for IKKε-mediated malignant transformation (Guo, Coppola et al. 2011).

RESULTS

TBK1 contributes to mTORC1 activity by amino acids

While I was examining potential signaling pathways that may be regulated by TBK1 through a gain-of-function approach, I found that expression of wildtype, but not kinase-dead, TBK1 was sufficient to drive auto-phosphorylation of mTOR at Ser2481 (Figure 3.1A). Coimmunoprecipitation assays also indicated that both wildtype and kinase-dead TBK1 interact with mTOR, and phosphorylation of mTOR at Ser2481 and Ser2448 was enhanced when mTOR associated with wild-type TBK1 (Figure 3.1B). It's been shown that mTORC1-associated mTOR Ser2481 autophosphorylation depends upon the presence of amino acids and phosphorylation of Ser2448 is dependent upon S6K activity (Chiang and Abraham 2005, Varma and Khandelwal 2007, Copp, Manning et al. 2009, Vazquez-Martin, Oliveras-Ferraros et al. 2009, Rosner, Siegel et al. 2010, Soliman, Acosta-Jaquez et al. 2010). These results prompted me to examine the functional relationship between TBK1 activation

and mTORC1 activity by amino acids. I hypothesized that TBK1 may participate in the amino acid-mediated mTORC1 signaling.

Figure 3.1

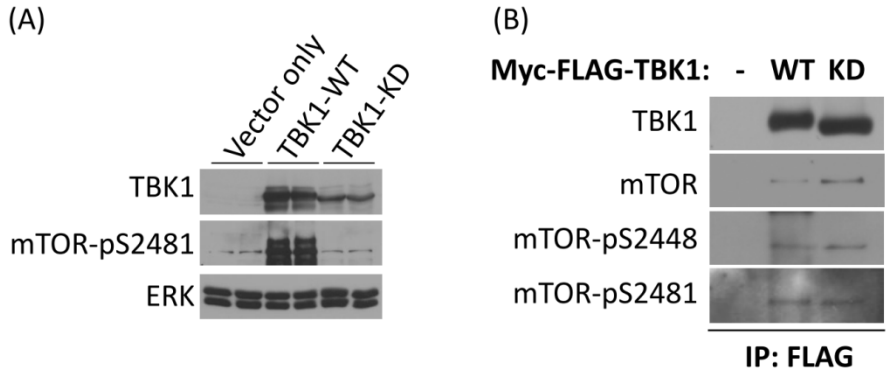

Figure 3.1. TBK1 drives mTORC1 activation.

(A) HEK293T cells were transfected with plasmids encoding wild-type (WT) or kinase-dead (KD) TBK1 as indicated. Two days post-transfection, whole cell lysates were assessed for TBK1 expression and accumulation of phosphorylated mTOR as indicated.

(B) Myc-FLAG-tagged TBK1 was expressed in HEK293T cells as indicated and then immunoprecipitated from HEK293T cell extracts. Immunoprecipitates were probed for the presence of TBK1, mTOR, and phosphorylation of mTOR at Ser2448 and Ser2481.

To examine whether amino acids regulate TBK1 activity, I first performed expression co-immunoprecipiation experiments and then analyzed the phosphorylation of TBK1-Ser172 that has been used as a marker of TBK1 kinase activity. My data demonstrated that addition of amino acids robustly induced phosphorylation of Ser172 on wildtype, but not kinase-dead, TBK1, implicating that amino acids stimulate TBK1 activity and phosphorylation of TBK1-Ser172 depends upon intact TBK1 kinase activity. Consistent with previous results, I found

that mTOR associated with TBK1 even in the amino acid-starved cells. Both wildtype and kinase-dead TBK1 associated with mTOR, whereas only wildtype TBK1 immunoprecipitates contained active mTOR, as indicated by Serine 2448 phosphorylation. Importantly, mTORC1 component Raptor also interacted with TBK1 (Figure 3.2). I also found that autophagy kinase ULK1 and exocyst proteins, Sec5 and Exo70, were recruited to TBK1 in an amino-acid dependent manner. Taken together, my data suggest that significant amounts of endogenous mTOR and Raptor are recruited to TBK1 in response to amino acids, and also implicates that TBK1 may play a novel role in regulating amino acid-mediated mTORC1 activation through a kinase-dependent mechanism.

Figure 3.2

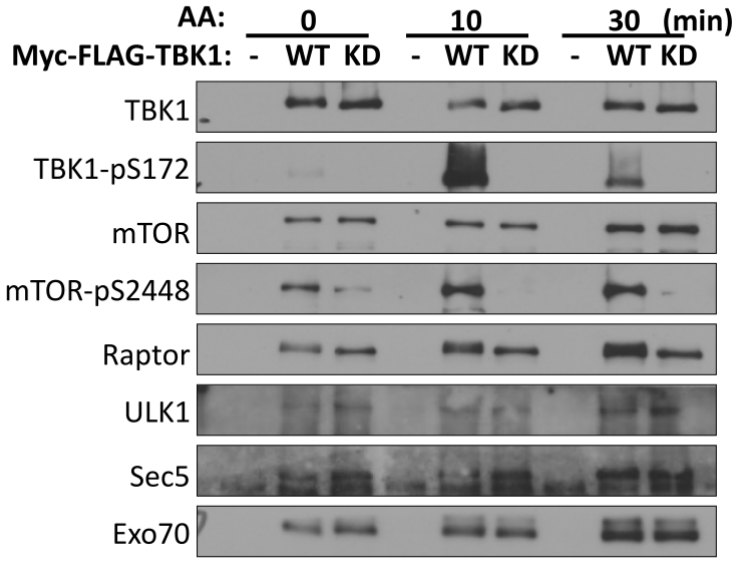

Figure 3.2. TBK1 is stimulated by amino acids and recruits mTORC1. Myc-FLAG-tagged TBK1 was expressed in HEK293T cells as indicated. Two days post-transfection, amino acids were depleted for 50 minutes and then cells were stimulated with amino acid as indicated. Immunoprecipitates were probed for the presence of indicated proteins.

To examine native TBK1/mTOR complex assembly, I tested the capacity of endogenous TBK1 to coimmunoprecipitate endogenous mTOR upon amino acids exposure. In amino acid starved condition, TBK1 interacts with mTOR. Furthermore, upon amino acid stimulation TBK1 recruited more endogenous mTOR that also displayed higher activity as indicated by phosphorylation of Ser2448 (Figure 3.3A).

To assess the contribution of TBK1 to amino acid-induced mTORC1 activation, the responsiveness of TBK1 and IKKε double knockout MEFs to amino acids was evaluated. Amino acid-mediated mTORC1/S6K activity was impaired in the TBK1 and IKKε-deficient MEFs (Figure 3.3B). Consistent with this observation, amino acid-induced mTORC1 signaling was also partially blunted in TBK1 knockout MEFs (unpublished data from Jonathan Cooper, Michael White Lab). Depletion of TBK1 by siRNA in HeLa cells blunted amino acid-induced mTOR activation (Figure 3.3C), indicating that TBK1 is a novel component of the mTORC1 signaling pathway.

Figure 3.3

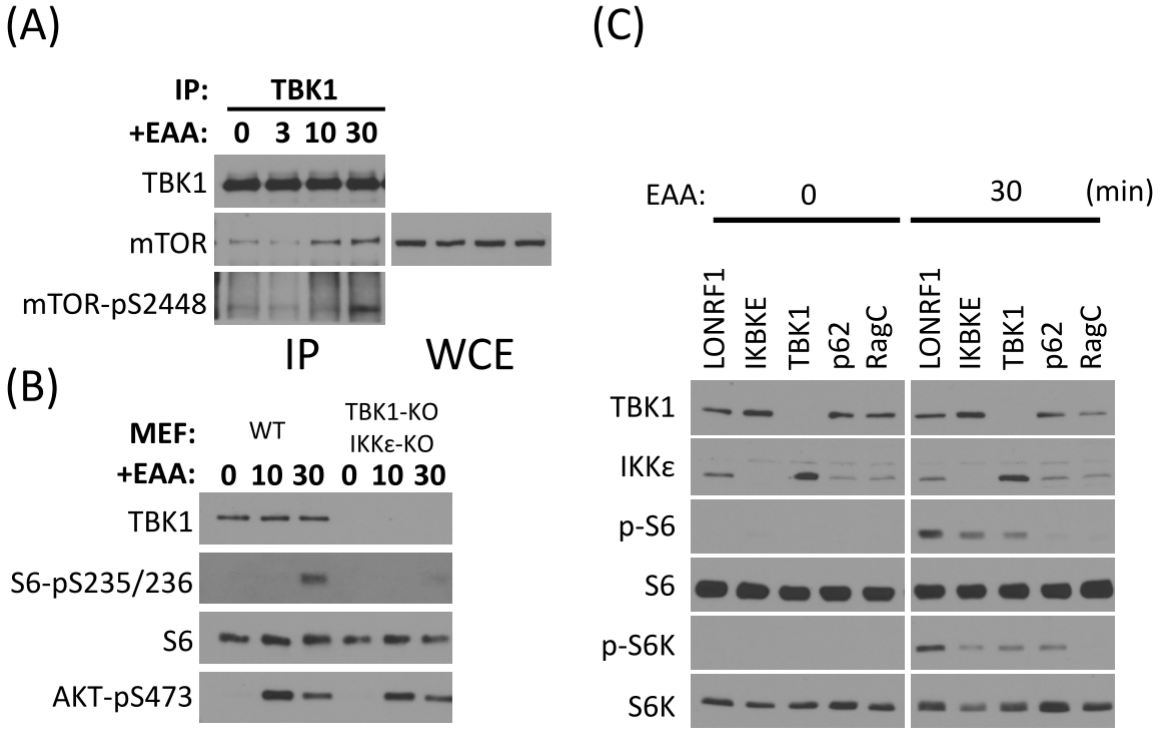

Figure 3.3. TBK1 interacts with mTORC1 and supports mTORC1 activation.

(A) HEK293T cells were plated in DMEM containing 10% FBS. After 24 hours, cells were washed twice by EBSS and then incubated with EBSS. Before EAA treatment, cells were preincubated with additional 2mM L-Glutamine and 10 uM Insulin for 1hr. EAA-treated cells were harvested and lysed. Immunoprecipitation was performed using anti-TBK1 antibody. Immunoprecipitates were probed for the presence of indicated proteins.

(B) WT and DKO (TBK1-/- and IKKε-/-) cells were plated in DMEM containing 10% FBS. After 24 hours, cells were washed twice by EBSS and then incubated with EBSS. Before EAA treatment, cells were preincubated with additional 2mM L-Glutamine for 1hr. EAA-treated cells were harvested and lysed directly by 1x SDS sample buffer at indicated time-points.

(C) HeLa cells were plated overnight in DMEM containing 10% FBS, and then transfected with the indicated siRNAs. After 3 days, cells were washed twice by EBSS and then incubated with EBSS. Before EAA treatment, cells were preincubated with additional 2mM L-Glutamine for 1hr. EAA-treated cells were harvested and lysed directly by 1x SDS sample buffer at indicated time-points.

IKKε contributes to amino acid-induced mTORC1 signaling.

I previously demonstrated that TBK1 contributes to amino acid-induced mTORC1 activation. It's been well documented that TBK1 and IKKε not only share high degrees of amino acid sequence homology, but also modulate common substrates, such as IRF3/IRF7 and AKT. Moreover, my preliminary experiments also demonstrated that knockdown of IKKε partially impaired amino acid-mediated mTORC1 signaling. (Figure 3.3B, C) These observations led me to examine whether IKKε supports mTORC1 activity by amino acids.

IKKε interacts with mTORC1

To investigate the biochemical relationship between IKKε and mTORC1, co-immunoprecipitation was performed using lysates from amino acid-treated HEK293T cells. IKKε immunoprecipitates from amino acid starved cells contained mTORC1 components, mTOR and Raptor, as well as mTORC1 substrate S6K. Of note, autophagy-initiating kinase ATG1/ULK1 were found in the same immunoprecipitates. Moreover, amino acids stimulation disrupted the interaction between IKKε and mTORC1/S6K/ULK1, which demonstrated distinct dynamics of IKKε/mTORC1 complex assembly in contrast to previous studies observed in TBK1/mTORC1 complex formation (Figure 3.4A). To investigate the endogenous interaction of IKKε-mTOR complex, I examined the capacity of endogenous IKKε to coimmunoprecipitate endogenous mTOR upon amino acid exposure. I found that mTOR associated with IKKε in amino acid starved HEK293 cells (Figure 3.4B). Although I previously demonstrated that amino acid stimulation significantly induced the dissociation of

IKKε-mTOR complex, my endogenous coimmunoprecipitation experiments revealed that mTOR-IKKε interaction was only modestly disrupted.

Figure 3.4

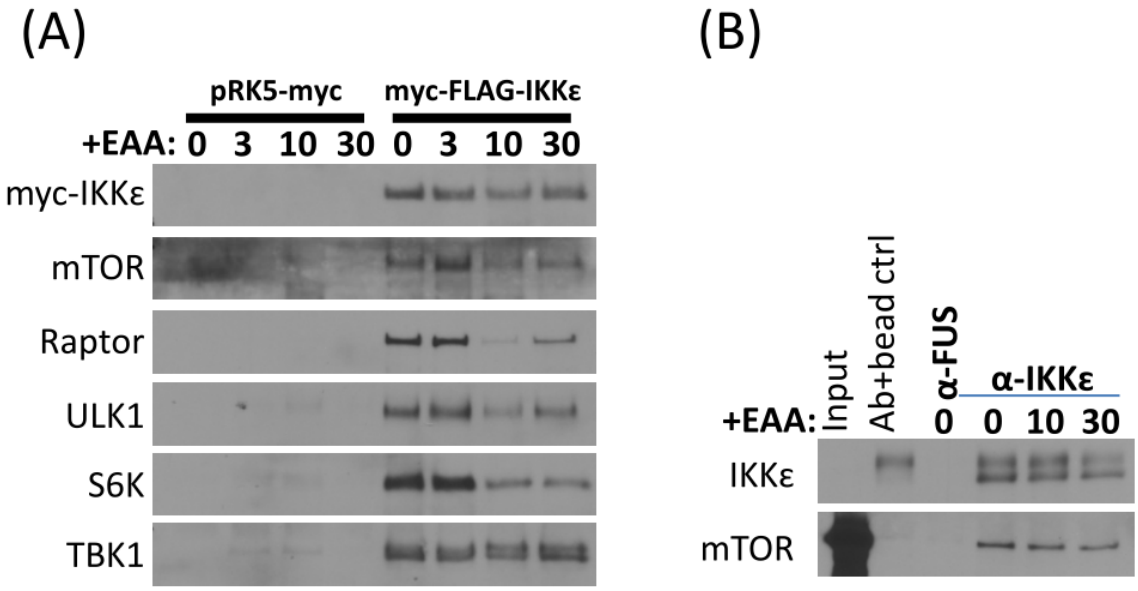

Figure 3.4. IKKε interacts with mTORC1.

(A) Myc-FLAG-tagged IKKε was expressed in HEK293T cells as indicated. Two days post-transfection, cells were washed twice by EBSS and then incubated with EBSS. Before EAA treatment, cells were preincubated with additional 2mM L-Glutamine for 1hr. EAA-treated cells were harvested and lysed. Immunoprecipitation was performed using anti-IKKε antibody. Immunoprecipitates were probed for the presence of indicated proteins.

(B) HEK293T cells were plated in DMEM containing 10% FBS. After 24 hours, cells were washed twice by EBSS and then incubated with EBSS. Before EAA treatment, cells were preincubated with additional 2mM L-Glutamine and 10 uM Insulin for 1hr. EAA-treated cells were harvested and lysed. Immunoprecipitation was performed using anti-TBK1 antibody. Immunoprecipitates were probed for the presence of indicated proteins.

Amino acids elevate IKKε kinase activity

To evaluate the effect of amino acid exposure to IKKε activity, I examined the autophosphorylation of IKKε at Ser172, which is positively correlated to IKKε specific kinase activity. After ten minutes of amino acid stimulation, I found that phosphorylation of IKKε-Ser172 was robustly induced and peaked at thirty minutes post-treatment. Moreover, phosphorylation of S6 also showed similar kinetics upon amino acid addition (Figure 3.5). These observations suggest that amino acids are a novel IKKε stimulus through an unknown mechanism and implicate that IKKε may play a role in amino acid-dependent mTORC1 activation.

Figure 3.5

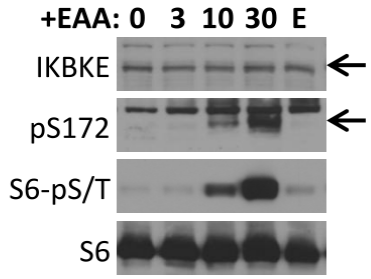

Figure 3.5. Amino acids stimulate IKKε. HEK293T cells were plated in DMEM containing 10% FBS. After 24 hours, cells were washed twice by EBSS and then incubated with EBSS. Before EAA treatment, cells were preincubated with additional 2mM L-Glutamine and 10μM Insulin for 1hr. EAA-treated cells were harvested and lysed directly by 1x SDS sample buffer at indicated time-points.

Knockdown of IKKε suppresses mTORC1 signaling

To further evaluate the contribution of IKKε to mTORC1 regulation, I depleted IKKε and RagA by pooled siRNA in HeLa cells (Figure 3.6A). Amino acid-induced mTOR activation was strongly diminished as indicated by blunted phosphorylation of S6 and S6K. Similar results were demonstrated in IKKε knockdown HEK293 cells (Figure 3.6B). To validate these results, multiple siRNAs against IKKε were examined in HeLa cells. Consistent with my results using pooled siRNAs, all three individual siRNAs impaired amino

acid-mediated mTOR activation to a similar extent (Figure 3.6C). Suppression of both TBK1 and IKKε by a TBK1/IKKε dual inhibitor from GlaxoSmithKline (GSK) substantially blocked mTORC1 activation by amino acids (Figure 3.6D). Collectively, my data suggest that IKKε may play an important role in the mTORC1 pathway, although it remains elusive how IKKε senses amino acid levels inside the cells and how IKKε contributes to amino acid-mediated mTORC1 signaling.

Figure 3.6

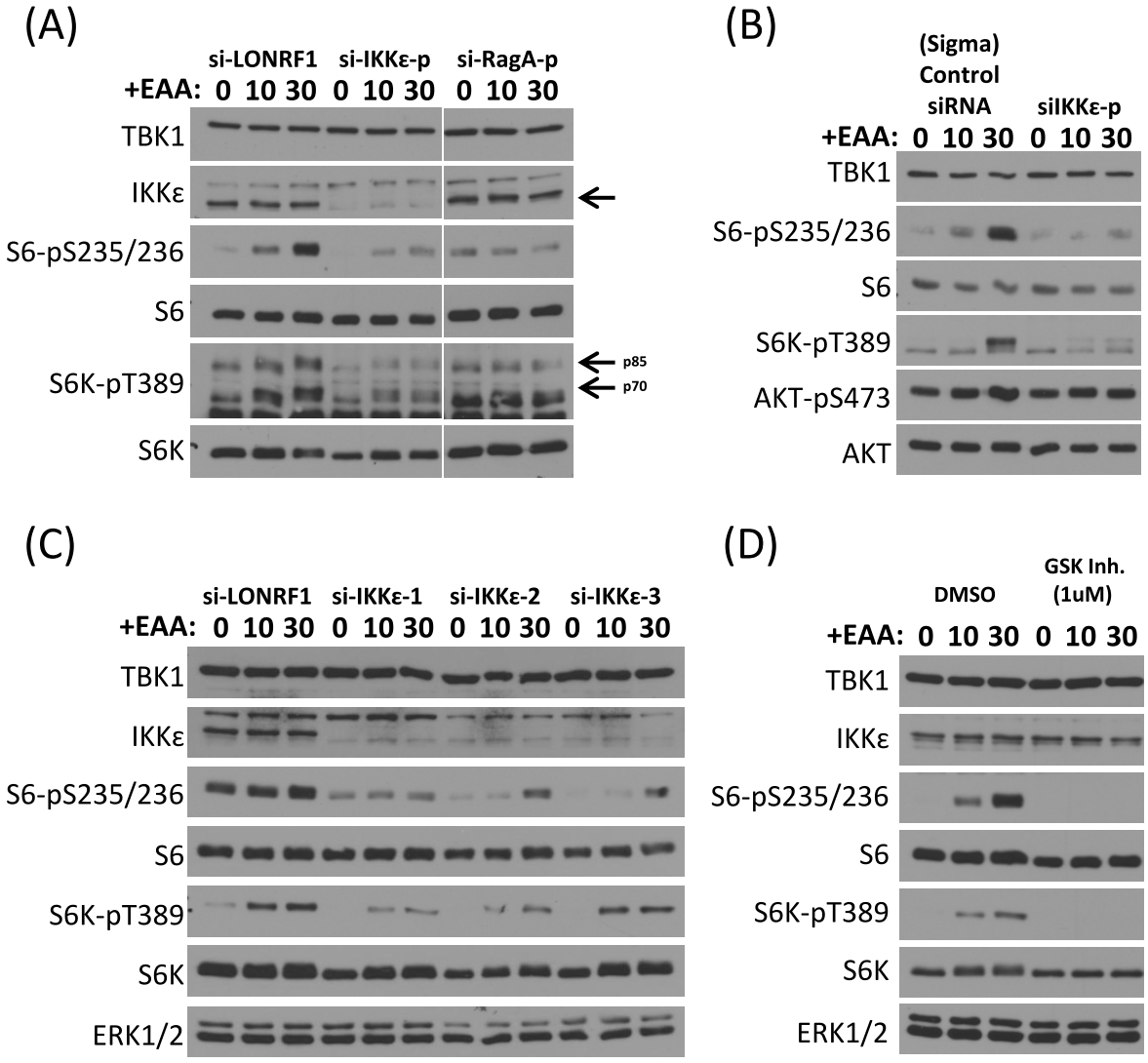

Figure 3.6. IKKε supports mTORC1 activation by amino acids.

(A) HeLa cells were plated overnight in DMEM containing 10% FBS, and then transfected with the indicated siRNAs. After 3 days, cells were washed twice by EBSS and then incubated with EBSS. Before EAA treatment, cells were preincubated with additional 2mM L-Glutamine for 1hr. EAA-treated cells were harvested and lysed directly by 1x SDS sample buffer at indicated time-points.

(B) HEK293T cells were plated in DMEM containing 10% FBS. After seeded overnight, cells were washed twice by EBSS and then incubated with EBSS. Before EAA treatment, cells were preincubated with additional 2mM L-Glutamine and 10uM Insulin for 1hr. EAA-treated cells were harvested and lysed directly by 1x SDS sample buffer at indicated time-points.

(C) HeLa cells were plated overnight in DMEM containing 10% FBS, and then transfected with the indicated siRNAs. After 3 days, cells were washed twice by EBSS and then incubated with EBSS. Before EAA treatment, cells were preincubated with additional 2mM L-Glutamine for 1hr. EAA-treated cells were harvested and lysed directly by 1x SDS sample buffer at indicated time-points.

(D) HeLa cells were plated overnight in DMEM containing 10% FBS, and then transfected with the indicated siRNAs. After 3 days, cells were washed twice by EBSS and then incubated with EBSS. Before EAA treatment, cells were preincubated with additional 2mM L-Glutamine for 1hr and treated with GSK inhibitor for 30mins. EAA-treated cells were harvested and lysed directly by 1x SDS sample buffer at indicated time points.

Candidate-based mini screen

To understand the molecular mechanism by which TBK1 and IKKε contributes to amino acid-induced mTORC1 pathway, I decided to perform a small-scale screen by knocking down known TBK1/IKKε interacting proteins and substrates. Depletion of several candidate genes significantly suppressed amino acid-mediated mTORC1 activation as indicated by phosphorylation of S6 or S6K. For example, knockdown of positive controls (taste receptor TAS1R1/TAS1R3 and amino acid transporter SLC7A5/SLC1A5/SLC3A2), TBK1/IKKε adaptor protein NAP1, suppressor CYLD, small GTPase RalA, and exocyst components Sec3, Sec6, Sec8, Sec10, and Sec15, dramatically impaired amino acid-mediated mTORC1 signaling. However, depletion of adaptor protein NEMO; suppressors SIKE, SHIP2, and A20; autophagy proteins ATG7 and ATG9, and innate immune response proteins p62, NDP52, optineurin, and STING; only modestly inhibit amino acid-induced mTORC1 activation. Interestingly, suppression of adaptor protein TANK and exocyst proteins Exo70 robustly enhanced amino acid-dependent mTORC1 activity.

Figure 3.7

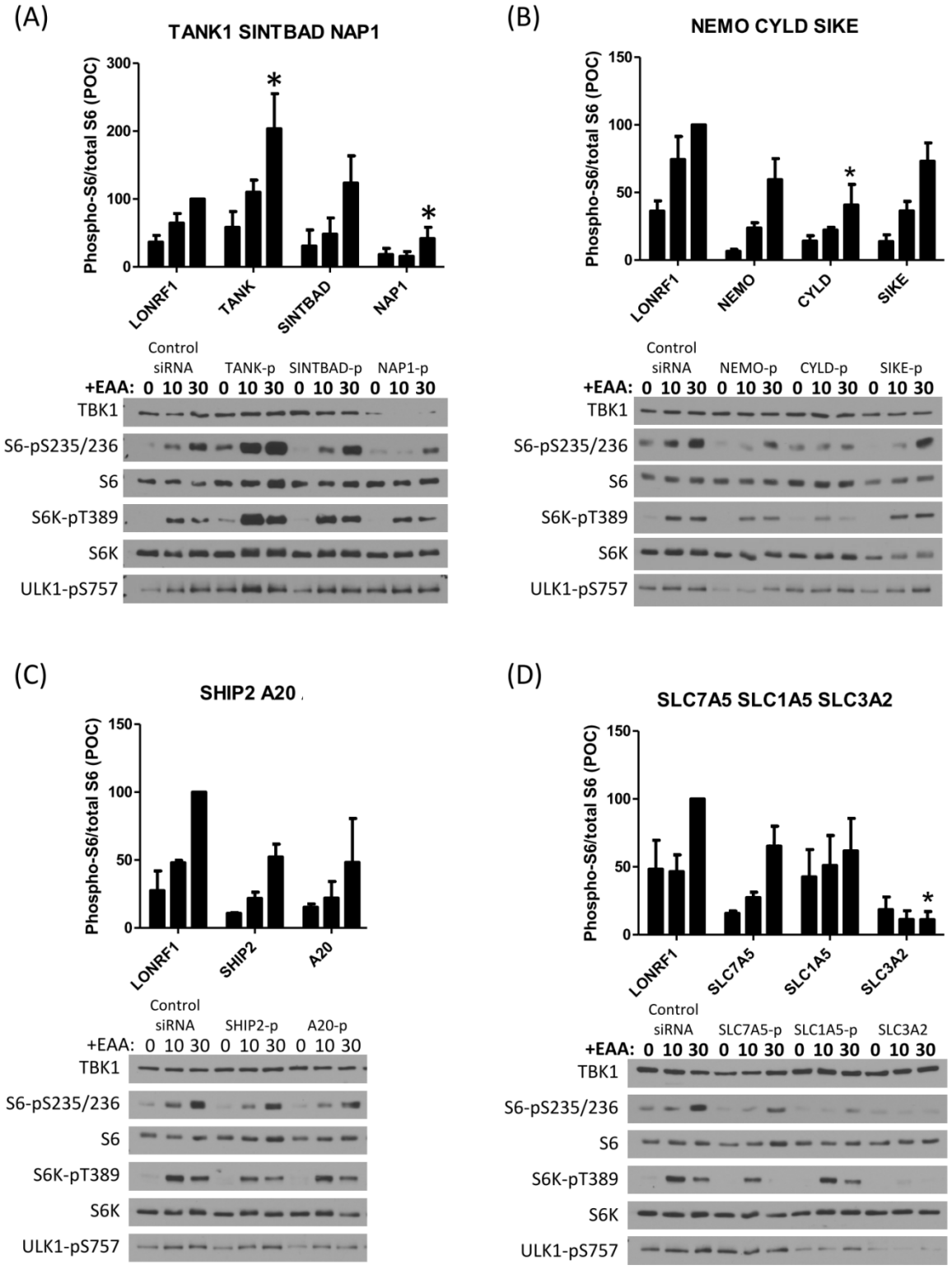
(A)
TANK1 SINTBAD NAP1
Phospho-S6/total S6 (POC)
300
200
100
0
*
*
LONRF1
TANK
SINTBAD
NAP1
Control siRNA
TANK-p
SINTBAD-p
NAP1-p
+EAA: 0 10 30 0 10 30 0 10 30 0 10 30
TBK1
S6-pS235/236
S6
S6K-pT389
S6K
ULK1-pS757
(B)
NEMO CYLD SIKE
Phospho-S6/total S6 (POC)
150
100
50
0
*
LONRF1
NEMO
CYLD
SIKE
Control siRNA
NEMO-p
CYLD-p
SIKE-p
+EAA: 0 10 30 0 10 30 0 10 30 0 10 30
TBK1
S6-pS235/236
S6
S6K-pT389
S6K
ULK1-pS757
(C)
SHIP2 A20
Phospho-S6/total S6 (POC)
150
100
50
0
LONRF1
SHIP2
A20
Control siRNA
SHIP2-p
A20-p
+EAA: 0 10 30 0 10 30 0 10 30
TBK1
S6-pS235/236
S6
S6K-pT389
S6K
ULK1-pS757
(D)
SLC7A5 SLC1A5 SLC3A2
Phospho-S6/total S6 (POC)
150
100
50
0
*
LONRF1
SLC7A5
SLC1A5
SLC3A2
Control siRNA
SLC7A5-p
SLC1A5-p
SLC3A2
+EAA: 0 10 30 0 10 30 0 10 30 0 10 30
TBK1
S6-pS235/236
S6
S6K-pT389
S6K
ULK1-pS757

Figure 3.7

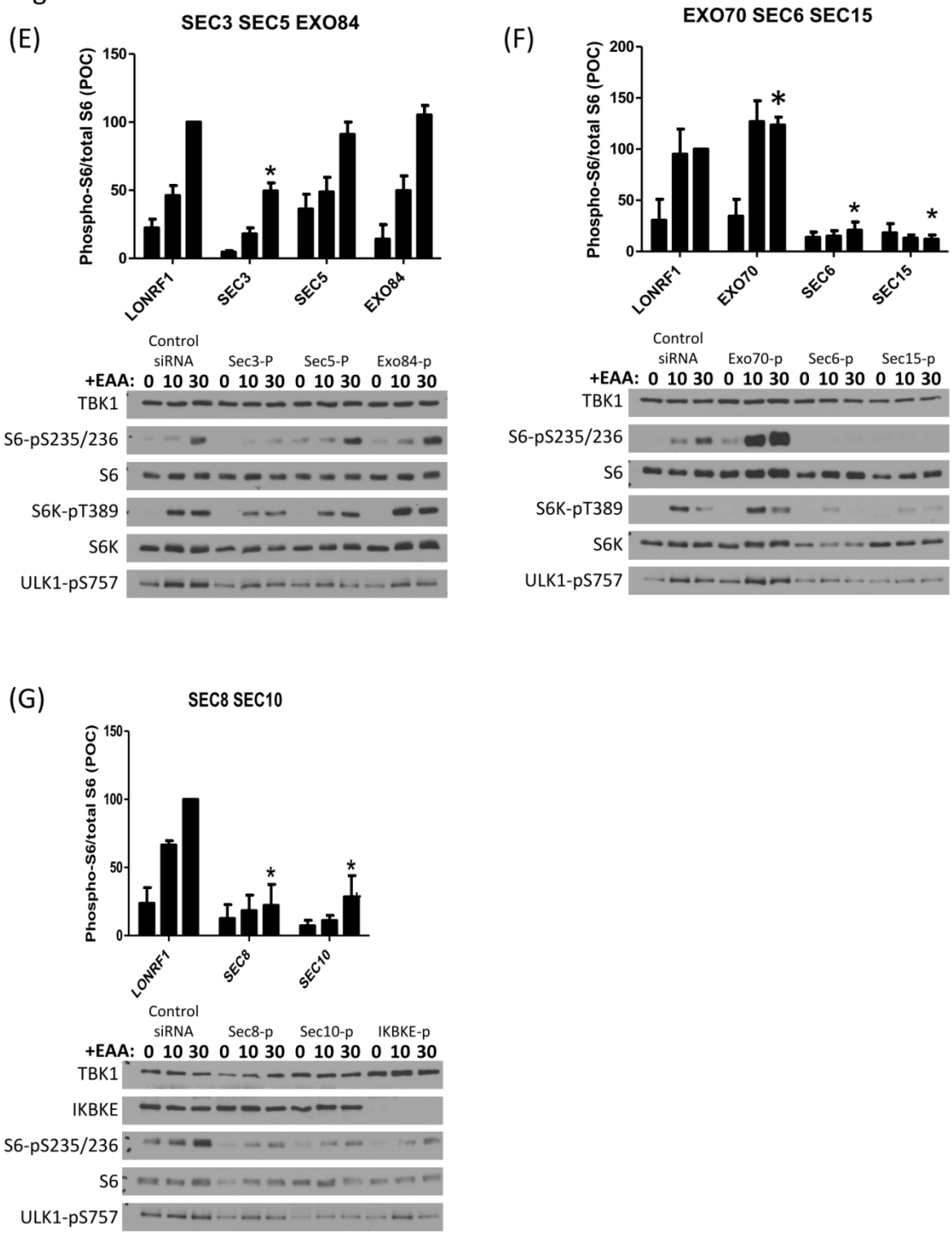
(E)
SEC3 SEC5 EXO84
Phospho-S6/total S6 (POC)
150
100
50
0
*
LONRF1
SEC3
SEC5
EXO84
Control siRNA
Sec3-P
Sec5-P
Exo84-p
+EAA: 0 10 30 0 10 30 0 10 30 0 10 30
TBK1
S6-pS235/236
S6
S6K-pT389
S6K
ULK1-pS757
(F)
EXO70 SEC6 SEC15
Phospho-S6/total S6 (POC)
200
150
100
50
0
*
*
*
LONRF1
EXO70
SEC6
SEC15
Control siRNA
Exo70-p
Sec6-p
Sec15-p
+EAA: 0 10 30 0 10 30 0 10 30 0 10 30
TBK1
S6-pS235/236
S6
S6K-pT389
S6K
ULK1-pS757
(G)
SEC8 SEC10
Phospho-S6/total S6 (POC)
150
100
50
0
*
*
LONRF1
SEC8
SEC10
Control siRNA
Sec8-p
Sec10-p
IKBKE-p
+EAA: 0 10 30 0 10 30 0 10 30 0 10 30
TBK1
IKBKE
S6-pS235/236
S6
ULK1-pS757

Figure 3.7

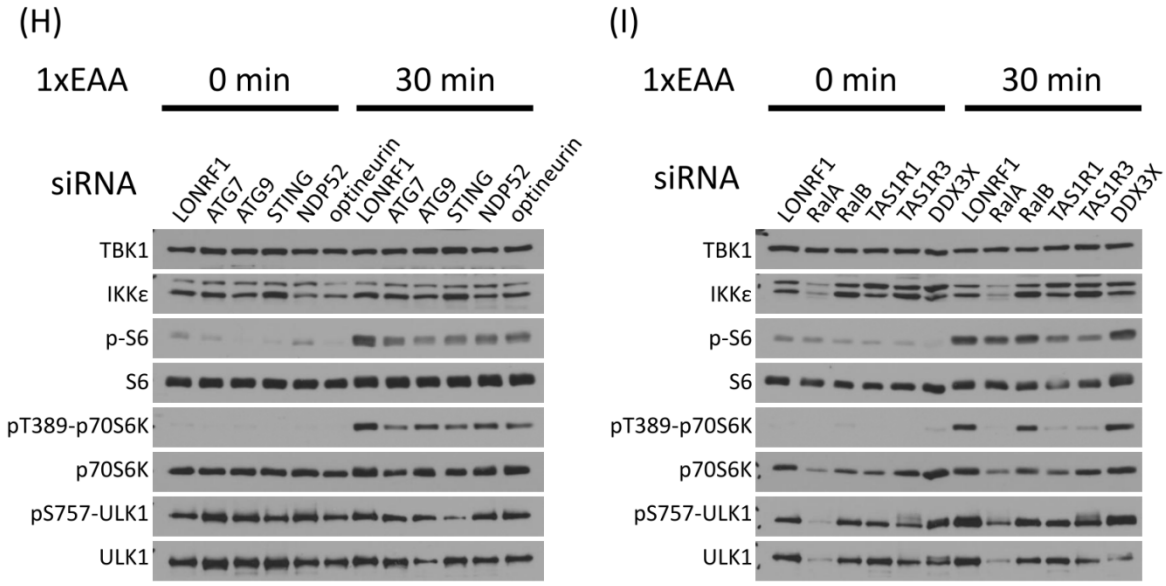

Figure 3.7. A novel set of TBK1 substrates and interacting proteins contributes to mTORC1 activation by amino acids. HeLa cells were plated overnight in DMEM containing 10% FBS, and then transfected with the indicated siRNAs. After 3 days, cells were washed twice by EBSS and then incubated with EBSS. Before EAA treatment, cells were preincubated with additional 2mM L-Glutamine for 1hr. EAA-treated cells were harvested and lysed directly by 1x SDS sample buffer at indicated time points. Significance was evaluated by T-Test. *, indicates $p<0.05$.

The MAP3K3-MAP2K5-ERK5 kinase cascade supports amino acid-induced mTORC1 activation.

Innate immunity modulator TBK1 contributes to autophagic clearance of cytosolic bacteria by phosphorylating autophagic receptor p62 at Ser403, which is critical for p62-mediated cargo capture and degradation (Pilli, Arko-Mensah et al. 2012). In addition to its role in autophagy, p62 supports amino acid-mediated mTORC1 activation by functioning as a scaffold protein to mediate heterodimerization of Rag proteins and to recruit mTORC1 to lysosomes. Of note, genetic depletion of p62 only impairs activation of mTORC1 by amino acids, but not insulin, suggesting p62 is a critical regulator of amino acid sensing in the mTORC1 pathway and p62 supports mTORC1 signaling in a context-specific manner (Duran, Amanchy et al. 2011). Nevertheless, it remains unclear how p62 senses the level of amino acids inside the cells and how p62 is regulated in response to amino acids. Although we previously demonstrated that TBK1 supports amino acid-induced mTORC1 activation, it remains unknown whether TBK1 mediates mTORC1 activation through a p62-dependent mechanism and whether p62 is regulated by another unidentified upstream kinase in response to amino acids. It has been shown that MAP3K3 and MAP2K5 both interact with p62 through PB1 domain (White 2012). Thus, I hypothesize that MAP3K3 and MAP2K5 may act as p62 upstream kinases and contribute to amino acid-dependent activation of mTORC1 via p62.

To investigate whether MAP2K5 contributes to amino acid-induced mTORC1 activation, I evaluated the responsiveness of HeLa cells to amino acids in the presence of a specific MAP2K5 inhibitor (BIX02189) (Tatake, O'Neill et al. 2008). Chemical perturbation

of MAP2K5 robustly suppressed amino acid-mediated mTORC1 activation (Figure 3.8A). Interestingly, like depletion of p62, BIX02189 did not affect mTORC1 activation by insulin (unpublished data from Malia Potts, Michael White Lab). Moreover, knockdown of MAP2K5 and p62 by pooled siRNAs substantially reduced amino acid-mediated mTORC1 signaling (Figure 3.8B). Depletion of MAP3K3 and ERK5, a MAP2K5 substrate, by siRNAs also showed similar results as knockdown of MAP2K5 (Figure 3.8C). These findings were validated by multiple siRNAs targeting individual genes. Knockdown of MAP2K5 and MAP3K3 by multiple single siRNAs blunted mTORC1 activation by amino acids (Figure 3.8D). However, it remains unknown how this MAP3K3-MAP2K5-ERK5 kinase cascade participates in amino acid-induced mTORC1 activation and what is the biochemical relationship between this kinase cascade and p62/mTORC1 complex. Of note, I also found that ULK1 immunoprecipitated with MAP2K5 from cycling cells (Figure 3.8E). Since there is a Yin-Yang relationship between mTORC1 complex and ULK1, it would be critical to understand whether MAP3K3-MAP2K5-ERK5 kinase cascade directly regulates ULK1 rather than mTORC1 complex, or like p62, contributes to both autophagy and amino acid-mediated mTORC1 activation.

Figure 3.8

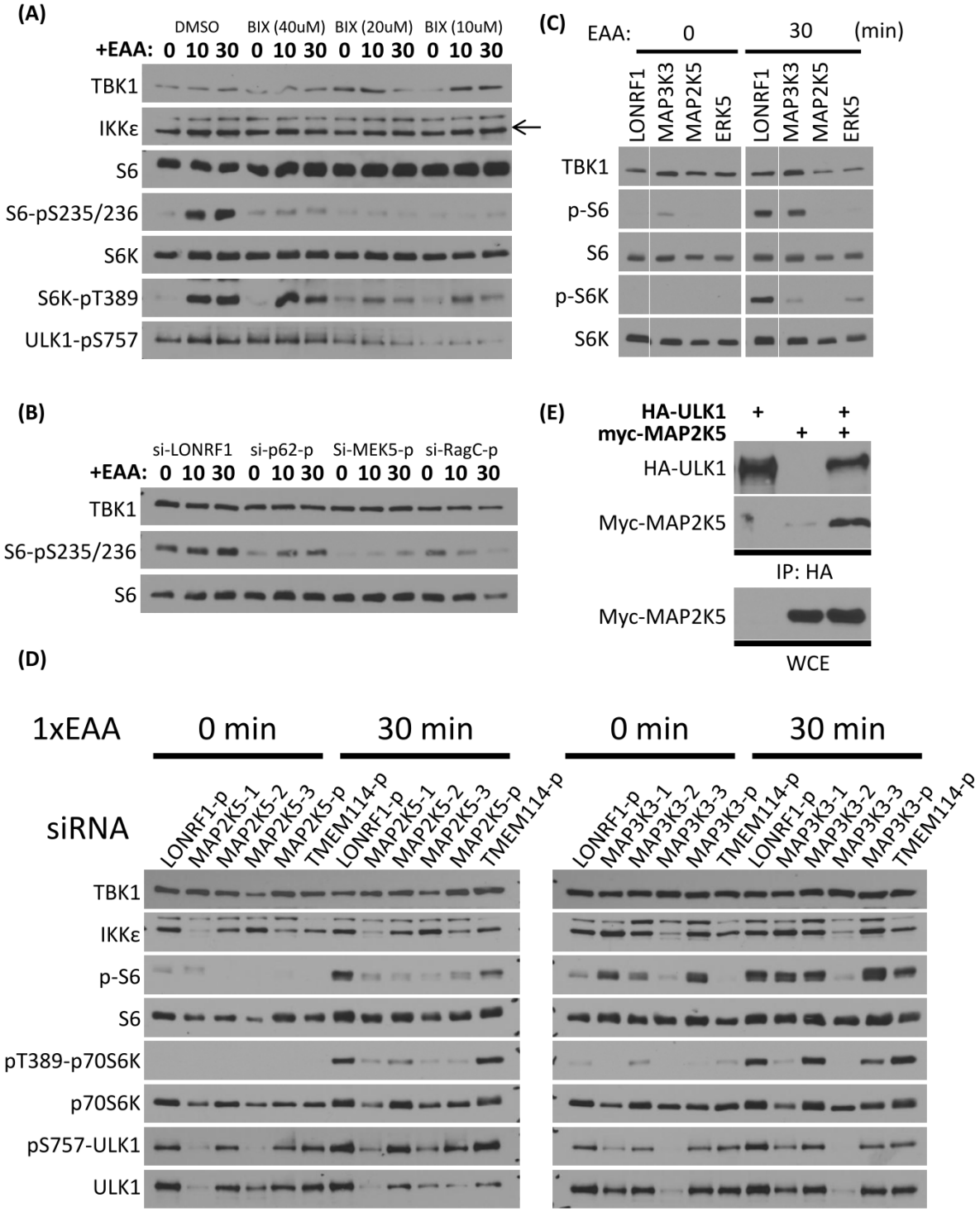
(A)
DMSO
BIX (40uM)
BIX (20uM)
BIX (10uM)
+EAA: 0 10 30 0 10 30 0 10 30 0 10 30
TBK1
IKKε
S6
S6-pS235/236
S6K
S6K-pT389
ULK1-pS757
(C)
EAA: 0 30 (min)
LONRF1
MAP3K3
MAP2K5
ERK5
TBK1
p-S6
S6
p-S6K
S6K
(B)
si-LONRF1
si-p62-p
Si-MEK5-p
si-RagC-p
+EAA: 0 10 30 0 10 30 0 10 30 0 10 30
TBK1
S6-pS235/236
S6
(E)
HA-ULK1 + +
myc-MAP2K5 + +
HA-ULK1
Myc-MAP2K5
IP: HA
Myc-MAP2K5
WCE
(D)
1xEAA
0 min
30 min
0 min
30 min
siRNA
LONRF1-p
MAP2K5-1
MAP2K5-2
MAP2K5-3
MAP2K5-p
TMEM114-p
MAP3K3-1
MAP3K3-2
MAP3K3-3
MAP3K3-p
TBK1
IKKε
p-S6
S6
pT389-p70S6K
p70S6K
pS757-ULK1
ULK1

Figure 3.8. MAP2K5 supports mTORC1 activation by amino acids.

(A) HeLa cells were plated in DMEM containing 10% FBS. After seeded overnight, cells were washed twice by EBSS and then treated with EBSS containing either DMSO or indicated concentration of BIX compound (BIX02189) for 2hr. Before EAA treatment, cells were preincubated with additional 2mM L-Glutamine for 1hr. EAA-treated cells were harvested and lysed directly by 1x SDS sample buffer at indicated time points.

(B), (C) and (D) HeLa cells were plated overnight in DMEM containing 10% FBS, and then transfected with the indicated siRNAs. After 3 days, cells were washed twice by EBSS and then incubated with EBSS. Before EAA treatment, cells were preincubated with additional 2mM L-Glutamine for 1hr. EAA-treated cells were harvested and lysed directly by 1x SDS sample buffer at indicated time points.

(E) HeLa cells were plated overnight in DMEM containing 10% FBS, and then transfected with the indicated siRNAs. After 3 days, cells were washed twice by EBSS and then incubated with EBSS. Before EAA treatment, cells were preincubated with additional 2mM L-Glutamine for 1hr and treated with GSK inhibitor for 30mins. EAA-treated cells were harvested and lysed directly by 1x SDS sample buffer at indicated time points.

DISCUSSION

My results suggest that TBK1 and IKKε as well as some of their interacting proteins and exocyst components, including NAP1, CYLD, Sec3, Sec6, Sec8, Sec10, and Sec15, support amino acid-induced mTORC1 signaling. Moreover, my data also indicates that the MAP3K3-MAP2K5-ERK5 kinase cascade participates in mTORC1 activation by amino acids.

Several groups reported that AKT is directly phosphorylated and activated by TBK1 and IKKε in response to growth factors and other stimuli, which disrupts the TSC1/TSC2 inhibitory complex, allowing for GTP-bound Rheb to stimulate mTORC1 activity (Guo, Coppola et al. 2011, Joung, Park et al. 2011, Ou, Torres et al. 2011, Xie, Zhang et al. 2011,

Mahajan and Mahajan 2012). Here, my results suggest that in addition to TBK1-AKT-TSC axis, TBK1 and IKKε may activate mTORC1 signaling through an alternative route. This hypothesis is supported by the results that amino acid-induced phosphorylation of AKT at Ser473 shows no significant difference between wildtype and TBK1/ IKKε double knockout MEFs, whereas mTORC1 activation by amino acids is impaired in TBK1/ IKKε dual deficient cells as indicated by phosphorylation of S6. However, it remains unclear how TBK1 and IKKε contribute to mTORC1 signaling. Since both proteins are kinases, one possibility is that TBK1 and IKKε directly phosphorylate and regulate mTORC1 key components. My data suggest that upon amino acids stimulation, the scaffold protein Raptor is not only recruited to active TBK1 complexes as indicated by TBK1-pS172, but also shows a significant band shift by western blot, implying that Raptor is phosphorylated by an unknown upstream kinase. It's been demonstrated that upon energy stress AMPK suppresses mTORC1 by direct phosphorylation of Raptor on Ser722/Ser792, suggesting that Raptor is a potential target for signal transduction (Gwinn, Shackelford et al. 2008). Moreover, p62 is also a direct substrate of TBK1 and participates in autophagy-dependent bacterial clearance (Pilli, Arko-Mensah et al. 2012). It would be important to examine whether Raptor, p62, and other core mTORC1 components are TBK1 (or IKKε) direct substrates in response to amino acids. It is also important to determine whether TBK1 and IKKε crosstalk to taste receptors TAS1R1 and TAS1R3, Leucyl-tRNA synthetase, and amino acid transporters (Nicklin, Bergman et al. 2009, Duran and Hall 2012, Elorza, Soro-Arnaiz et al. 2012, Han, Jeong et al. 2012, Wauson, Zaganjor et al. 2012, Wauson, Zaganjor et al. 2013).

The scaffold proteins, TANK, NAP1, and SINTBAD are all required for IRF3-mediated interferon production by TBK1 and IKKε and perform similar functions in TBK1 and IKKε activation due to structural similarities (Chau, Gioia et al. 2008, Kumar, Kawai et al. 2009). NAP1 and SINTBAD are required for TBK1 recruitment to ubiquitin-coated bacteria recognized by autophagy receptor NDP52 and p62 (Thurston, Ryzhakov et al. 2009, Weidberg and Elazar 2011). Moreover, expression of NAP1 is sufficient to activate TBK1 (Fujita, Taniguchi et al. 2003). My results suggest that NAP1 may play a unique role in mTORC1 signaling by amino acids. However, it remains unclear if NAP1 supports mTORC1 activation through a TBK1-dependent mechanism.

TBK1 somatic and germline mutations were found in human cancers and HSE patients respectively (Cerami, Gao et al. 2012, Herman, Ciancanelli et al. 2012). However, the consequences of TBK1 mutations in cancer are poorly defined. It would be critical to determine the cell biological and biochemical properties of those mutations and to investigate the roles of those mutants in tumorigenesis. Furthermore, it would be important to examine the metabolic profiles of human patients carrying TBK1 loss-of-function mutations.

The exocyst is a conserved multi-protein complex composed of eight subunits including Sec3, Sec5, Sec6, Sec8, Sec10, Sec15, Exo70 and Exo84. Mounting evidence indicates that exocyst is a downstream effector of Ral proteins contributing to basolateral membrane protein targeting (Bodemann and White 2008). Recent studies suggest that sub-exocyst complexes may exist and participate in autophagy and cancer cell survival (Chien, Kim et al. 2006, Bodemann, Orvedahl et al. 2011). For example, RalB-Sec5 is selectively required for cancer cell to suppress apoptosis. RalB-Exo84 sub-complex is required for

autophagosome assembly upon nutrient deprivation. Here, my results show that five out of eight exocyst complex proteins, including Sec3, Sec6, Sec8, Sec10, and Sec15, are required for amino-acid induced mTORC1 signaling, suggesting the existence of novel exocyst sub-complexes. Of note, Sec3 and Exo70 both interact with TBK1, whereas only Sec3 is required for both AKT signaling by serum and mTORC1 pathway by amino acids, indicating that Sec3 functions diversely in different contexts (Ou, Torres et al. 2011). Further investigation would be required to determine how this exocyst sub-complex supports amino acid-induced mTORC1 activity. Nevertheless, it's been shown that Sec5 sub-complex is required for STING and TBK1 targeting to perinuclear vesicles upon exposure to intracellular DNA (Ishikawa, Ma et al. 2009). It's possible that exocyst sub-complexes may participate in the activation of mTORC1 by targeting mTORC1 complex to lysosomes, where mTORC1 is activated by amino acids.

Autophagic receptor p62 is required for the activation of mTORC1 by amino acids, but not by insulin (Duran, Amanchy et al. 2011). Interaction among MAP3K3, MAP2K5, and p62 depends on PB1 domain and MAP2K5 is also a direct substrate of MAP3K3 (White 2012). My data suggest that p62-interacting proteins MAP3K3 and MAP2K5 are also involved in amino acid-induced mTORC1 activation. It's possible that MAP3K3 and MAP2K5 contribute to mTORC1 activity through p62. Furthermore, amino acid-mediated mTORC1 signaling is impaired when MAP2K5 is pharmacologically inhibited. However, MAP2K5 inhibitor has no effect toward insulin-stimulated mTORC1 activation, which phenocopies the results obtained from p62 deficient MEFs and suggests critical roles of p62 and MAP2K5 in mTORC1 signaling by amino acids. (Duran, Amanchy et al. 2011)

(Unpublished data from Malia Potts, Michael White Lab). Thus, there are several important questions remain unanswered. For example, is p62 a substrate of MAP2K5 and MAP3K3 upon amino acids exposure? Does p62 also recruit MAP2K5 and MAP3K3 to the lysosomes in the presence of amino acids? Do MAP2K5 and MAP3K3 modulate mTORC1 activity by phosphorylating and regulating mTORC1 key components or ULK1? Are enzymatic activities of MAP2K5 and MAP3K3 altered upon exposure to amino acids? It would be critical to answer these questions in order to understand how MAP2K5 and MAP3K3 contribute to amino acids-mediated mTORC1 signaling.

In conclusion, my observations reveal a novel group of TBK1 interacting proteins and substrates contributing to mTORC1 activation by amino acids (Figure 3.9).

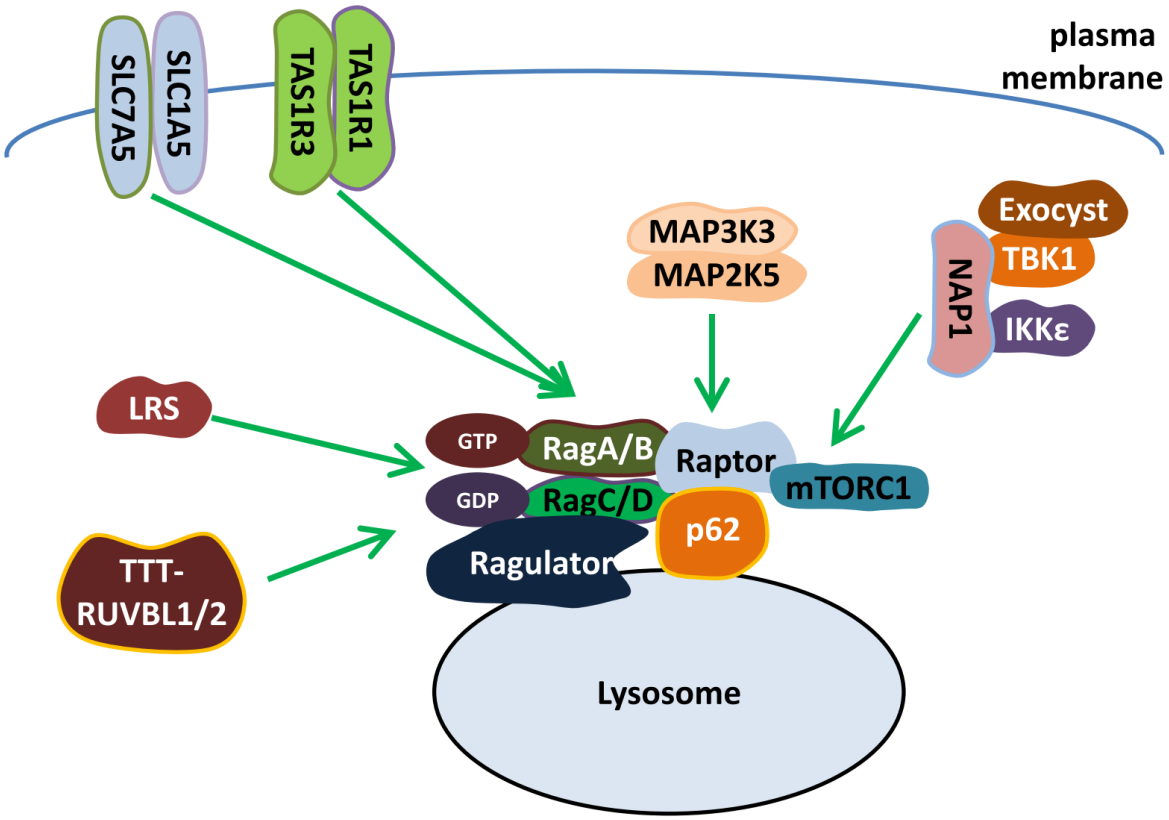

Figure 3.9. Amino acid sensing and regulation of mTORC1

CHAPTER FOUR

CONCLUDING REMARKS

Dissecting the molecular mechanisms underlying oncogene-driven cell transformation is key for personalized therapeutic intervention. I found that the innate immune response kinase TBK1 contributes to cancer cell survival by directly engaging AKT signaling. My data suggest that TBK1 is required for AKT activation in a context-dependent manner. I also showed that TBK1 directly phosphorylates AKT on both the activation loop Thr308 and the hydrophobic motif Ser473, which leads to the activation of AKT kinase activity and connects TBK1 to prosurvival signaling. Furthermore, I demonstrated that pharmacological perturbation of TBK1, by a novel class of chemical inhibitors, impairs oncogenic AKT activation and cancer cell survival. In conclusion, my findings suggest that AKT is an immediate effector of TBK1 and demonstrate that a non-canonical TBK1-AKT axis supports oncogenic transformation. In addition, I discover a novel set of proteins, including TBK1, IKKε, exocyst proteins, and MAP2K5/MAP3K3, supporting mTORC1 activation by amino acids. By investigating the molecular mechanisms underlying oncogenic transformation, I hope my work contributes to prediction of clinical outcomes and provides novel therapeutic opportunities.

BIBLIOGRAPHY

Ablasser, A., F. Bauernfeind, G. Hartmann, E. Latz, K. A. Fitzgerald and V. Hornung (2009). "RIG-I-dependent sensing of poly(dA:dT) through the induction of an RNA polymerase III-transcribed RNA intermediate." Nat Immunol **10**(10): 1065-1072.

Ahn, J. Y., R. Rong, T. G. Kroll, E. G. Van Meir, S. H. Snyder and K. Ye (2004). "PIKE (phosphatidylinositol 3-kinase enhancer)-A GTPase stimulates Akt activity and mediates cellular invasion." J Biol Chem **279**(16): 16441-16451.

Alessi, D. R., S. R. James, C. P. Downes, A. B. Holmes, P. R. Gaffney, C. B. Reese and P. Cohen (1997). "Characterization of a 3-phosphoinositide-dependent protein kinase which phosphorylates and activates protein kinase Balpha." Curr Biol **7**(4): 261-269.

Altomare, D. A. and J. R. Testa (2005). "Perturbations of the AKT signaling pathway in human cancer." Oncogene **24**(50): 7455-7464.

An, H., W. Zhao, J. Hou, Y. Zhang, Y. Xie, Y. Zheng, H. Xu, C. Qian, J. Zhou, Y. Yu, S. Liu, G. Feng and X. Cao (2006). "SHP-2 phosphatase negatively regulates the TRIF adaptor protein-dependent type I interferon and proinflammatory cytokine production." Immunity **25**(6): 919-928.

Arnoult, D., F. Soares, I. Tattoli and S. E. Girardin (2011). "Mitochondria in innate immunity." EMBO Rep **12**(9): 901-910.

Bain, J., L. Plater, M. Elliott, N. Shpiro, C. J. Hastie, H. McLauchlan, I. Klevernic, J. S. Arthur, D. R. Alessi and P. Cohen (2007). "The selectivity of protein kinase inhibitors: a further update." Biochem J **408**(3): 297-315.

Bamborough, P., J. A. Christopher, G. J. Cutler, M. C. Dickson, G. W. Mellor, J. V. Morey, C. B. Patel and L. M. Shewchuk (2006). "5-(1H-Benzimidazol-1-yl)-3-alkoxy-2-thiophenecarbonitriles as potent, selective, inhibitors of IKK-epsilon kinase." Bioorg Med Chem Lett **16**(24): 6236-6240.

Barbie, D. A., P. Tamayo, J. S. Boehm, S. Y. Kim, S. E. Moody, I. F. Dunn, A. C. Schinzel, P. Sandy, E. Meylan, C. Scholl, S. Frohling, E. M. Chan, M. L. Sos, K. Michel, C. Mermel, S. J. Silver, B. A. Weir, J. H. Reiling, Q. Sheng, P. B. Gupta, R. C. Wadlow, H. Le, S. Hoersch, B. S. Wittner, S. Ramaswamy, D. M. Livingston, D. M. Sabatini, M. Meyerson, R. K. Thomas, E. S. Lander, J. P. Mesirov, D. E. Root, D. G. Gilliland, T. Jacks and W. C. Hahn (2009). "Systematic RNA interference reveals that oncogenic KRAS-driven cancers require TBK1." Nature **462**(7269): 108-112.

Bartel, P., C. T. Chien, R. Sternglanz and S. Fields (1993). "Elimination of false positives that arise in using the two-hybrid system." Biotechniques **14**(6): 920-924.

Beg, A. A., W. C. Sha, R. T. Bronson, S. Ghosh and D. Baltimore (1995). "Embryonic lethality and liver degeneration in mice lacking the RelA component of NF-kappa B." Nature **376**(6536): 167-170.

Bellacosa, A., T. O. Chan, N. N. Ahmed, K. Datta, S. Malstrom, D. Stokoe, F. McCormick, J. Feng and P. Tsichlis (1998). "Akt activation by growth factors is a multiple-step process: the role of the PH domain." Oncogene **17**(3): 313-325.

Ben-Sahra, I., J. J. Howell, J. M. Asara and B. D. Manning (2013). "Stimulation of de novo pyrimidine synthesis by growth signaling through mTOR and S6K1." Science **339**(6125): 1323-1328.

Berwick, D. C., G. C. Dell, G. I. Welsh, K. J. Heesom, I. Hers, L. M. Fletcher, F. T. Cooke and J. M. Tavare (2004). "Protein kinase B phosphorylation of PIKfyve regulates the trafficking of GLUT4 vesicles." J Cell Sci **117**(Pt 25): 5985-5993.

Blume-Jensen, P., R. Janknecht and T. Hunter (1998). "The kit receptor promotes cell survival via activation of PI 3-kinase and subsequent Akt-mediated phosphorylation of Bad on Ser136." Curr Biol **8**(13): 779-782.

Bodemann, B. O., A. Orvedahl, T. Cheng, R. R. Ram, Y. H. Ou, E. Formstecher, M. Maiti, C. C. Hazelett, E. M. Wauson, M. Balakireva, J. H. Camonis, C. Yeaman, B. Levine and M. A. White (2011). "RalB and the exocyst mediate the cellular starvation response by direct activation of autophagosome assembly." Cell **144**(2): 253-267.

Bodemann, B. O. and M. A. White (2008). "Ral GTPases and cancer: linchpin support of the tumorigenic platform." Nat Rev Cancer **8**(2): 133-140.

Boehm, J. S., J. J. Zhao, J. Yao, S. Y. Kim, R. Firestein, I. F. Dunn, S. K. Sjostrom, L. A. Garraway, S. Weremowicz, A. L. Richardson, H. Greulich, C. J. Stewart, L. A. Mulvey, R. R. Shen, L. Ambrogio, T. Hirozane-Kishikawa, D. E. Hill, M. Vidal, M. Meyerson, J. K. Grenier, G. Hinkle, D. E. Root, T. M. Roberts, E. S. Lander, K. Polyak and W. C. Hahn (2007). "Integrative genomic approaches identify IKBKE as a breast cancer oncogene." Cell **129**(6): 1065-1079.

Bonnard, M., C. Mirtsos, S. Suzuki, K. Graham, J. Huang, M. Ng, A. Itie, A. Wakeham, A. Shahinian, W. J. Henzel, A. J. Elia, W. Shillinglaw, T. W. Mak, Z. Cao and W. C. Yeh (2000). "Deficiency of T2K leads to apoptotic liver degeneration and impaired NF-kappaB-dependent gene transcription." EMBO J **19**(18): 4976-4985.

Boormans, J. L., H. Korsten, A. C. Ziel-van der Made, G. J. van Leenders, P. C. Verhagen and J. Trapman (2010). "E17K substitution in AKT1 in prostate cancer." Br J Cancer **102**(10): 1491-1494.

Boulbes, D., C. H. Chen, T. Shaikenov, N. K. Agarwal, T. R. Peterson, T. A. Addona, H. Keshishian, S. A. Carr, M. A. Magnuson, D. M. Sabatini and D. Sarbassov dos (2010). "Rictor phosphorylation on the Thr-1135 site does not require mammalian target of rapamycin complex 2." Mol Cancer Res **8**(6): 896-906.

Bowie, A. (2012). "The STING in the tail for cytosolic DNA-dependent activation of IRF3." Sci Signal **5**(214): pe9.

Bozulic, L. and B. A. Hemmings (2009). "PIKKing on PKB: regulation of PKB activity by phosphorylation." Curr Opin Cell Biol **21**(2): 256-261.

Buller, C. L., C. W. Heilig and F. C. Brosius, 3rd (2011). "GLUT1 enhances mTOR activity independently of TSC2 and AMPK." Am J Physiol Renal Physiol **301**(3): F588-596.

Buller, C. L., R. D. Loberg, M. H. Fan, Q. Zhu, J. L. Park, E. Vesely, K. Inoki, K. L. Guan and F. C. Brosius, 3rd (2008). "A GSK-3/TSC2/mTOR pathway regulates glucose uptake and GLUT1 glucose transporter expression." Am J Physiol Cell Physiol **295**(3): C836-843.

Buss, H., A. Dorrie, M. L. Schmitz, E. Hoffmann, K. Resch and M. Kracht (2004). "Constitutive and interleukin-1-inducible phosphorylation of p65 NF-{kappa}B at serine 536 is mediated by multiple protein kinases including I{kappa}B kinase (IKK)-{alpha}, IKK{beta}, IKK{epsilon}, TRAF family member-associated (TANK)-binding kinase 1 (TBK1), and an unknown kinase and couples p65 to TATA-binding protein-associated factor II31-mediated interleukin-8 transcription." J Biol Chem **279**(53): 55633-55643.

Cardone, M. H., N. Roy, H. R. Stennicke, G. S. Salvesen, T. F. Franke, E. Stanbridge, S. Frisch and J. C. Reed (1998). "Regulation of cell death protease caspase-9 by phosphorylation." Science **282**(5392): 1318-1321.

Carpten, J. D., A. L. Faber, C. Horn, G. P. Donoho, S. L. Briggs, C. M. Robbins, G. Hostetter, S. Boguslawski, T. Y. Moses, S. Savage, M. Uhlik, A. Lin, J. Du, Y. W. Qian, D. J. Zeckner, G. Tucker-Kellogg, J. Touchman, K. Patel, S. Mousses, M. Bittner, R. Schevitz, M. H. Lai, K. L. Blanchard and J. E. Thomas (2007). "A transforming mutation in the pleckstrin homology domain of AKT1 in cancer." Nature **448**(7152): 439-444.

Cerami, E., J. Gao, U. Dogrusoz, B. E. Gross, S. O. Sumer, B. A. Aksoy, A. Jacobsen, C. J. Byrne, M. L. Heuer, E. Larsson, Y. Antipin, B. Reva, A. P. Goldberg, C. Sander and N. Schultz (2012). "The cBio cancer genomics portal: an open platform for exploring multidimensional cancer genomics data." Cancer Discov **2**(5): 401-404.

Chalhoub, N. and S. J. Baker (2009). "PTEN and the PI3-kinase pathway in cancer." Annu Rev Pathol **4**: 127-150.

Chan, C. H., C. F. Li, W. L. Yang, Y. Gao, S. W. Lee, Z. Feng, H. Y. Huang, K. K. Tsai, L. G. Flores, Y. Shao, J. D. Hazle, D. Yu, W. Wei, D. Sarbassov, M. C. Hung, K. I. Nakayama and H. K. Lin (2012). "The Skp2-SCF E3 ligase regulates Akt ubiquitination, glycolysis, herceptin sensitivity, and tumorigenesis." Cell **149**(5): 1098-1111.

Chan, E. Y. (2009). "mTORC1 phosphorylates the ULK1-mAtg13-FIP200 autophagy regulatory complex." Sci Signal **2**(84): pe51.

Chau, T. L., R. Gioia, J. S. Gatot, F. Patrascu, I. Carpentier, J. P. Chapelle, L. O'Neill, R. Beyaert, J. Piette and A. Chariot (2008). "Are the IKKs and IKK-related kinases TBK1 and IKK-epsilon similarly activated?" Trends Biochem Sci **33**(4): 171-180.

Chen, C. C., S. M. Jeon, P. T. Bhaskar, V. Nogueira, D. Sundararajan, I. Tonic, Y. Park and N. Hay (2010). "FoxOs inhibit mTORC1 and activate Akt by inducing the expression of Sestrin3 and Rictor." Dev Cell **18**(4): 592-604.

Cheng, A., J. Guo, E. Henderson-Jackson, D. Kim, M. Malafa and D. Coppola (2011). "IkappaB Kinase epsilon expression in pancreatic ductal adenocarcinoma." Am J Clin Pathol **136**(1): 60-66.

Chiang, G. G. and R. T. Abraham (2005). "Phosphorylation of mammalian target of rapamycin (mTOR) at Ser-2448 is mediated by p70S6 kinase." J Biol Chem **280**(27): 25485-25490.

Chien, Y., S. Kim, R. Bumeister, Y. M. Loo, S. W. Kwon, C. L. Johnson, M. G. Balakireva, Y. Romeo, L. Kopelovich, M. Gale, Jr., C. Yeaman, J. H. Camonis, Y. Zhao and M. A. White (2006). "RalB GTPase-mediated activation of the IkappaB family kinase TBK1 couples innate immune signaling to tumor cell survival." Cell **127**(1): 157-170.

Chien, Y. and M. A. White (2003). "RAL GTPases are linchpin modulators of human tumour-cell proliferation and survival." EMBO Rep **4**(8): 800-806.

Chiu, Y. H., J. B. Macmillan and Z. J. Chen (2009). "RNA polymerase III detects cytosolic DNA and induces type I interferons through the RIG-I pathway." Cell **138**(3): 576-591.

Cho, H., J. Mu, J. K. Kim, J. L. Thorvaldsen, Q. Chu, E. B. Crenshaw, 3rd, K. H. Kaestner, M. S. Bartolomei, G. I. Shulman and M. J. Birnbaum (2001). "Insulin resistance and a diabetes mellitus-like syndrome in mice lacking the protein kinase Akt2 (PKB beta)." Science **292**(5522): 1728-1731.

Clark, K., L. Plater, M. Peggie and P. Cohen (2009). "Use of the pharmacological inhibitor BX795 to study the regulation and physiological roles of TBK1 and IkappaB

kinase epsilon: a distinct upstream kinase mediates Ser-172 phosphorylation and activation." J Biol Chem **284**(21): 14136-14146.

Clement, J. F., S. Meloche and M. J. Servant (2008). "The IKK-related kinases: from innate immunity to oncogenesis." Cell Res **18**(9): 889-899.

Copp, J., G. Manning and T. Hunter (2009). "TORC-specific phosphorylation of mammalian target of rapamycin (mTOR): phospho-Ser2481 is a marker for intact mTOR signaling complex 2." Cancer Res **69**(5): 1821-1827.

Dan, H. C., M. Sun, L. Yang, R. I. Feldman, X. M. Sui, C. C. Ou, M. Nellist, R. S. Yeung, D. J. Halley, S. V. Nicosia, W. J. Pledger and J. Q. Cheng (2002). "Phosphatidylinositol 3-kinase/Akt pathway regulates tuberous sclerosis tumor suppressor complex by phosphorylation of tuberin." J Biol Chem **277**(38): 35364-35370.

DeBerardinis, R. J., J. J. Lum, G. Hatzivassiliou and C. B. Thompson (2008). "The biology of cancer: metabolic reprogramming fuels cell growth and proliferation." Cell Metab **7**(1): 11-20.

Delhase, M., S. Y. Kim, H. Lee, A. Naiki-Ito, Y. Chen, E. R. Ahn, K. Murata, S. J. Kim, N. Lautsch, K. S. Kobayashi, T. Shirai, M. Karin and M. Nakanishi (2012). "TANK-binding kinase 1 (TBK1) controls cell survival through PAI-2/serpinB2 and transglutaminase 2." Proc Natl Acad Sci U S A **109**(4): E177-186.

Deprez, J., D. Vertommen, D. R. Alessi, L. Hue and M. H. Rider (1997). "Phosphorylation and activation of heart 6-phosphofructo-2-kinase by protein kinase B and other protein kinases of the insulin signaling cascades." J Biol Chem **272**(28): 17269-17275.

Der, C. J., T. G. Krontiris and G. M. Cooper (1982). "Transforming genes of human bladder and lung carcinoma cell lines are homologous to the ras genes of Harvey and Kirsten sarcoma viruses." Proc Natl Acad Sci U S A **79**(11): 3637-3640.

DeYoung, M. P., P. Horak, A. Sofer, D. Sgroi and L. W. Ellisen (2008). "Hypoxia regulates TSC1/2-mTOR signaling and tumor suppression through REDD1-mediated 14-3-3 shuttling." Genes Dev **22**(2): 239-251.

Dibble, C. C., W. Elis, S. Menon, W. Qin, J. Klekota, J. M. Asara, P. M. Finan, D. J. Kwiatkowski, L. O. Murphy and B. D. Manning (2012). "TBC1D7 is a third subunit of the TSC1-TSC2 complex upstream of mTORC1." Mol Cell **47**(4): 535-546.

Dineen, S. P., K. D. Lynn, S. E. Holloway, A. F. Miller, J. P. Sullivan, D. S. Shames, A. W. Beck, C. C. Barnett, J. B. Fleming and R. A. Brekken (2008). "Vascular endothelial growth factor receptor 2 mediates macrophage infiltration into orthotopic pancreatic tumors in mice." Cancer Res **68**(11): 4340-4346.

Do, H., R. Salemi, C. Murone, P. L. Mitchell and A. Dobrovic (2010). "Rarity of AKT1 and AKT3 E17K mutations in squamous cell carcinoma of lung." Cell Cycle **9**(21): 4411-4412.

Downward, J. (2003). "Targeting RAS signalling pathways in cancer therapy." Nat Rev Cancer **3**(1): 11-22.

Dunlop, E. A., D. K. Hunt, H. A. Acosta-Jaquez, D. C. Fingar and A. R. Tee (2011). "ULK1 inhibits mTORC1 signaling, promotes multisite Raptor phosphorylation and hinders substrate binding." Autophagy **7**(7): 737-747.

Duran, A., R. Amanchy, J. F. Linares, J. Joshi, S. Abu-Baker, A. Porollo, M. Hansen, J. Moscat and M. T. Diaz-Meco (2011). "p62 is a key regulator of nutrient sensing in the mTORC1 pathway." Mol Cell **44**(1): 134-146.

Duran, R. V. and M. N. Hall (2012). "Leucyl-tRNA synthetase: double duty in amino acid sensing." Cell Res **22**(8): 1207-1209.

Duran, R. V., W. Oppliger, A. M. Robitaille, L. Heiserich, R. Skendaj, E. Gottlieb and M. N. Hall (2012). "Glutaminolysis activates Rag-mTORC1 signaling." Mol Cell **47**(3): 349-358.

Efeyan, A., R. Zoncu and D. M. Sabatini (2012). "Amino acids and mTORC1: from lysosomes to disease." Trends Mol Med **18**(9): 524-533.

Elorza, A., I. Soro-Arnaiz, F. Melendez-Rodriguez, V. Rodriguez-Vaello, G. Marsboom, G. de Carcer, B. Acosta-Iborra, L. Albacete-Albacete, A. Ordonez, L. Serrano-Oviedo, J. M. Gimenez-Bachs, A. Vara-Vega, A. Salinas, R. Sanchez-Prieto, R. Martin del Rio, F. Sanchez-Madrid, M. Malumbres, M. O. Landazuri and J. Aragones (2012). "HIF2alpha acts as an mTORC1 activator through the amino acid carrier SLC7A5." Mol Cell **48**(5): 681-691.

Engelman, J. A. (2009). "Targeting PI3K signalling in cancer: opportunities, challenges and limitations." Nat Rev Cancer **9**(8): 550-562.

Ericson, K., C. Gan, I. Cheong, C. Rago, Y. Samuels, V. E. Velculescu, K. W. Kinzler, D. L. Huso, B. Vogelstein and N. Papadopoulos (2010). "Genetic inactivation of AKT1, AKT2, and PDPK1 in human colorectal cancer cells clarifies their roles in tumor growth regulation." Proc Natl Acad Sci U S A **107**(6): 2598-2603.

Fitzgerald, K. A., S. M. McWhirter, K. L. Faia, D. C. Rowe, E. Latz, D. T. Golenbock, A. J. Coyle, S. M. Liao and T. Maniatis (2003). "IKKepsilon and TBK1 are essential components of the IRF3 signaling pathway." Nat Immunol **4**(5): 491-496.

Forbes, S. A., G. Tang, N. Bindal, S. Bamford, E. Dawson, C. Cole, C. Y. Kok, M. Jia, R. Ewing, A. Menzies, J. W. Teague, M. R. Stratton and P. A. Futreal (2009). "COSMIC (the Catalogue of Somatic Mutations in Cancer): a resource to investigate acquired mutations in human cancer." Nucleic Acids Res.

Formstecher, E., S. Aresta, V. Collura, A. Hamburger, A. Meil, A. Trehin, C. Reverdy, V. Betin, S. Maire, C. Brun, B. Jacq, M. Arpin, Y. Bellaiche, S. Bellusci, P. Benaroch, M. Bornens, R. Chanet, P. Chavrier, O. Delattre, V. Doye, R. Fehon, G. Faye, T. Galli, J. A. Girault, B. Goud, J. de Gunzburg, L. Johannes, M. P. Junier, V. Mirouse, A. Mukherjee, D. Papadopoulo, F. Perez, A. Plessis, C. Rosse, S. Saule, D. Stoppa-Lyonnet, A. Vincent, M. White, P. Legrain, J. Wojcik, J. Camonis and L. Daviet (2005). "Protein interaction mapping: a Drosophila case study." Genome Res **15**(3): 376-384.

Friedman, C. S., M. A. O'Donnell, D. Legarda-Addison, A. Ng, W. B. Cardenas, J. S. Yount, T. M. Moran, C. F. Basler, A. Komuro, C. M. Horvath, R. Xavier and A. T. Ting (2008). "The tumour suppressor CYLD is a negative regulator of RIG-I-mediated antiviral response." EMBO Rep **9**(9): 930-936.

Fromont-Racine, M., J. C. Rain and P. Legrain (1997). "Toward a functional analysis of the yeast genome through exhaustive two-hybrid screens." Nat Genet **16**(3): 277-282.

Fujita, F., Y. Taniguchi, T. Kato, Y. Narita, A. Furuya, T. Ogawa, H. Sakurai, T. Joh, M. Itoh, M. Delhase, M. Karin and M. Nakanishi (2003). "Identification of NAP1, a regulatory subunit of IkappaB kinase-related kinases that potentiates NF-kappaB signaling." Mol Cell Biol **23**(21): 7780-7793.

Ganley, I. G., H. Lam du, J. Wang, X. Ding, S. Chen and X. Jiang (2009). "ULK1.ATG13.FIP200 complex mediates mTOR signaling and is essential for autophagy." J Biol Chem **284**(18): 12297-12305.

Garofalo, R. S., S. J. Orena, K. Rafidi, A. J. Torchia, J. L. Stock, A. L. Hildebrandt, T. Coskran, S. C. Black, D. J. Brees, J. R. Wicks, J. D. McNeish and K. G. Coleman (2003). "Severe diabetes, age-dependent loss of adipose tissue, and mild growth deficiency in mice lacking Akt2/PKB beta." J Clin Invest **112**(2): 197-208.

George, S., J. J. Rochford, C. Wolfrum, S. L. Gray, S. Schinner, J. C. Wilson, M. A. Soos, P. R. Murgatroyd, R. M. Williams, C. L. Acerini, D. B. Dunger, D. Barford, A. M. Umpleby, N. J. Wareham, H. A. Davies, A. J. Schafer, M. Stoffel, S. O'Rahilly and I. Barroso (2004). "A family with severe insulin resistance and diabetes due to a mutation in AKT2." Science **304**(5675): 1325-1328.

Goldfarb, M., K. Shimizu, M. Perucho and M. Wigler (1982). "Isolation and preliminary characterization of a human transforming gene from T24 bladder carcinoma cells." Nature **296**(5856): 404-409.

Grindstaff, K. K., C. Yeaman, N. Anandasabapathy, S. C. Hsu, E. Rodriguez-Boulan, R. H. Scheller and W. J. Nelson (1998). "Sec6/8 complex is recruited to cell-cell contacts and specifies transport vesicle delivery to the basal-lateral membrane in epithelial cells." Cell **93**(5): 731-740.

Guan, H., H. Zhang, J. Cai, J. Wu, J. Yuan, J. Li, Z. Huang and M. Li (2011). "IKBKE is over-expressed in glioma and contributes to resistance of glioma cells to apoptosis via activating NF-kappaB." J Pathol **223**(3): 436-445.

Guertin, D. A., D. M. Stevens, C. C. Thoreen, A. A. Burds, N. Y. Kalaany, J. Moffat, M. Brown, K. J. Fitzgerald and D. M. Sabatini (2006). "Ablation in mice of the mTORC components raptor, rictor, or mLST8 reveals that mTORC2 is required for signaling to Akt-FOXO and PKCalpha, but not S6K1." Dev Cell **11**(6): 859-871.

Guo, J. P., D. Coppola and J. Q. Cheng (2011). "IKBKE protein activates Akt independent of phosphatidylinositol 3-kinase/PDK1/mTORC2 and the pleckstrin homology domain to sustain malignant transformation." J Biol Chem **286**(43): 37389-37398.

Guo, J. P., S. K. Shu, L. He, Y. C. Lee, P. A. Kruk, S. Grenman, S. V. Nicosia, G. Mor, M. J. Schell, D. Coppola and J. Q. Cheng (2009). "Deregulation of IKBKE is associated with tumor progression, poor prognosis, and cisplatin resistance in ovarian cancer." Am J Pathol **175**(1): 324-333.

Guo, W., M. Sacher, J. Barrowman, S. Ferro-Novick and P. Novick (2000). "Protein complexes in transport vesicle targeting." Trends Cell Biol **10**(6): 251-255.

Gwinn, D. M., D. B. Shackelford, D. F. Egan, M. M. Mihaylova, A. Mery, D. S. Vasquez, B. E. Turk and R. J. Shaw (2008). "AMPK phosphorylation of raptor mediates a metabolic checkpoint." Mol Cell **30**(2): 214-226.

Hacker, H. and M. Karin (2006). "Regulation and function of IKK and IKK-related kinases." Sci STKE **2006**(357): re13.

Han, J. M., S. J. Jeong, M. C. Park, G. Kim, N. H. Kwon, H. K. Kim, S. H. Ha, S. H. Ryu and S. Kim (2012). "Leucyl-tRNA synthetase is an intracellular leucine sensor for the mTORC1-signaling pathway." Cell **149**(2): 410-424.

Hanahan, D. and R. A. Weinberg (2011). "Hallmarks of cancer: the next generation." Cell **144**(5): 646-674.

Harrington, L. S., G. M. Findlay, A. Gray, T. Tolkacheva, S. Wigfield, H. Rebholz, J. Barnett, N. R. Leslie, S. Cheng, P. R. Shepherd, I. Gout, C. P. Downes and R. F. Lamb (2004). "The TSC1-2 tumor suppressor controls insulin-PI3K signaling via regulation of IRS proteins." J Cell Biol **166**(2): 213-223.

Hay, N. (2011). "Akt isoforms and glucose homeostasis - the leptin connection." Trends Endocrinol Metab **22**(2): 66-73.

Herman, M., M. Ciancanelli, Y. H. Ou, L. Lorenzo, M. Klaudel-Dreszler, E. Pauwels, V. Sancho-Shimizu, R. Perez de Diego, A. Abhyankar, E. Israelsson, Y. Guo, A. Cardon, F. Rozenberg, P. Lebon, M. Tardieu, E. Heropolitanska-Pliszka, D. Chaussabel, M. A. White, L. Abel, S. Y. Zhang and J. L. Casanova (2012). "Heterozygous TBK1 mutations impair TLR3 immunity and underlie herpes simplex encephalitis of childhood." J Exp Med **209**(9): 1567-1582.

Hiscott, J. (2007). "Convergence of the NF-kappaB and IRF pathways in the regulation of the innate antiviral response." Cytokine Growth Factor Rev **18**(5-6): 483-490.

Horak, P., A. R. Crawford, D. D. Vadysirisack, Z. M. Nash, M. P. DeYoung, D. Sgroi and L. W. Ellisen (2010). "Negative feedback control of HIF-1 through REDD1-regulated ROS suppresses tumorigenesis." Proc Natl Acad Sci U S A **107**(10): 4675-4680.

Hosokawa, N., T. Hara, T. Kaizuka, C. Kishi, A. Takamura, Y. Miura, S. Iemura, T. Natsume, K. Takehana, N. Yamada, J. L. Guan, N. Oshiro and N. Mizushima (2009). "Nutrient-dependent mTORC1 association with the ULK1-Atg13-FIP200 complex required for autophagy." Mol Biol Cell **20**(7): 1981-1991.

Howell, J. J. and B. D. Manning (2011). "mTOR couples cellular nutrient sensing to organismal metabolic homeostasis." Trends Endocrinol Metab **22**(3): 94-102.

Hresko, R. C. and M. Mueckler (2005). "mTOR.RICTOR is the Ser473 kinase for Akt/protein kinase B in 3T3-L1 adipocytes." J Biol Chem **280**(49): 40406-40416.

Hsu, P. P., S. A. Kang, J. Rameseder, Y. Zhang, K. A. Ottina, D. Lim, T. R. Peterson, Y. Choi, N. S. Gray, M. B. Yaffe, J. A. Marto and D. M. Sabatini (2011). "The mTOR-regulated phosphoproteome reveals a mechanism of mTORC1-mediated inhibition of growth factor signaling." Science **332**(6035): 1317-1322.

Hutti, J. E., R. R. Shen, D. W. Abbott, A. Y. Zhou, K. M. Sprott, J. M. Asara, W. C. Hahn and L. C. Cantley (2009). "Phosphorylation of the tumor suppressor CYLD by the breast cancer oncogene IKKepsilon promotes cell transformation." Mol Cell **34**(4): 461-472.

Inoki, K., J. Kim and K. L. Guan (2012). "AMPK and mTOR in cellular energy homeostasis and drug targets." Annu Rev Pharmacol Toxicol **52**: 381-400.

Inoki, K., Y. Li, T. Zhu, J. Wu and K. L. Guan (2002). "TSC2 is phosphorylated and inhibited by Akt and suppresses mTOR signalling." Nat Cell Biol **4**(9): 648-657.

Inoki, K., T. Zhu and K. L. Guan (2003). "TSC2 mediates cellular energy response to control cell growth and survival." Cell **115**(5): 577-590.

Ishikawa, H. and G. N. Barber (2008). "STING is an endoplasmic reticulum adaptor that facilitates innate immune signalling." Nature **455**(7213): 674-678.

Ishikawa, H., Z. Ma and G. N. Barber (2009). "STING regulates intracellular DNA-mediated, type I interferon-dependent innate immunity." Nature **461**(7265): 788-792.

Jacinto, E., V. Facchinetti, D. Liu, N. Soto, S. Wei, S. Y. Jung, Q. Huang, J. Qin and B. Su (2006). "SIN1/MIP1 maintains rictor-mTOR complex integrity and regulates Akt phosphorylation and substrate specificity." Cell **127**(1): 125-137.

Jewell, J. L., R. C. Russell and K. L. Guan (2013). "Amino acid signalling upstream of mTOR." Nat Rev Mol Cell Biol **14**(3): 133-139.

Joung, S. M., Z. Y. Park, S. Rani, O. Takeuchi, S. Akira and J. Y. Lee (2011). "Akt contributes to activation of the TRIF-dependent signaling pathways of TLRs by interacting with TANK-binding kinase 1." J Immunol **186**(1): 499-507.

Julien, L. A., A. Carriere, J. Moreau and P. P. Roux (2010). "mTORC1-activated S6K1 phosphorylates Rictor on threonine 1135 and regulates mTORC2 signaling." Mol Cell Biol **30**(4): 908-921.

Jung, C. H., C. B. Jun, S. H. Ro, Y. M. Kim, N. M. Otto, J. Cao, M. Kundu and D. H. Kim (2009). "ULK-Atg13-FIP200 complexes mediate mTOR signaling to the autophagy machinery." Mol Biol Cell **20**(7): 1992-2003.

Jung, C. H., M. Seo, N. M. Otto and D. H. Kim (2011). "ULK1 inhibits the kinase activity of mTORC1 and cell proliferation." Autophagy **7**(10): 1212-1221.

Karnoub, A. E. and R. A. Weinberg (2008). "Ras oncogenes: split personalities." Nat Rev Mol Cell Biol **9**(7): 517-531.

Kawai, T. and S. Akira (2007). "Signaling to NF-kappaB by Toll-like receptors." Trends Mol Med **13**(11): 460-469.

Kim, S. G., G. R. Hoffman, G. Poulogiannis, G. R. Buel, Y. J. Jang, K. W. Lee, B. Y. Kim, R. L. Erikson, L. C. Cantley, A. Y. Choo and J. Blenis (2013). "Metabolic stress controls mTORC1 lysosomal localization and dimerization by regulating the TTT-RUVBL1/2 complex." Mol Cell **49**(1): 172-185.

Kishore, N., Q. K. Huynh, S. Mathialagan, T. Hall, S. Rouw, D. Creely, G. Lange, J. Caroll, B. Reitz, A. Donnelly, H. Boddupalli, R. G. Combs, K. Kretzmer and C. S. Tripp (2002). "IKK-i and TBK-1 are enzymatically distinct from the homologous enzyme IKK-

2: comparative analysis of recombinant human IKK-i, TBK-1, and IKK-2." J Biol Chem **277**(16): 13840-13847.

Korherr, C., H. Gille, R. Schafer, K. Koenig-Hoffmann, J. Dixelius, K. A. Egland, I. Pastan and U. Brinkmann (2006). "Identification of proangiogenic genes and pathways by high-throughput functional genomics: TBK1 and the IRF3 pathway." Proc Natl Acad Sci U S A **103**(11): 4240-4245.

Kumar, H., T. Kawai and S. Akira (2009). "Toll-like receptors and innate immunity." Biochem Biophys Res Commun **388**(4): 621-625.

Kuo, Y. C., K. Y. Huang, C. H. Yang, Y. S. Yang, W. Y. Lee and C. W. Chiang (2008). "Regulation of phosphorylation of Thr-308 of Akt, cell proliferation, and survival by the B55alpha regulatory subunit targeting of the protein phosphatase 2A holoenzyme to Akt." J Biol Chem **283**(4): 1882-1892.

Laplante, M. and D. M. Sabatini (2010). "mTORC1 activates SREBP-1c and uncouples lipogenesis from gluconeogenesis." Proc Natl Acad Sci U S A **107**(8): 3281-3282.

Lee, D. F., H. P. Kuo, C. T. Chen, J. M. Hsu, C. K. Chou, Y. Wei, H. L. Sun, L. Y. Li, B. Ping, W. C. Huang, X. He, J. Y. Hung, C. C. Lai, Q. Ding, J. L. Su, J. Y. Yang, A. A. Sahin, G. N. Hortobagyi, F. J. Tsai, C. H. Tsai and M. C. Hung (2007). "IKK beta suppression of TSC1 links inflammation and tumor angiogenesis via the mTOR pathway." Cell **130**(3): 440-455.

Li, H., L. Chen, A. Zhang, G. Wang, L. Han, K. Yu, P. Pu, C. Kang and Q. Huang (2012). "Silencing of IKKepsilon using siRNA inhibits proliferation and invasion of glioma cells in vitro and in vivo." Int J Oncol **41**(1): 169-178.

Li, Q., D. Van Antwerp, F. Mercurio, K. F. Lee and I. M. Verma (1999). "Severe liver degeneration in mice lacking the IkappaB kinase 2 gene." Science **284**(5412): 321-325.

Li, X., Y. Lu, W. Jin, K. Liang, G. B. Mills and Z. Fan (2006). "Autophosphorylation of Akt at threonine 72 and serine 246. A potential mechanism of regulation of Akt kinase activity." J Biol Chem **281**(19): 13837-13843.

Liao, Y. and M. C. Hung (2010). "Physiological regulation of Akt activity and stability." Am J Transl Res **2**(1): 19-42.

Ma, X. M. and J. Blenis (2009). "Molecular mechanisms of mTOR-mediated translational control." Nat Rev Mol Cell Biol **10**(5): 307-318.

Mahajan, K. and N. P. Mahajan (2012). "PI3K-independent AKT activation in cancers: a treasure trove for novel therapeutics." J Cell Physiol **227**(9): 3178-3184.

Manning, B. D. and L. C. Cantley (2007). "AKT/PKB signaling: navigating downstream." Cell **129**(7): 1261-1274.

Martina, J. A., Y. Chen, M. Gucek and R. Puertollano (2012). "MTORC1 functions as a transcriptional regulator of autophagy by preventing nuclear transport of TFEB." Autophagy **8**(6): 903-914.

Martina, J. A. and R. Puertollano (2013). "Rag GTPases mediate amino acid-dependent recruitment of TFEB and MITF to lysosomes." J Cell Biol **200**(4): 475-491.

Matern, H. T., C. Yeaman, W. J. Nelson and R. H. Scheller (2001). "The Sec6/8 complex in mammalian cells: characterization of mammalian Sec3, subunit interactions, and expression of subunits in polarized cells." Proc Natl Acad Sci U S A **98**(17): 9648-9653.

Matheny, R. W., Jr. and M. L. Adamo (2009). "Current perspectives on Akt Akt-ivation and Akt-ions." Exp Biol Med (Maywood) **234**(11): 1264-1270.

Mattioli, I., H. Geng, A. Sebald, M. Hodel, C. Bucher, M. Kracht and M. L. Schmitz (2006). "Inducible phosphorylation of NF-kappa B p65 at serine 468 by T cell costimulation is mediated by IKK epsilon." J Biol Chem **281**(10): 6175-6183.

Mendoza, M. C., E. E. Er and J. Blenis (2011). "The Ras-ERK and PI3K-mTOR pathways: cross-talk and compensation." Trends Biochem Sci **36**(6): 320-328.

Mitin, N., K. L. Rossman and C. J. Der (2005). "Signaling interplay in Ras superfamily function." Curr Biol **15**(14): R563-574.

Moscat, J. and M. T. Diaz-Meco (2011). "Feedback on fat: p62-mTORC1-autophagy connections." Cell **147**(4): 724-727.

Moskalenko, S., D. O. Henry, C. Rosse, G. Mirey, J. H. Camonis and M. A. White (2002). "The exocyst is a Ral effector complex." Nat Cell Biol **4**(1): 66-72.

Newman, A. C., C. L. Scholefield, A. J. Kemp, M. Newman, E. G. McIver, A. Kamal and S. Wilkinson (2012). "TBK1 kinase addiction in lung cancer cells is mediated via autophagy of Tax1bp1/Ndp52 and non-canonical NF-kappaB signalling." PLoS One **7**(11): e50672.

Nicklin, P., P. Bergman, B. Zhang, E. Triantafellow, H. Wang, B. Nyfeler, H. Yang, M. Hild, C. Kung, C. Wilson, V. E. Myer, J. P. MacKeigan, J. A. Porter, Y. K. Wang, L. C. Cantley, P. M. Finan and L. O. Murphy (2009). "Bidirectional transport of amino acids regulates mTOR and autophagy." Cell **136**(3): 521-534.

O'Neill, A. K., M. J. Niederst and A. C. Newton (2013). "Suppression of survival signalling pathways by the phosphatase PHLPP." FEBS J **280**(2): 572-583.

O'Neill, L. A. (2008). "When signaling pathways collide: positive and negative regulation of toll-like receptor signal transduction." Immunity **29**(1): 12-20.

Obenauer, J. C., L. C. Cantley and M. B. Yaffe (2003). "Scansite 2.0: Proteome-wide prediction of cell signaling interactions using short sequence motifs." Nucleic Acids Res **31**(13): 3635-3641.

Ou, Y. H., M. Torres, R. Ram, E. Formstecher, C. Roland, T. Cheng, R. Brekken, R. Wurz, A. Tasker, T. Polverino, S. L. Tan and M. A. White (2011). "TBK1 directly engages Akt/PKB survival signaling to support oncogenic transformation." Mol Cell **41**(4): 458-470.

Owen, J. L., Y. Zhang, S. H. Bae, M. S. Farooqi, G. Liang, R. E. Hammer, J. L. Goldstein and M. S. Brown (2012). "Insulin stimulation of SREBP-1c processing in transgenic rat hepatocytes requires p70 S6-kinase." Proc Natl Acad Sci U S A **109**(40): 16184-16189.

Parada, L. F., C. J. Tabin, C. Shih and R. A. Weinberg (1982). "Human EJ bladder carcinoma oncogene is homologue of Harvey sarcoma virus ras gene." Nature **297**(5866): 474-478.

Pelengaris, S., M. Khan and G. Evan (2002). "c-MYC: more than just a matter of life and death." Nat Rev Cancer **2**(10): 764-776.

Pena-Llopis, S., S. Vega-Rubin-de-Celis, J. C. Schwartz, N. C. Wolff, T. A. Tran, L. Zou, X. J. Xie, D. R. Corey and J. Brugarolas (2011). "Regulation of TFEB and V-ATPases by mTORC1." EMBO J **30**(16): 3242-3258.

Perry, A. K., E. K. Chow, J. B. Goodnough, W. C. Yeh and G. Cheng (2004). "Differential requirement for TANK-binding kinase-1 in type I interferon responses to toll-like receptor activation and viral infection." J Exp Med **199**(12): 1651-1658.

Peterson, T. R., M. Laplante, C. C. Thoreen, Y. Sancak, S. A. Kang, W. M. Kuehl, N. S. Gray and D. M. Sabatini (2009). "DEPTOR is an mTOR inhibitor frequently overexpressed in multiple myeloma cells and required for their survival." Cell **137**(5): 873-886.

Peterson, T. R., S. S. Sengupta, T. E. Harris, A. E. Carmack, S. A. Kang, E. Balderas, D. A. Guertin, K. L. Madden, A. E. Carpenter, B. N. Finck and D. M. Sabatini (2011). "mTOR complex 1 regulates lipin 1 localization to control the SREBP pathway." Cell **146**(3): 408-420.

Pilli, M., J. Arko-Mensah, M. Ponpuak, E. Roberts, S. Master, M. A. Mandell, N. Dupont, W. Ornatowski, S. Jiang, S. B. Bradfute, J. A. Bruun, T. E. Hansen, T. Johansen

and V. Deretic (2012). "TBK-1 promotes autophagy-mediated antimicrobial defense by controlling autophagosome maturation." Immunity **37**(2): 223-234.

Poduri, A., G. D. Evrony, X. Cai, P. C. Elhosary, R. Beroukhim, M. K. Lehtinen, L. B. Hills, E. L. Heinzen, A. Hill, R. S. Hill, B. J. Barry, B. F. Bourgeois, J. J. Riviello, A. J. Barkovich, P. M. Black, K. L. Ligon and C. A. Walsh (2012). "Somatic activation of AKT3 causes hemispheric developmental brain malformations." Neuron **74**(1): 41-48.

Polak, P. and M. N. Hall (2009). "mTOR and the control of whole body metabolism." Curr Opin Cell Biol **21**(2): 209-218.

Pomerantz, J. L. and D. Baltimore (1999). "NF-kappaB activation by a signaling complex containing TRAF2, TANK and TBK1, a novel IKK-related kinase." EMBO J **18**(23): 6694-6704.

Porstmann, T., C. R. Santos, C. Lewis, B. Griffiths and A. Schulze (2009). "A new player in the orchestra of cell growth: SREBP activity is regulated by mTORC1 and contributes to the regulation of cell and organ size." Biochem Soc Trans **37**(Pt 1): 278-283.

Potter, C. J., L. G. Pedraza and T. Xu (2002). "Akt regulates growth by directly phosphorylating Tsc2." Nat Cell Biol **4**(9): 658-665.

Proud, C. G. (2011). "mTOR Signalling in Health and Disease." Biochem Soc Trans **39**(2): 431-436.

Pulciani, S., E. Santos, A. V. Lauver, L. K. Long, K. C. Robbins and M. Barbacid (1982). "Oncogenes in human tumor cell lines: molecular cloning of a transforming gene from human bladder carcinoma cells." Proc Natl Acad Sci U S A **79**(9): 2845-2849.

Rain, J. C., L. Selig, H. De Reuse, V. Battaglia, C. Reverdy, S. Simon, G. Lenzen, F. Petel, J. Wojcik, V. Schachter, Y. Chemama, A. Labigne and P. Legrain (2001). "The protein-protein interaction map of Helicobacter pylori." Nature **409**(6817): 211-215.

Renner, F., R. Moreno and M. L. Schmitz (2010). "SUMOylation-dependent localization of IKKepsilon in PML nuclear bodies is essential for protection against DNA-damage-triggered cell death." Mol Cell **37**(4): 503-515.

Robitaille, A. M., S. Christen, M. Shimobayashi, M. Cornu, L. L. Fava, S. Moes, C. Prescianotto-Baschong, U. Sauer, P. Jenoe and M. N. Hall (2013). "Quantitative phosphoproteomics reveal mTORC1 activates de novo pyrimidine synthesis." Science **339**(6125): 1320-1323.

Roczniak-Ferguson, A., C. S. Petit, F. Froehlich, S. Qian, J. Ky, B. Angarola, T. C. Walther and S. M. Ferguson (2012). "The transcription factor TFEB links mTORC1 signaling to transcriptional control of lysosome homeostasis." Sci Signal **5**(228): ra42.

Roland, C. L., S. P. Dineen, K. D. Lynn, L. A. Sullivan, M. T. Dellinger, L. Sadegh, J. P. Sullivan, D. S. Shames and R. A. Brekken (2009). "Inhibition of vascular endothelial growth factor reduces angiogenesis and modulates immune cell infiltration of orthotopic breast cancer xenografts." Mol Cancer Ther **8**(7): 1761-1771.

Rosner, M., N. Siegel, A. Valli, C. Fuchs and M. Hengstschlager (2010). "mTOR phosphorylated at S2448 binds to raptor and rictor." Amino Acids **38**(1): 223-228.

Rudolph, D., W. C. Yeh, A. Wakeham, B. Rudolph, D. Nallainathan, J. Potter, A. J. Elia and T. W. Mak (2000). "Severe liver degeneration and lack of NF-kappaB activation in NEMO/IKKgamma-deficient mice." Genes Dev **14**(7): 854-862.

Salhia, B., C. Van Cott, T. Tegeler, A. Polpitiya, R. A. Duquette, M. Gale, G. Hostteter, K. Petritis and J. Carpten (2012). "Differential effects of AKT1(p.E17K) expression on human mammary luminal epithelial and myoepithelial cells." Hum Mutat **33**(8): 1216-1227.

Salmena, L., A. Carracedo and P. P. Pandolfi (2008). "Tenets of PTEN tumor suppression." Cell **133**(3): 403-414.

Sancak, Y., C. C. Thoreen, T. R. Peterson, R. A. Lindquist, S. A. Kang, E. Spooner, S. A. Carr and D. M. Sabatini (2007). "PRAS40 is an insulin-regulated inhibitor of the mTORC1 protein kinase." Mol Cell **25**(6): 903-915.

Sano, H., L. Eguez, M. N. Teruel, M. Fukuda, T. D. Chuang, J. A. Chavez, G. E. Lienhard and T. E. McGraw (2007). "Rab10, a target of the AS160 Rab GAP, is required for insulin-stimulated translocation of GLUT4 to the adipocyte plasma membrane." Cell Metab **5**(4): 293-303.

Sano, H., W. G. Roach, G. R. Peck, M. Fukuda and G. E. Lienhard (2008). "Rab10 in insulin-stimulated GLUT4 translocation." Biochem J **411**(1): 89-95.

Sarbassov, D. D., D. A. Guertin, S. M. Ali and D. M. Sabatini (2005). "Phosphorylation and regulation of Akt/PKB by the rictor-mTOR complex." Science **307**(5712): 1098-1101.

Sasaki, H., K. Okuda, O. Kawano, H. Yukiue, M. Yano and Y. Fujii (2008). "AKT1 and AKT2 mutations in lung cancer in a Japanese population." Mol Med Rep **1**(5): 663-666.

Sato, S., N. Fujita and T. Tsuruo (2000). "Modulation of Akt kinase activity by binding to Hsp90." Proc Natl Acad Sci U S A **97**(20): 10832-10837.

Sato, S., M. Sugiyama, M. Yamamoto, Y. Watanabe, T. Kawai, K. Takeda and S. Akira (2003). "Toll/IL-1 receptor domain-containing adaptor inducing IFN-beta (TRIF) associates with TNF receptor-associated factor 6 and TANK-binding kinase 1, and

activates two distinct transcription factors, NF-kappa B and IFN-regulatory factor-3, in the Toll-like receptor signaling." J Immunol **171**(8): 4304-4310.

Schroder, M., M. Baran and A. G. Bowie (2008). "Viral targeting of DEAD box protein 3 reveals its role in TBK1/IKKepsilon-mediated IRF activation." EMBO J **27**(15): 2147-2157.

Sengupta, S., T. R. Peterson and D. M. Sabatini (2010). "Regulation of the mTOR complex 1 pathway by nutrients, growth factors, and stress." Mol Cell **40**(2): 310-322.

Seth, R. B., L. Sun, C. K. Ea and Z. J. Chen (2005). "Identification and characterization of MAVS, a mitochondrial antiviral signaling protein that activates NF-kappaB and IRF 3." Cell **122**(5): 669-682.

Settembre, C., R. Zoncu, D. L. Medina, F. Vetrini, S. Erdin, S. Erdin, T. Huynh, M. Ferron, G. Karsenty, M. C. Vellard, V. Facchinetti, D. M. Sabatini and A. Ballabio (2012). "A lysosome-to-nucleus signalling mechanism senses and regulates the lysosome via mTOR and TFEB." EMBO J **31**(5): 1095-1108.

Shackelford, D. B., D. S. Vasquez, J. Corbeil, S. Wu, M. Leblanc, C. L. Wu, D. R. Vera and R. J. Shaw (2009). "mTOR and HIF-1alpha-mediated tumor metabolism in an LKB1 mouse model of Peutz-Jeghers syndrome." Proc Natl Acad Sci U S A **106**(27): 11137-11142.

Shah, O. J., Z. Wang and T. Hunter (2004). "Inappropriate activation of the TSC/Rheb/mTOR/S6K cassette induces IRS1/2 depletion, insulin resistance, and cell survival deficiencies." Curr Biol **14**(18): 1650-1656.

Shao, W. and P. J. Espenshade (2012). "Expanding roles for SREBP in metabolism." Cell Metab **16**(4): 414-419.

Sharma, S., B. R. tenOever, N. Grandvaux, G. P. Zhou, R. Lin and J. Hiscott (2003). "Triggering the interferon antiviral response through an IKK-related pathway." Science **300**(5622): 1148-1151.

Shaw, R. J. and L. C. Cantley (2006). "Ras, PI(3)K and mTOR signalling controls tumour cell growth." Nature **441**(7092): 424-430.

Shen, R. R. and W. C. Hahn (2011). "Emerging roles for the non-canonical IKKs in cancer." Oncogene **30**(6): 631-641.

Shih, C. and R. A. Weinberg (1982). "Isolation of a transforming sequence from a human bladder carcinoma cell line." Cell **29**(1): 161-169.

Shiota, C., J. T. Woo, J. Lindner, K. D. Shelton and M. A. Magnuson (2006). "Multiallelic disruption of the rictor gene in mice reveals that mTOR complex 2 is essential for fetal growth and viability." Dev Cell **11**(4): 583-589.

Singh, A., P. Greninger, D. Rhodes, L. Koopman, S. Violette, N. Bardeesy and J. Settleman (2009). "A gene expression signature associated with "K-Ras addiction" reveals regulators of EMT and tumor cell survival." Cancer Cell **15**(6): 489-500.

Soliman, G. A., H. A. Acosta-Jaquez, E. A. Dunlop, B. Ekim, N. E. Maj, A. R. Tee and D. C. Fingar (2010). "mTOR Ser-2481 autophosphorylation monitors mTORC-specific catalytic activity and clarifies rapamycin mechanism of action." J Biol Chem **285**(11): 7866-7879.

Song, M. S., L. Salmena and P. P. Pandolfi (2012). "The functions and regulation of the PTEN tumour suppressor." Nat Rev Mol Cell Biol **13**(5): 283-296.

Soulat, D., T. Burckstummer, S. Westermayer, A. Goncalves, A. Bauch, A. Stefanovic, O. Hantschel, K. L. Bennett, T. Decker and G. Superti-Furga (2008). "The DEAD-box helicase DDX3X is a critical component of the TANK-binding kinase 1-dependent innate immune response." EMBO J **27**(15): 2135-2146.

Stephens, P. J., P. S. Tarpey, H. Davies, P. Van Loo, C. Greenman, D. C. Wedge, S. Nik-Zainal, S. Martin, I. Varela, G. R. Bignell, L. R. Yates, E. Papaemmanuil, D. Beare, A. Butler, A. Cheverton, J. Gamble, J. Hinton, M. Jia, A. Jayakumar, D. Jones, C. Latimer, K. W. Lau, S. McLaren, D. J. McBride, A. Menzies, L. Mudie, K. Raine, R. Rad, M. S. Chapman, J. Teague, D. Easton, A. Langerod, C. Oslo Breast Cancer, M. T. Lee, C. Y. Shen, B. T. Tee, B. W. Huimin, A. Broeks, A. C. Vargas, G. Turashvili, J. Martens, A. Fatima, P. Miron, S. F. Chin, G. Thomas, S. Boyault, O. Mariani, S. R. Lakhani, M. van de Vijver, L. van 't Veer, J. Foekens, C. Desmedt, C. Sotiriou, A. Tutt, C. Caldas, J. S. Reis-Filho, S. A. Aparicio, A. V. Salomon, A. L. Borresen-Dale, A. L. Richardson, P. J. Campbell, P. A. Futreal and M. R. Stratton (2012). "The landscape of cancer genes and mutational processes in breast cancer." Nature **486**(7403): 400-404.

Stockli, J., D. J. Fazakerley and D. E. James (2011). "GLUT4 exocytosis." J Cell Sci **124**(Pt 24): 4147-4159.

Takaoka, A., Z. Wang, M. K. Choi, H. Yanai, H. Negishi, T. Ban, Y. Lu, M. Miyagishi, T. Kodama, K. Honda, Y. Ohba and T. Taniguchi (2007). "DAI (DLM-1/ZBP1) is a cytosolic DNA sensor and an activator of innate immune response." Nature **448**(7152): 501-505.

Tan, C. Y. and T. Hagen (2013). "Post-translational regulation of mTOR complex 1 in hypoxia and reoxygenation." Cell Signal **25**(5): 1235-1244.

Tang, X., S. W. Jang, X. Wang, Z. Liu, S. M. Bahr, S. Y. Sun, D. Brat, D. H. Gutmann and K. Ye (2007). "Akt phosphorylation regulates the tumour-suppressor merlin through ubiquitination and degradation." Nat Cell Biol **9**(10): 1199-1207.

Tatake, R. J., M. M. O'Neill, C. A. Kennedy, A. L. Wayne, S. Jakes, D. Wu, S. Z. Kugler, Jr., M. A. Kashem, P. Kaplita and R. J. Snow (2008). "Identification of pharmacological inhibitors of the MEK5/ERK5 pathway." Biochem Biophys Res Commun **377**(1): 120-125.

Thedieck, K., P. Polak, M. L. Kim, K. D. Molle, A. Cohen, P. Jeno, C. Arrieumerlou and M. N. Hall (2007). "PRAS40 and PRR5-like protein are new mTOR interactors that regulate apoptosis." PLoS One **2**(11): e1217.

Thurston, T. L., G. Ryzhakov, S. Bloor, N. von Muhlinen and F. Randow (2009). "The TBK1 adaptor and autophagy receptor NDP52 restricts the proliferation of ubiquitin-coated bacteria." Nat Immunol **10**(11): 1215-1221.

Tojima, Y., A. Fujimoto, M. Delhase, Y. Chen, S. Hatakeyama, K. Nakayama, Y. Kaneko, Y. Nimura, N. Motoyama, K. Ikeda, M. Karin and M. Nakanishi (2000). "NAK is an IkappaB kinase-activating kinase." Nature **404**(6779): 778-782.

Topisirovic, I. and N. Sonenberg (2011). "mRNA translation and energy metabolism in cancer: the role of the MAPK and mTORC1 pathways." Cold Spring Harb Symp Quant Biol **76**: 355-367.

Treins, C., P. H. Warne, M. A. Magnuson, M. Pende and J. Downward (2010). "Rictor is a novel target of p70 S6 kinase-1." Oncogene **29**(7): 1003-1016.

Ugi, S., T. Imamura, H. Maegawa, K. Egawa, T. Yoshizaki, K. Shi, T. Obata, Y. Ebina, A. Kashiwagi and J. M. Olefsky (2004). "Protein phosphatase 2A negatively regulates insulin's metabolic signaling pathway by inhibiting Akt (protein kinase B) activity in 3T3-L1 adipocytes." Mol Cell Biol **24**(19): 8778-8789.

Vadysirisack, D. D., F. Baenke, B. Ory, K. Lei and L. W. Ellisen (2011). "Feedback control of p53 translation by REDD1 and mTORC1 limits the p53-dependent DNA damage response." Mol Cell Biol **31**(21): 4356-4365.

Varma, S. and R. L. Khandelwal (2007). "Effects of rapamycin on cell proliferation and phosphorylation of mTOR and p70(S6K) in HepG2 and HepG2 cells overexpressing constitutively active Akt/PKB." Biochim Biophys Acta **1770**(1): 71-78.

Vasudevan, K. M. and L. A. Garraway (2010). "AKT signaling in physiology and disease." Curr Top Microbiol Immunol **347**: 105-133.

Vazquez-Martin, A., C. Oliveras-Ferraros, L. Bernado, E. Lopez-Bonet and J. A. Menendez (2009). "The serine 2481-autophosphorylated form of mammalian Target Of Rapamycin (mTOR) is localized to midzone and midbody in dividing cancer cells." Biochem Biophys Res Commun **380**(3): 638-643.

Vega, I. E. and S. C. Hsu (2001). "The exocyst complex associates with microtubules to mediate vesicle targeting and neurite outgrowth." J Neurosci **21**(11): 3839-3848.

Vousden, K. H. and C. Prives (2009). "Blinded by the Light: The Growing Complexity of p53." Cell **137**(3): 413-431.

Wang, L., T. E. Harris and J. C. Lawrence, Jr. (2008). "Regulation of proline-rich Akt substrate of 40 kDa (PRAS40) function by mammalian target of rapamycin complex 1 (mTORC1)-mediated phosphorylation." J Biol Chem **283**(23): 15619-15627.

Wang, L., T. E. Harris, R. A. Roth and J. C. Lawrence, Jr. (2007). "PRAS40 regulates mTORC1 kinase activity by functioning as a direct inhibitor of substrate binding." J Biol Chem **282**(27): 20036-20044.

Wang, X. and C. G. Proud (2011). "mTORC1 signaling: what we still don't know." J Mol Cell Biol **3**(4): 206-220.

Wauson, E. M., E. Zaganjor and M. H. Cobb (2013). "Amino acid regulation of autophagy through the GPCR TAS1R1-TAS1R3." Autophagy **9**(3): 418-419.

Wauson, E. M., E. Zaganjor, A. Y. Lee, M. L. Guerra, A. B. Ghosh, A. L. Bookout, C. P. Chambers, A. Jivan, K. McGlynn, M. R. Hutchison, R. J. Deberardinis and M. H. Cobb (2012). "The G protein-coupled taste receptor T1R1/T1R3 regulates mTORC1 and autophagy." Mol Cell **47**(6): 851-862.

Weidberg, H. and Z. Elazar (2011). "TBK1 mediates crosstalk between the innate immune response and autophagy." Sci Signal **4**(187): pe39.

Welsh, G. I., I. Hers, D. C. Berwick, G. Dell, M. Wherlock, R. Birkin, S. Leney and J. M. Tavare (2005). "Role of protein kinase B in insulin-regulated glucose uptake." Biochem Soc Trans **33**(Pt 2): 346-349.

White, E. (2012). "Deconvoluting the context-dependent role for autophagy in cancer." Nat Rev Cancer **12**(6): 401-410.

Whitehurst, A. W., B. O. Bodemann, J. Cardenas, D. Ferguson, L. Girard, M. Peyton, J. D. Minna, C. Michnoff, W. Hao, M. G. Roth, X. J. Xie and M. A. White (2007). "Synthetic lethal screen identification of chemosensitizer loci in cancer cells." Nature **446**(7137): 815-819.

Wojcik, J., I. G. Boneca and P. Legrain (2002). "Prediction, assessment and validation of protein interaction maps in bacteria." J Mol Biol **323**(4): 763-770.

Wolf, A., S. Agnihotri, J. Micallef, J. Mukherjee, N. Sabha, R. Cairns, C. Hawkins and A. Guha (2011). "Hexokinase 2 is a key mediator of aerobic glycolysis and promotes tumor growth in human glioblastoma multiforme." J Exp Med **208**(2): 313-326.

Wolff, N. C., S. Vega-Rubin-de-Celis, X. J. Xie, D. H. Castrillon, W. Kabbani and J. Brugarolas (2011). "Cell-type-dependent regulation of mTORC1 by REDD1 and the tumor suppressors TSC1/TSC2 and LKB1 in response to hypoxia." Mol Cell Biol **31**(9): 1870-1884.

Wullschleger, S., R. Loewith and M. N. Hall (2006). "TOR signaling in growth and metabolism." Cell **124**(3): 471-484.

Xie, X., D. Zhang, B. Zhao, M. K. Lu, M. You, G. Condorelli, C. Y. Wang and K. L. Guan (2011). "IkappaB kinase epsilon and TANK-binding kinase 1 activate AKT by direct phosphorylation." Proc Natl Acad Sci U S A **108**(16): 6474-6479.

Yamamoto, M., S. Sato, H. Hemmi, K. Hoshino, T. Kaisho, H. Sanjo, O. Takeuchi, M. Sugiyama, M. Okabe, K. Takeda and S. Akira (2003). "Role of adaptor TRIF in the MyD88-independent toll-like receptor signaling pathway." Science **301**(5633): 640-643.

Yang, W. L., J. Wang, C. H. Chan, S. W. Lee, A. D. Campos, B. Lamothe, L. Hur, B. C. Grabiner, X. Lin, B. G. Darnay and H. K. Lin (2009). "The E3 ligase TRAF6 regulates Akt ubiquitination and activation." Science **325**(5944): 1134-1138.

Yecies, J. L. and B. D. Manning (2011). "mTOR links oncogenic signaling to tumor cell metabolism." J Mol Med (Berl) **89**(3): 221-228.

Yecies, J. L. and B. D. Manning (2011). "Transcriptional control of cellular metabolism by mTOR signaling." Cancer Res **71**(8): 2815-2820.

Yu, Y., S. O. Yoon, G. Poulogiannis, Q. Yang, X. M. Ma, J. Villen, N. Kubica, G. R. Hoffman, L. C. Cantley, S. P. Gygi and J. Blenis (2011). "Phosphoproteomic analysis identifies Grb10 as an mTORC1 substrate that negatively regulates insulin signaling." Science **332**(6035): 1322-1326.

Zhang, H., X. Zha, Y. Tan, P. V. Hornbeck, A. J. Mastrangelo, D. R. Alessi, R. D. Polakiewicz and M. J. Comb (2002). "Phosphoprotein analysis using antibodies broadly reactive against phosphorylated motifs." J Biol Chem **277**(42): 39379-39387.

Zhang, M., X. Wu, A. J. Lee, W. Jin, M. Chang, A. Wright, T. Imaizumi and S. C. Sun (2008). "Regulation of IkappaB kinase-related kinases and antiviral responses by tumor suppressor CYLD." J Biol Chem **283**(27): 18621-18626.

Zhang, X., N. Tang, T. J. Hadden and A. K. Rishi (2011). "Akt, FoxO and regulation of apoptosis." Biochim Biophys Acta **1813**(11): 1978-1986.

Zhao, W. (2013). "Negative regulation of TBK1-mediated antiviral immunity." FEBS Lett **587**(6): 542-548.

Zhou, Q. L., Z. Y. Jiang, J. Holik, A. Chawla, G. N. Hagan, J. Leszyk and M. P. Czech (2008). "Akt substrate TBC1D1 regulates GLUT1 expression through the mTOR pathway in 3T3-L1 adipocytes." Biochem J **411**(3): 647-655.

Zoncu, R., A. Efeyan and D. M. Sabatini (2011). "mTOR: from growth signal integration to cancer, diabetes and ageing." Nat Rev Mol Cell Biol **12**(1): 21-35.